Aus dem Max von Pettenkofer-Institut
für Hygiene und Medizinische Mikrobiologie
der Ludwig-Maximilians-Universität München
Lehrstuhl Virologie
Vorstand: Prof. Dr. med. Oliver T. Keppler

The role of the murine cytomegalovirus (MCMV) chemokine MCK2 in infection and as part of MCMV vaccine vectors

Dissertation
zum Erwerb des Doktorgrades der Naturwissenschaften
an der Medizinischen Fakultät der
Ludwig-Maximilians-Universität zu München

vorgelegt von
Marwa Abdualraheem Mohammed Eletreby
aus
Gharbeya, Ägypten
2021

Mit Genehmigung der Medizinischen Fakultät

der Universität München

Betreuerin:	Priv. Doz. Dr. Barbara Adler
Zweitgutachterin:	Priv. Doz. Dr. Ursula Zimber-Strobl
Dekan:	Prof. Dr. med. Thomas Gudermann
Tag der mündlichen Prüfung:	07/12/2021

Printed with the support of the German Academic Exchange Service (DAAD)

Affidavit

LMU LUDWIG-MAXIMILIANS-UNIVERSITÄT MÜNCHEN | Promotionsbüro Medizinische Fakultät | MMRS

Eidesstattliche Versicherung

Eletreby, Marwa Abdualraheem Mohammed

Ich erkläre hiermit an Eides statt, dass ich die vorliegende Dissertation mit dem Titel:

“The role of the murine cytomegalovirus (MCMV) chemokine MCK2 in infection and as part of MCMV vaccine vectors”

selbständig verfasst, mich außer der angegebenen keiner weiteren Hilfsmittel bedient und alle Erkenntnisse, die aus dem Schrifttum ganz oder annähernd übernommen sind, als solche kenntlich gemacht und nach ihrer Herkunft unter Bezeichnung der Fundstelle einzeln nachgewiesen habe.

Ich erkläre des Weiteren, dass die hier vorgelegte Dissertation nicht in gleicher oder in ähnlicher Form bei einer anderen Stelle zur Erlangung eines akademischen Grades eingereicht wurde.

München, 2.01.2022 Marwa Eletreby

_____ _____

Ort, Datum Unterschrift Doktorandin bzw. Doktorand

Table of contents

Acknowledgements

Undertaking a PhD is not an easy journey, but it is made both bearable and enjoyable, by those who surround you during this journey. Firstly, I would firstly like to express my deepest gratitude to my supervisor Barbara Adler for her patience, excellent supervision throughout this journey, and endless support from the very beginning of the PhD to the end. I admire not only her scientific work and passion for research, but also her leadership skills which inspired me as a woman. Therefore, she left a deep fingerprint on my character, as they say in German "*Ihr Einfluss wird unvergesslich sein".*

I would like to thank everyone in our lab. I would like to gratefully acknowledge Lucie Kubic for her technical help. A special thanks to Katharina Jäger for her continuous help and support in my stressful times and for making the lab a more enjoyable place.

I would like to thank Prof. Dr. Heiko Adler for his great help and support during vaccination experiments. I would like also to acknowledge Dr. Xaver Sewald for his outstanding suggestions in my thesis advisory committee.

I would like to extend my most profound gratitude to my beloved family, my parents and my sisters, Mona, Maha, Manar and the lovely twins Mohammed and Marium (M empire) ☺ for supporting my decision of studying abroad, their encouragement, and endless emotional support. Special thanks to my friends in Germany, Samah Mahmoud, Nesma Mustafa, Soha Hassan, Sara Mobarez for their continuous support and sharing a lot of exciting moments in Germany.

Finally, there are no words to express my gratitude to DAAD for offering me the opportunities to make my PhD in Germany and have this wonderful experience.

Dedication

I dedicate this thesis to the first teacher in my life, the person who believed in me since I was three years old, the constant source of strength, unconditional love and happiness throughout every step in my life, **my lovely mother**. You are the light of my life. I could not have done this without you.

Zusammenfassung

Das humane Cytomegalovirus (HCMV) gehört zur Familie der Herpesviridae. Die Infektion immunkompetenter Menschen verläuft überwiegend asymptomatisch, eine Infektion immungeschwächter Patienten kann jedoch zu lebensbedrohlichen Erkrankungen führen. Cytomegaloviren (CMV) ziehen auch als potenzielle Impfstoffvektoren, die in der Lage sind, Fremdantigene effizient zu präsentieren und lang anhaltende $CD8^+$-T-Zellantworten auszulösen, viel Aufmerksamkeit auf sich. Cytomegalieviren kodieren für viele immunmodulatorische Gene, die dem Virus helfen, der Immunantwort des Wirts zu entkommen. Darunter befinden sich zum Beispiel virale CC-Chemokine, wie das UL128 Protein von HCMV, das als Chemokin Monozyten anlocken kann, aber auch mit gH/gL-Glykoproteinen im Virion einen Komplex bilden und den Viruseintritt vermitteln kann. Die Infektion von Mäusen mit dem murinen Cytomegalovirus (MCMV) ist ein gut etabliertes Tiermodell, um HCMV-Infektionen *in vivo* zu untersuchen. Das MCMV Chemokin MCK2 hat wie sein HCMV Homolog UL128 eine Doppelfunktion: Es ist ein aktives Chemokin, das ebenfalls Monozyten anlockt und zusätzlich als Teil eines gH/gL/MCK2 Hüllglykoprotein Komplexes die Infektion von MCMV-Wirtszellen vermittelt. MCK2 vermittelt *in vivo* die Virusdissemination und moduliert die antivirale Immunantwort.

Zu Beginn dieser Arbeit war nicht bekannt, ob die *in vivo* beobachteten Phänotypen für MCMV Mutanten, die kein MCK2 exprimieren, auf die Chemokinfunktion von MCK2 oder seine Rolle im gH/gL/MCK2 Komplex oder beides zurückzuführen sind. Das erste Ziel dieser Arbeit war die Charakterisierung verschiedener MCK2 Mutanten *in vitro* und *in vivo.* Die Mutationen wurden so konzipiert, dass entweder die Chemokinfunktion von MCK2 oder die Komplexbindungskapazität oder beides zerstört wurde. *In vitro* konnte gezeigt werden, dass die Infektion von Makrophagen und dendritischen Zellen durch den gH/gL/MCK2 Komplex vermittelt wird. *In vivo* fördert der gH/gL/MCK2 Komplex die Dissemination der MCMV-Infektion in die Speicheldrüsen. Die Mutation der Chemokinfunktion führte zu einer verstärkten frühen $CD8^+$ T-Zell-Antwort, begleitet von reduzierten Titern beispielsweise in der Lunge. Das deutete darauf hin, dass das MCK2-Chemokin die frühe antivirale CD8-T-Zell-Antwort dämpft, um eine effiziente Infektion sicherzustellen. Diese Ergebnisse zeigten zum ersten Mal, dass die MCK2-Chemokinaktivität und der gH/gL/MCK2-abhängige Virusinfektion unabhängige Funktionen von MCK2 sind. Außerdem wurde untersucht,

wie MCK2 eine Vakzinierung mit MCMV Vektoren beeinflusst. Als Modell diente die Vakzinierung von Mäusen gegen eine Infektion mit dem murinen Gammaherpesvirus 68 (MHV-68). Es wurden MCMV-Impfstoffvektoren kloniert, die verschiedene MCK2-Mutationen tragen und das ORF6-Protein von MHV-68 exprimieren, das ein T-Zell Antigen ist. Bereits nach einer Immunisierung induzierten alle MCMV-Vektoren ORF6-spezifische $CD8^+$-T-Zellantworten. Die lytische MHV-68 Infektion in der Lunge wurde unabhängig von der MCK2-Expression effizient kontrolliert. Im Gegensatz dazu war der Schutz immunisierter Mäuse vor der MHV-68-Latenz eindeutig MCK2-abhängig. Diese Studie beleuchtet die Rolle der CMV CC-Chemokine und gH/gL-Chemokin Komplexe für die antivirale Immunantwort sowohl im Rahmen einer CMV-Infektion als auch beim Einsatz von CMV als Impfstoffvektoren.

Summary

Human cytomegalovirus (HCMV) belongs to the family of Herpesviridae. Infection of immunocompetent humans is predominantly asymptomatic, but infection of immunocompromised patients can result in life-threating diseases. Cytomegaloviruses (CMV) also attract much attention as potential vaccine vectors, which are able to efficiently deliver vaccine antigens and elicit long lasting $CD8^+$ T cell responses. CMV code for many immunomodulatory genes, which help the virus to escape from the host immune response. Among them are viral CC-chemokines, for example the UL128 protein of HCMV, which can act as a classical chemokine and attract for example monocytes, and additionally can also form a complex with gH/gL glycoproteins in the virion and promote virus entry. The infection of mice with murine cytomegalovirus (MCMV) is a well-established animal model to study HCMV infections *in vivo*. Like the HCMV UL128 gene product, its MCMV homolog MCK2 has a dual function: It is an active chemokine attracting for example monocytes, and additionally it promotes infection of MCMV host cells as part of a gH/gL/MCK2 envelope glycoprotein complex. MCK2 expression has a profound effect on MCMV viral dissemination and antiviral response. Before the start of this thesis, it was not known whether phenotypes observed for MCMV mutants lacking MCK2 *in vivo* are due to the chemokine function of MCK2 or its entry function as a part of the gH/gL/MCK2 complex or both. The first aim of this thesis was to characterize a set of MCMV mutants carrying different MCK2 mutations *in vitro* and *in vivo*. The mutations were designed in a way that either MCK2's chemokine function or the complex binding capacity or both were destroyed. *In vitro*, it could be shown that infection of macrophages and dendritic cells is promoted by the gH/gL/MCK2 complex. *In vivo*, the gH/gL/MCK2 complex promotes dissemination of MCMV infection to the salivary glands. Mutation of the chemokine function resulted in an enhanced early $CD8^+$ T cell response accompanied by reduced titers, for example in lungs, indicating that the MCK2 chemokine dampens the early antiviral $CD8^+$ T cell response to secure efficient infection. These findings for the first time demonstrated that the MCK2 chemokine activity and gH/gL/MCK2-dependent virus entry are separate and independent functions of MCK2.

Additionally, it was studied whether MCK2 shapes the vaccination success when MCMV was used as a vaccine vector. Vaccination of mice against infection with the murine gamma herpes virus 68 (MHV-68) was used as a model. MCMV vaccine vectors

carrying different MCK2 mutations and expressing the ORF6 protein of MHV-68, which is a classical target of antiviral T cell responses, were generated. After one round of immunization, all MCMV vaccine vectors induced ORF6-specific $CD8^+$ T cell responses and all of immunized mice could efficiently control lytic infection of MHV-68 in the lungs, independently of MCK2 expression or mutation of MCK2. In contrast, the protection of immunized mice against MHV-68 latency was clearly influenced by MCK2 functions. This study highlights the role of the CMV CC-chemokines and chemokine-containing gH/gL complexes for the antiviral immune response both in the context of a CMV infection and also when CMV are used as vaccine vectors.

1. Introduction

1.1 Herpesviruses

Herpesviruses are large, enveloped DNA viruses. Their hosts include mammals, birds, and reptiles (McGeoch & Gatherer, 2005). The family of *herpesviridae* is subdivided into three subfamilies: *alpaherpesviridae*, *betaherpesviridae,* and *gammaherpesviridae.* Members of *herpesviridae* family exhibit a common structure, a linear double-stranded (ds) DNA genome, ranging from 125 to 295 kbp in length, encapsidated by an approximately 125nm (diameter) icosahedral capsid consisting of 162 capsomeres, implanted in a protein layer called tegument and surrounded by an envelope (Roizman et al., 1993).

Herpesviruses enter their host cells either by direct fusion at the plasma membrane or by membrane fusion in endocytotic vesicles (Compton et al., 1992; Ryckman et al., 2006). The viral capsid is transported to the nucleus, where the genome is released and the transcription of immediate early (IE) proteins is started. These proteins work as transcriptional activators, which are required for the expression of cellular and viral genes. Early proteins then initiate genome replication in the nucleus. After replication, late genes that encode for envelope glycoproteins, tegument proteins, and capsid components are expressed. In the final stage of the infection cycle, late proteins initiate virion assembly and finally infectious viruses are released from the cytoplasm (Gibson, 1996). After primary infection, herpesviruses evade and overcome the host immune response by different mechanisms and establish a lifelong latent infection. Viral latency can be described as the presence of functional viral genomes in a cell without production of infectious viral particles. These genomes can be reactivated to produce viruses (Redpath et al., 2001).

Eight human herpesviruses have been identified: Herpes Simplex Virus 1 and 2 and Varizella Zoster virus (*alpaherpesviridae*), Human Cytomegalovirus and Human Herpesviruses 6A, 6B and 7 (*betaherpesviridae*), Epstein-Barr virus and Karposi´s sarcoma-associated herpesvirus (*gammaherpesviridae*) (Mocarski et al., 2013).

1.2 Human cytomegalovirus (HCMV)

Human cytomegalovirus belongs to the *betaherpesviridae* subfamily of herpesviruses. HCMV infection has a morphological impact upon the cells, as it causes increase in the size of the cells, a phenomenon called “cytomegaly”, which gave HCMV its name (Weller et al., 1957). It was first isolated from tissues of infected infants and cultivated in 1956 (Smith 1956; Weller et al., 1957). Cytomegaloviruses infect a wide range of hosts, including for example rhesus monkeys (RhCMV), mice (MCMV) or guinea pigs (Guinean pig CMV). They are all restricted to their host species (Mocarski et al., 2013). HCMV has a genome size of 235 kbp and its virion has a diameter of 200–300 nm (Mocarski et al., 2013). The nucleocapsid is made up of seven proteins, including the conserved major and minor capsid proteins. A protein-rich tegument layer surrounds the capsid, which is enclosed within a lipid bilayer envelope (Mocarski et al., 2013) (Figure 1).

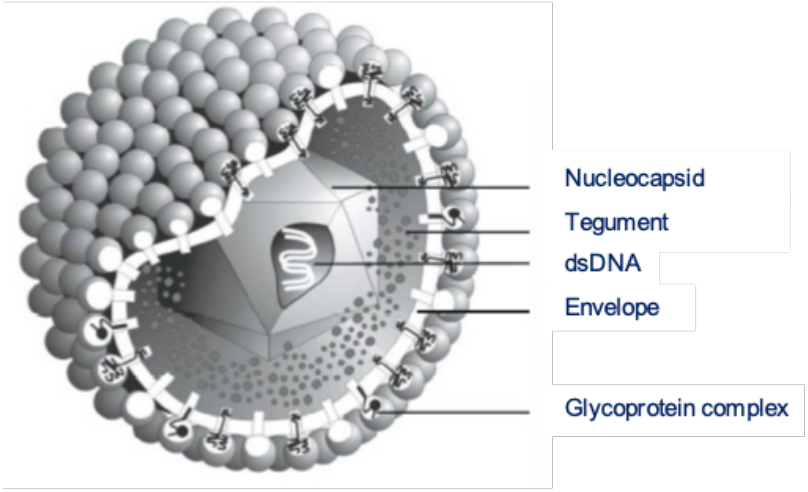

Figure 1: Schematic presentation of the HCMV virion (adapted from Reschke, 1994).

HCMV virions contain at least thirty proteins, the majority of the virion proteins are located in the tegument layer. Tegument proteins play several roles in viral entry and modulating the host cell response upon virus entry (Mocarski et al., 2013). The surrounding envelope is rich of proteins of both viral and cellular origin. The major glycoproteins/ glycoprotein complexes embedded in the envelope are glycoprotein B (gB), gM/gN gH/gL/gO, and gH/gL/pUL(128,130,131A). They play a crucial role in mediating viral entry and determine the broad cell tropism of HCMV (Wille et al., 2013; Ryckman et al., 2008).

1.2.1 HCMV prevalence and transmission

HCMV is distributed worldwide and the seroprevalence varies from 40 to nearly 100% (Staras et al., 2006). HCMV seroprevalence in Germany is about 40-50% (Lachmann et al., 2018). HCMV is not highly contagious and transmission occurs mainly through close contact with an infected individual, who sheds virus in bodily fluids like urine or saliva (Pass, 2001). HCMV can also be sexually transmitted (Chandler et al., 1985; Pereira et al., 1990). Additionally, HCMV can be transmitted vertically from mother to child either transplacentally, postpartum or intrapartum. The most prevalent route of HCMV transfer from mother to child is postpartum transmission during breastfeeding (Pass, 2001). The intrauterine transmission rate of HCMV for HCMV-positive mothers experiencing reactivation of latent virus or superinfection is 0.1–1%, whereas the intrauterine transmission in seronegative mothers experiencing primary infection is about 35% (Forbes, 1989; Mocarski et al., 2013; Pass & Anderson, 2014).

1.2.2 HCMV Pathogenesis

As the immune response plays a major role in controlling HCMV infection and limits lytic viral replication, the pathogenesis of HCMV is highly correlated with the immune competence of infected individuals. HCMV mostly causes asymptomatic infections in immunocompetent individuals or rarely results in a mononucleosis syndrome (Crough & Khanna, 2009) characterized by malaise, fever, lymphocytosis with abnormal liver function and atypical lymphocytes (Friel et al., 2010). In immunocompromised individuals, HCMV can cause life-threating diseases. After organ or bone marrow transplantation, suppression of T cells results in a reduced antiviral T cell surveillance. Therefore, the risk of developing HCMV disease is high in both recipients of solid organ transplants (i.e., kidney and liver) or hematopoietic stem cell transplants (HSCT). The immunosuppressed transplant recipients develop serious diseases like hepatitis or pneumonia (Drago et al., 2000). Also, immunocompromised patients like HIV-infected individuals are at a high risk to develop HCMV disease like for example retinitis (Centers 1997; Palella Jr et al., 1998). Intrauterine infection of HCMV causes a high rate of morbidity and mortality in the newborn or prematurely borne children. Furthermore, the surviving children can suffer from a number of serious neurological, hearing, and developmental problems (Malm & Engman, 2007).

1.2.3. Treatment of HCMV disease and HCMV vaccines

Ganciclovir (GCV) is known as the gold standard drug for HCMV infection in immunocompromised patients. GCV is a nucleoside analogue that is administrated by intravenous infusion, and targets the viral DNA polymerase and prevents virus replication (Lischka & Zimmermann, 2008). Furthermore, there are also other groups of anti-HCMV drugs like Cidofovir (CDV), Foscarnet (FOS), which also target the viral polymerase (Härter & Michel, 2012; Razonable, 2011) or Letermovir and Maribavir, which target packaging of the viral genome or particle assembly, respectively (Foolad et al., 2018; Goldberg et al., 2011).

All these drugs have drawbacks, like development of resistance (Schreiber et al., 2009; Keyvani et al., 2016) and association with adverse side effects like anaemia and thrombocytopenia (Upadhyayula & Michaels, 2013).

Many efforts are directed to the development of a vaccine against HCMV. A vaccine could protect immunocompromised individuals from developing HCMV disease as well as prevent HCMV infection during pregnancy. Currently, no licensed anti-HCMV vaccine is available. However, there are many clinical trials up to phase III, which tested for example recombinant gB and the tegument phosphoprotein 65 (pp65) (Anderholm et al., 2016). Additionally, DNA vaccines coding for pp65 and gB have shown some protection in transplant recipients (Smith et al., 2013). Most of the tested HCMV vaccine candidates work by inducing a humoral immunity, while pp65-based vaccines induce an antiviral T-cell response (Wloch et al., 2008; Anderholm et al., 2016). New platforms of vaccines have also been utilized for development of HCMV vaccine, for instance RNA-based technology (Anderholm et al., 2016; Loomis et al., 2013). Furthermore, viral vectored vaccines have been investigated, like canary box vector, modified vaccinia virus ankara (MVA) and alphavirus-based vectors were tested (Anderholm et al., 2016). Many different approaches for designing HCMV vaccine are in clinical trials up to phase III studies, yet none of them exceeded a 50% protection from infection (Anderholm et al., 2016). Currently, new studies are focusing on the gH/gL/pUL(128,130,131A) glycoprotein complex as a promising vaccine target, because in the human infection, potent neutralizing antibodies are elicited (Wen et al., 2014; Macagno et al., 2010).

1.3 HCMV Glycoproteins

The entry process of HCMV is mediated by envelope glycoproteins: gM/gN, gB, gH/gH complexes (Figure 2). The initial attachment of virions to the target cells is mediated by HCMV gM/gN complex, which binds to cell surface heparan sulfate glycosaminoglycans (Kari & Gehrz, 1992). HCMV gB is a trimer and considered to be the most abundant viral glycoprotein in the virion envelope, which works together in concert with gH/gL as a core fusion machinery, the attachment of HCMV virions is followed by the interaction of gH/gL complexes with specific cellular receptors, mediating viral entry (Nguyen & Kamil, 2018).

1.3.1 HCMV gH/gL complexes

HCMV can infect nearly all organs and many different cell types *in vivo* (Bissinger et al., 2002). In culture, HCMV can infect predominantly primary cells such as fibroblasts, epithelial cells, endothelial cells, hepatocytes, macrophages (MΦ), dendritic cells, neurons and trophoblasts (Adler & Sinzger, 2009). The broad cell tropism of HCMV is attributed to two glycoprotein complexes of HCMV, the trimeric gH/gL/gO complex (TC) and the pentameric gH/gL/pUL(128,130,131A) complex (PC) (Heldwein & Krummenacher, 2008; Nguyen & Kamil, 2018).

1.3.1.1 gH/gL/gO

A recent study has determined the structure of trimeric complex using cryogenic electron microscopy and confirmed that the three subunit gH, gL and gO are arranged in a boot-like structure, and the architecture structure of the trimeric complex is similar to the pentameric complex, in terms of length and shape (Kschonsak et al., 2021). It has been proposed that UL128/UL130/UL131A and gO bind to the same position on gH/gL and form a disulfide bond with gL-Cys144 (Ciferri et al., 2015). The gH/gL/gO complex is required for the recognition of the platelet-derived growth factor-α (PDGFR-α) as an entry receptor in fibroblasts (Kabanova et al., 2016; Wu et al., 2017; Stegmann et al., 2017). Furthermore, the infection of all cell types are enhanced by the trimeric gH/gL/gO complex (Wille et al., 2010; Zhou et al., 2015). The gH/gL/gO-PDGFR-α interaction promotes entry of free virus into fibroblasts. Moreover, the gH/gL/gO complex could enhance infection of epithelial and endothelial cells, independent of PDGFR-α receptor (Kabanova et al., 2016; Wu et al., 2017).

HCMV mutants with low levels of gH/gL/gO in their envelopes, or lacking gO have been shown a distinct phenotype, they were attenuated for entry into all tested cell types, including macrophages, fibroblasts, epithelial cells, and endothelial cell (Nguyen & Kamil, 2018). Infection with HCMV mutants lacking gO, results in a cell-associated spread pattern in cell cultures and production of virus particles with reducing titers (<1000) than the wildtype (Wille et al., 2010; Li & Kamil, 2016).

1.3.1.2 gH/gL/pUL(128,130,131A)

The gH/gL/pUL(128,130,131A) pentameric complex is indispensable for viral entry into epithelial, endothelial, dendritic cells and leukocytes (Hahn et al., 2004; Gerna et al., 2005; Chandramouli et al., 2017; Nguyen & Kamil, 2018). Interestingly, the UL128 protein in PC complex is distinguished with its chemokine activity and acts as a CC chemokine, attracting monocytes (Zheng et al., 2012; Frascaroli et al., 2006). The gH/gL/pUL(128,130,131A) complex uses Neuropilin-2 as a cell entry receptor (Martinez-Martin et al., 2018; Nguyen & Kamil, 2018). Moreover, the olfactory receptor family member OR14I1 has been recently discovered as an additional cellular receptor for the pentameric complex, which mediates HCMV infection of epithelial cells (Xiaofei et al., 2019).

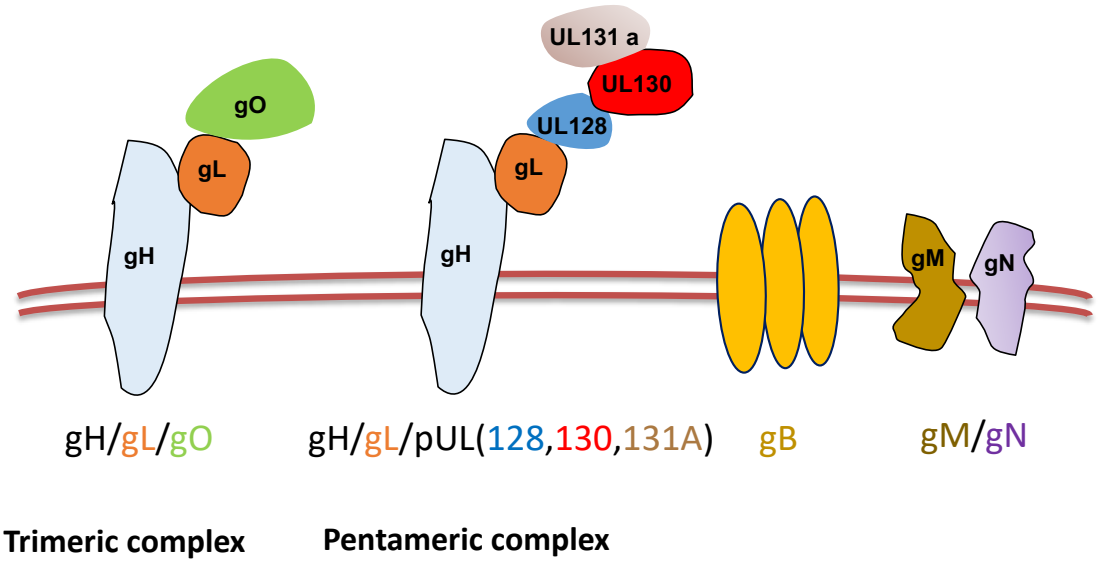

Figure 2: Schematic presentation of HCMV envelope glycoproteins.

1.4 Anti-HCMV immune responses

1.4.1 Innate immune response

HCMV can trigger a powerful innate immune response, which provides an antiviral state and protects the infected and surrounding cells. Once the virus enters the cells, the innate immune response is initiated and HCMV can be detected by pattern recognition receptors (PRRs), including Toll-like receptors (TLR) 2, which is expressed on the plasma membrane and acts as a sensor of HCMV envelope glycoproteins B (gB) and glycoprotein H (gH). Recognition of gB and gH leads to activation of the NF-κB pathway, which in turn induces the production of inflammatory cytokines such as IL-6, IL-12, and IFN-β (Boehme et al., 2006; Compton et al., 2003). NK (natural killer) cells are classical innate lymphocytes, which support the innate arm of immune system for controlling viral infection. NK cells can lyse HCMV-infected cells and produce antiviral cytokines including IFN-γ and TNF-α (Magri et al., 2011; Fauriat et al., 2010; Wu et al., 2013). The adaptive immune response is highly affected by NK cells, therefore NK modulation by HCMV can have a significant impact on the antiviral host immune response (Goodier et al., 2018).

1.4.2 Antibody response

Antibodies against HCMV are shortly produced after primary infection (Nielsen et al., 1988). The majority of the antibodies target envelope glycoproteins like gB (Britt et al., 1990; Marshall et al., 1992), or gH (Fouts et al., 2012; Wussow et al., 2017). Interestingly, antibodies produced against the pentameric complex were shown to be highly neutralizing *in vitro* (Wen et al., 2014; Macagno et al., 2010), although they can only neutralize infection of specific cells like epithelial, endothelial and myeloid cells (Fouts et al., 2012). The role of neutralizing antibodies in protection against congenital HCMV infection is controversial. An early development of antibodies against the PC has been correlated with better protection from fetal transmission and congenital diseases, suggesting that PC antibodies may protect from intrauterine infection (Lilleri et al., 2013). The existence of maternal antibodies to HCMV in seropositive mothers reduces the risk of intrauterine HCMV infection (Fowler et al., 1992). Furthermore, administration of high-titer CMV hyperimmunoglobulin has been shown to decrease both the rate and severity of the disabilities caused by CMV after a primary maternal infection in the first half of pregnancy (Nigro & Adler, 2013).

A recent study has shown that monoclonal antibodies against the pentameric complex could reduce the spread of HCMV in developing placentas (Tabata et al., 2019; Sandonís et al., 2020).

Yet, a double-blind study has been reported that administration of hyperimmunoglobulin was not efficient in preventing congenital infection (Revello et al., 2014). Furthermore, another recent study has reported that the trimer- and pentamer-specific neutralizing antibodies do not provide protection against transmission of HCMV infection from mothers to fetus during nonprimary infection (Vanarsdall et al., 2019; Sandonís et al., 2020) .

1.4.3 T cell response

T cells play a crucial role in protection from intracellular pathogens like viruses. One of the unique features of HCMV is its ability to induce strong $CD8^+$ and $CD4^+$ T cell responses that comprise 10-20% of all circulating memory T cells in CMV-positive individuals (Sylwester et al., 2005). After primary infection, antigen specific $CD8^+$ T cells encounter antigen, proliferate and differentiate into effector T cells, which kill infected cells through perforin and granzyme production, and secret cytokines like IFN-γ and TNF-α to eradicate the infection. Whereas in most viral infections the effector $CD8^+$ T cells enter the memory phase and contract over time (Kaech et al., 2003; Sarkar et al., 2008), in HCMV infection, specific anti-HCMV $CD8^+$ T cell responses do not contract in the memory phase and are maintained at a high frequency (Figure 3), with a distinct phenotype and functional profile. This specific $CD8^+$ T cell behavior has been termed “memory inflation” and is considered to be one of the hallmarks of HCMV infection (Karrer et al., 2003).

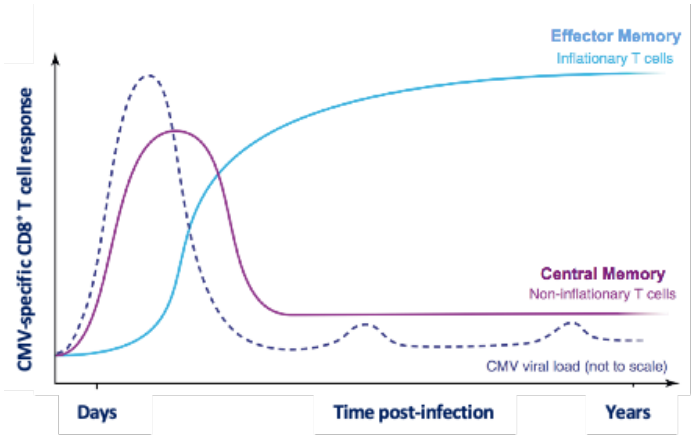

Figure 3: **Development of CMV-specific memory T cell populations**, modified from (O’Hara et al., 2012).

HCMV-specific T cells are typically defined as effector memory T cells (T_{EM}) cells, as they lack expression of lymph node-homing markers CD62L and CCR7. Furthermore, HCMV-specific T cells are characterized by expression of T cell maturation markers, including the expression of effector molecules such as perforin and granzyme B, downregulation of the co-receptors CD27 and CD28, and upregulation of the expression of CD57 and killer cell lectin-like receptor subfamily G member 1 (KLRG1) (Appay et al., 2002; Klenerman & Oxenius, 2016). High frequencies of HCMV-specific T cells are found in blood and tissues like the liver and lungs in HCMV infected individuals (Ward et al., 2004; Akulian et al., 2013).

Additionally, HCMV-specific $CD8^+$ T cells show no evidence of T cell exhaustion, as they maintain their function including cytotoxicity and production of antiviral cytokines like IFN-γ and TNF-α (van Stijn et al., 2008; Young & Uhrberg, 2002). IFN-γ is a proinflammatory cytokine. Besides its antiviral activity, IFN-γ plays a crucial role in activation and differentiation of immune cells, including macrophages, NK cells, and T cells (Delannoy et al., 1999; Cheeran et al., 2000; Sainz et al., 2005).

1.4.4 HCMV immunomodulatory genes

The HCMV genome exhibits more than 751 translated open reading frames (ORFs) (Patro, 2019; Ye et al., 2020). Many viral genes are dedicated to immune modulation and evasion, and many of these genes have been identified in HCMV (Miller-Kittrell & Sparer, 2009; Patro, 2019). The evasion mechanisms include downregulation of major histocompatibility complex (MHC) class I molecules, which leads to a downregulation of HCMV-directed $CD8^+$ T cell responses (Patro, 2019). HCMV encodes for US2, US11, US6, U3, US2 and US3 that downregulate the expression of MHC I (Noriega & Tortorella, 2009). The HCMV tegument protein pp65 (UL183) has been shown to be involved in blocking interferon-alpha activity (Browne & Shenk, 2003). For overcoming antiviral NK responses, HCMV UL18 and UL40 proteins which show sequence homologies to MHC class I on the surface of the infected cells, repress NK activity (Prod'homme et al., 2012). Additionally, HCMV encodes for RL11 and UL119, which show a Fcγ-binding capacity, therefore they block host FcγR activation and prevent subsequent antibody-dependent cellular cytotoxicity (ADCC) (Lilley et al., 2001; Sprague et al., 2008; Ndjamen et al., 2016). The viral protein US28 exhibits a high sequence homology to the cellular receptor CCR1, which enables it to bind to a number of CC1 chemokines like CCL2, CCL3, CCL4 and CCL5 (Gao & Murphy, 1994;

Kuhn et al., 1995). Additionally, US128 binds with high affinity to the CX3C chemokine, CX3CL1 (fractalkine) (Kledal et al., 1998). Besides chemokine receptors homologues, HCMV also codes for chemokine homologues.

1.5 Viral chemokines

Herpesvirus immune evasion factors are structurally and functionally similar to host immune regulatory proteins. One interesting group are viral chemokines. For subversion of the host's chemokine network, herpesviruses produce viral chemokines, chemokine receptors as well as chemokine-binding proteins (Alcami & Lira, 2010; Pontejo et al., 2018). Chemokines are small cytokines (7–12 kDa) with chemo-attractive activity. They are secreted from their producer cells to attract immune cells, which carry the respective chemokine receptors on their surface. This leads to a chemotactic gradient that initiates cell migration into tissue. Therefore, chemokines influence the migration and effector functions of immune cells (Alcami, 2003). Structurally, chemokines can be classified into subgroups based on the position of highly conserved N-terminal cysteine residues connected by disulfide bridges. The 4 classes are called CXC, CC, C and CX3C chemokines (Hughes & Nibbs, 2018). Viral chemokines very likely affect the host immune response including the cytokine network, through their antagonistic or synergistic effects on host chemokine receptors. Therefore, they may be novel therapeutic targets to combat herpesviruses (Pontejo & Murphy, 2017a). HCMV encodes for UL146 and UL147 with homology to CXC chemokines, also called vCXCL1 and vCXCL2, respectively. *In vitro* studies of recombinant vCXC-1 confirmed its activity as a fully functional chemokine, which was able to induce calcium mobilization, degranulation of neutrophils and chemotaxis (Penfold et al., 1999). Additionally, vCXCL1 has been reported to act as agonist not only for CXCR1 but also for CXCR2 (Lüttichau, 2010). Furthermore, the deletion of UL146-UL147 in an HCMV mutant, results in an impaired neutrophile infection, suggesting that these proteins contribute to the interaction between HCMV and neutrophils (Hahn et al., 2004; Miller-Kittrell & Sparer, 2009).

1.5.1 The UL128 chemokine

The UL128 component of the the pentameric complex is also a viral chemokine. The pUL128 protein is a small soluble protein without membrane anchor, but it has a signal peptide (Hahn et al., 2004).

pUL128 has 4 conserved cysteine motifs near its N-terminus, spaced like in CC chemokines, as shown in Figure 4. Homologs also exist in CMV from other species like MCMV, rat CMV (RCMV), simian CMV (SCMV) and chimpanzee CMV (CCMV) (Akter et al., 2003). Recombinant pUL128 has been shown to attract peripheral blood mononuclear cells (PBMC) *in vitro* and to affect macrophage (MΦ) activity (Hui-hui et al., 2013; Frascaroli et al., 2006). Additionally, pUL128 has been shown to antagonize CCL5 and CCL2 *in vitro* and downregulate CCR1, CCR2 and CCR5, thus blocking primary human monocyte chemotaxis (Straschewski et al., 2011). Investigating the crystal structure of the pentameric complex has revealed that pUL128 could correctly fold as an active chemokine within the complex (Chandramouli et al., 2017).

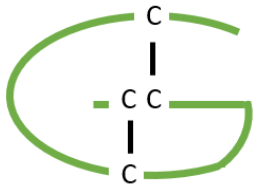

Figure 4: Schematic structure of a CC chemokine with disulphide bridges between cysteine residues, (adapted from de Munnik et al., 2015).

1.6 Cytomegaloviruses as vaccine vectors for infectious diseases

Most conventional vaccines induce neutralizing antibodies. However, they are not efficient in protection from chronic infections, in particular, from pathogens with high variability and pathogens which are less amenable to conventional vaccination strategies. Therefore, there is a need to develop novel vaccines, which induce strong and long-lasting cellular immune responses. There are many recombinant virus vectors that have been studied including adenoviruses, adeno-associated viruses, vesicular stomatitis virus, lentivirus and vaccina virus (Rollier et al., 2011; Méndez et al., 2019). CMV exhibit unique features, which make them promising and attractive vaccine vectors. CMV induce a potent and long-lasting $CD8^+$ T lymphocyte response that comprises on average 10% of the memory $CD8^+$ T lymphocytes in infected hosts like humans and mice (Sylwester et al., 2005; Karrer et al., 2003). Moreover, CMV is known to be able to superinfect hosts with a history of prior infection (Boppana et al., 2001) by using immune evasion strategies that let the virus escape from recognition by primed T-cells (Hansen et al., 2010). CMV vectors have been shown to provide protective immunity in vaccinated animals (Rhesus macaques and mice) with

documented prior exposure to CMV infection (Hansen et al., 2018; Beyranvand Nejad et al., 2019). Moreover, the large genome of CMV allows insertion of multiple vaccine antigens because more than 50 kb can be excised from HCMV without any effect on virus replication (Jarvis et al., 2013; Méndez et al., 2019).

Immunogenicity and safety are the two arms of vaccine development. Therefore, attenuated CMV vaccine vectors, which cannot cross the placental barrier or cause serious diseases, have to be used. Interestingly, infection of mice with attenuated-single cycle MCMV did not diminish the development of $CD8^+$ T cell memory inflation, confirming that only the establishment of latent infection in a certain number of cells is sufficient to induce memory inflation without the need of production of infectious virus (Méndez et al., 2019; Snyder et al., 2011). In addition, live-attenuated RhCMV vaccine vector was generated by deletion of specific gene encodes the pp71 tegument protein, which consequently inhibit lytic gene expression and thus viral genome replication (Hansen et al., 2019). Importantly, this attenuated vector expressing simian immunodeficiency virus (SIV) proteins still maintains its immunogenicity and could control SIV infection in 59% of vaccinated rhesus macaques (Hansen et al., 2019). Currently, HCMV-based vaccine vectors are in clinical trial I (Murray et al., 2017).

1.6.1 MCMV vaccine vectors

MCMV has repeatedly used as a vector in *in vivo* vaccination studies. An MCMV vector expressing a $CD8^+$ T cell epitope of the nucleoprotein of *Zaire ebolavirus (*ZEBOV), has been demonstrated to be efficient in inducing a durable $CD8^+$ T cell response against a lethal challenge with ZEBOV in a mouse- adapted ZEBOV variant (Tsuda et al., 2011). A recombinant MCMV vector expressing an MHC-I restricted epitope from influenza A virus (IAV) H1N1 was used for intranasal immunization of mice. Immunization resulted in induction of IAV-specific tissue-resident memory $CD8^+$ T ($CD8T_{RM}$) cells in the lungs, providing mucosal immunity at the sites of entry (Zheng et al., 2019). MCMV-based vaccines have also been used to immunize against *Mycobacterium tuberculosis*. Mice infected with recombinant murine CMV (MCMV) expressing *Mycobacterium tuberculosis* Ag 85A, showed a reduced mycobacterial load after challenge with *Mycobacterium tuberculosis* (Beverley et al., 2014). In another study, MCMV has been used as a vector expressing non-toxic tetanus toxin fragment C, in order to find an alternative for vaccination using inactivated tetanus toxin. The MCMV vector could successfully induce a long lasting anti-tetanus antibody

response after only one round of vaccination (Tierney et al., 2012). Additionally, an MCMV vector expressing the E7 epitope of human papilloma virus could elicit vaccine-induced $CD8^+$ T cell responses of more than 0.3% of the total circulating $CD8^+$ T cell population, and consequently protected the mice from lethal challenge of Human papillomavirus 16 (HPV 16) (Nejad et al., 2019). Beyond protection from viruses and bacteria, MCMV-based vaccine vectors have also been investigated as vaccine vectors to protect from cancer. One study has been conducted using the aggressive B16 lung metastatic melanoma model. Mice immunized with MCMV-expressing ovalbumin (OVA), showed a reduction of OVA-expressing B16 melanoma (Qiu et al., 2015).

1.6.2 Rhesus CMV vaccine vectors

RhCMV-based vaccine vectors expressing simian immunodeficiency virus (SIV) proteins have been shown to elicit a strong, tissue-resident effector memory T cell (T_{EM}) response, which translated into a 50% protection from SIV infection after mucosal SIV challenge (Hansen et al., 2009; Hansen et al., 2013). The protection of macaques using RhCMV-based vaccine was highly encouraging and raised the interest in using HCMV as a vector for the development of therapeutic or prophylactic vaccines against HIV (Liu et al., 2019). Interestingly, it was reported that RhCMV vaccine candidates elicited promiscuous MHC class I and class II-restricted $CD8^+$ T cell responses (Hansen et al., 2013), and not conventional anti-SIV responses. This was correlated with a particular RhCMV strain. RhCMV strain 68-1 is known as a fibroblast-adapted vector with a mutation in a region Rh157.4-6, which encodes proteins that are functionally homologous to HCMV pUL(128,130,131A) (Hansen et al., 2013; Lilja & Shenk, 2008; Malouli et al., 2012). RhCMV strain 68-1 with an additional deletion of the Rh189 gene (HCMV US11 homolog), which is responsible for downregulation of MHC class I in HCMV-infected cells was also tested. Vaccination of macaques with this vector induced both a canonical MHC I-restricted $CD8^+$ T cells response and an unconventional $CD8^+$ T cell response (Hansen et al., 2013; Früh & Picker, 2017). Taken together, the design of the CMV vector may be a useful tool to redirect and program for a particular pattern of $CD8^+$ T cell epitope recognition, which might give CMV-based vaccines an advantage over other vaccine vectors (Früh & Picker, 2017).

1.7 Mouse Cytomegalovirus as a model for HCMV

Due to its high species-specificity, host-pathogen interaction of HCMV can only be studied in animal models. Chimpanzee (Davison et al., 2003), rhesus macaque (Tarantal et al., 1998), guinea pig (for congenital infection) (Schleiss, 2002), rat (Suzanne et al , 2006; Kern et al , 2006), and mouse CMV infection of their respective hosts have been used (Fodil-Cornu et al., 2008; Reddehase & Lemmermann, 2018). All these animal models are restricted to their specific CMV viruses (Mocarski et al., 2013). Infection of mice with MCMV is the most frequently used model for studying CMV infection and the antiviral host immune response. The murine model of MCMV infection is considered highly valuable, as it shares great similarity to the HCMV infection of human, in terms of gene expression patterns or pathogenicity (except congenital diseases) (Simon et al., 2006). MCMV is able to infect the same organs as HCMV and shows the same cell-type tropism (Reddehase & Lemmermann, 2018). Moreover, the transmission of MCMV infection is similar to HCMV, as it occurs via shedding of bodily fluids like breast milk and saliva (Wu et al., 2011). Additionally, using this model, the immune evasion of HCMV was correctly predicted, and an adoptive immune cell transfer studied in mice could successfully be transferred to clinical immunotherapy of HCMV infection (Watanabe et al., 1992; Reddehase & Lemmermann, 2018).

Based on the susceptibility to MCMV infection, different mouse strains are more (BALB/c mice) or less (C57BL/6 mice) susceptible to infection, depending on their ability to mount an effective antiviral NK response (Krmpotic et al., 2003). The activation of NK cells after MCMV infection requires the Ly49H receptor recognizing the MCMV protein m157 (Arase et al., 2002; Smith et al., 2002). This activation of NK cells leads to an early control of viral replication (Bubić et al., 2004; Fodil-Cornu et al., 2008). This interaction between Ly49H receptor and m157 exists in C57BL/6 mice. In contrast, BALB/c mice lack the Ly49H receptor and therefore are unable to activate an effective NK cell response to MCMV. As a result, BALB/c mice develop viremia rapidly after infection with MCMV in many organs (e.g. liver, lungs, spleen and kidney), For this reason, BALB/c mice are often used for testing the efficiency of antiviral agents and studying CMV disease (Reddehase et al., 2002; Schleiss, 2013).

1.8 MCMV gH/gL complexes

Like HCMV, MCMV forms two distinct glycoprotein complexes that determine the cell tropism, gH/gL/gO (Scrivano et al., 2010) and gH/gL/MCK2 (Wagner et al., 2013) with unknown host cell target receptors. The gH/gL/gO complex of MCMV has been shown to be indispensable for infection of first target cells (Lemmermann et al., 2015). The following spread of virus within the tissues and infection of salivary glands, the main site of host-host transmission, are mediated by both the gH/gL/gO and the gH/gL/MCK2 complex (Lemmermann et al., 2015).

The trimeric gH/gL/MCK2 complex is functional homolog of the pentameric gH/gL/pUL(128,130,131A) of HCMV (Wagner et al., 2013). One hallmark of this complex is that it promotes infection of macrophages *in vitro* and *in vivo* (Wagner et al, 2013; Stahl et al., 2015). Besides binding to gH/gL, MCK2 works as CC chemokine (Noda et al., 2006; Wagner et al, 2013) (Figure 5).

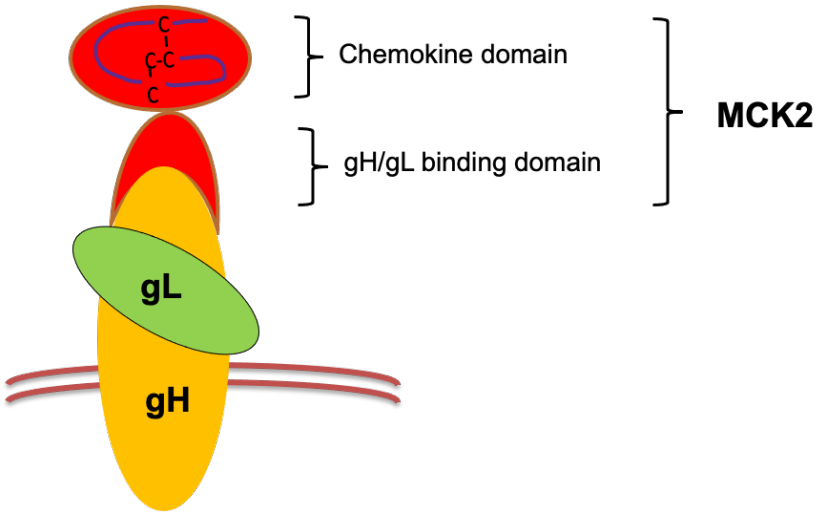

Figure 5: Schematic presentation of the gH/gL/MCK2 complex.

1.9 The murine CMV chemokine 2 (MCK2)

1.9.1 The MCK2 protein

The m131 ORF of MCMV codes for a protein of 81 amino acids. Because of sequence similarities between this gene product and other CC chemokines, this protein was given the name murine CMV chemokine 1 (MCK1) (Vieira et al., 1994; MacDonald et al., 1997). Two years later, a second gene product, called MCK2 was identified with an additional 199 amino acids and characterized as the product of RNA splicing between MCK1 and a downstream ORF, m129 (MacDonald et al., 1999; Fleming et al., 1999), as illustrated in Figure 6.

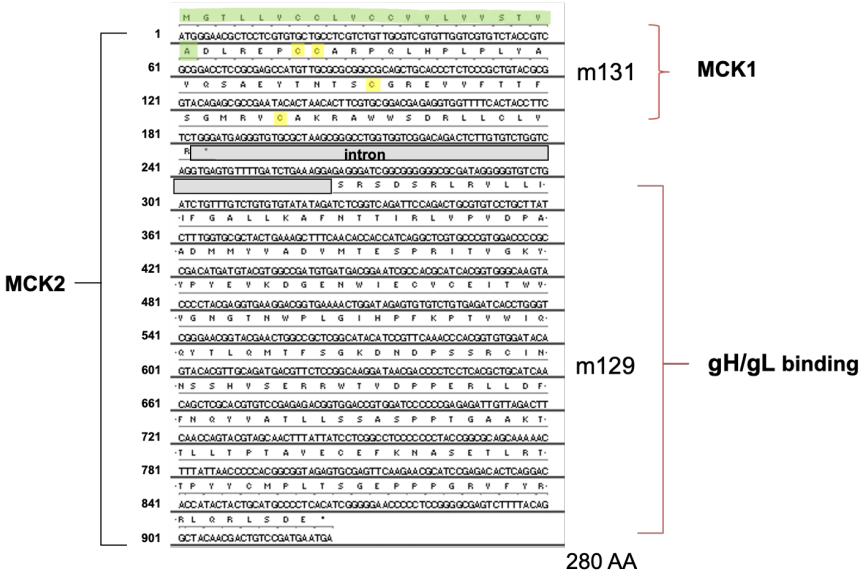

Figure 6: Sequence of MCK2, indicating ORF m131 and ORF m129. The putative signal peptide is highlighted in green, and conserved cysteine residues characteristic of CC chemokines are highlighted in yellow.

The specific receptor for MCK2 has not yet been identified. The first biochemical analysis of recombinant MCK2 showed that MCK2 shows two features of chemokines, (Miller-Kittrell & Sparer, 2009) glycosaminoglycans (GAGs)-binding and the ability to oligomerize on GAGs (Pontejo & Murphy, 2017b).

1.9.2 Chemokine activity of MCK2

First *in vitro* studies showed that MCK1 induced mobilization of Ca^{2+} in peritoneal exudates cells from mice infected with MCMV, suggesting that MCK1 may increase recruitment of the cells to the site of infection (Saederup et al., 1999; Miller-Kittrell & Sparer, 2009).

It has been reported that also MCK2 exhibits chemokine activities, as it enhances the migration of PBMCs to the site of inflammation (Saederup et al., 1999; Saederup et al., 2001). Infection of mice with MCMV-expressing MCK2, promotes recruitment of myelomonocytic leukocytes with an immature phenotype, and recombinant MCK2 proteins have the same action on this population of the cells even in the absence of virus infection (Noda et al., 2006). Remarkably, MCK2-positive MCMV recruited more monocytes into lungs than MCK2-negative MCMV at day 2 post-infection (Farrell, et al., 2016).

1.9.3 The role of MCK2 in virus dissemination

Mice infected with MCMV lacking MCK2 showed lower viral titers in salivary glands than mice infected with MCK2 positive MCMV. As salivary glands are primary sites of virus spread and horizontal virus shedding, this was a first evidence that MCK2 may also play a role in viral spread and dissemination (Fleming et al., 1999; Saederup et al., 2001; Jordan et al., 2011). During acute MCMV infection, infected dendritic cells work to spread infection (Farrell, et al., 2019a). MCK2 has been shown to promote infection of macrophages *in vitro* and *in vivo* (Wagner et al., 2013; Stahl et al., 2015). Furthermore, MCK2 mediates recruitment of CX3CR1^{hi} patrolling monocytes to become infected and then act as vehicles for dissemination of MCMV infection, and a source for seeding a persistent reservoir of infection (Daley-Bauer et al., 2014). It has been reported that there is no difference between the numbers of infected leukocytes in blood infected with wt MCMV and those infected with MCK2-negative MCMV at day 4 and 5 p.i (Farrell et al., 2016; Farrell et al., 2019a). In line with that, MCK2 has been proposed to enhance proficient MCMV dissemination to salivary glands, but only late after the initial seeding of infection (Farrell et al., 2019a).

1.9.4 Immunomodulatory activities of MCK2

An MCMV infection leads to a strong inflammation at the site of infection, which is mediated by the chemokine activity of MCK2, as it enhances the migration of PBMCs to the site of inflammation (Saederup et al., 1999; Daley-Bauer et al., 2012). MCK2 also plays a role at a very early stage of viral infection (Wikstrom et al., 2013). It has been shown that MCK2 induces the activation of plasmacytoid dendritic cells, and accordingly enhances the production of IFN-α in mice infected with wt MCMV (intact MCK2) at 40 hours post infection, in comparison with low IFN-α production in mice

infected with MCMV lacking MCK2 (Wikstrom et al., 2013). The influence of MCK2 on the adaptive immune response of the host has also been investigated. MCK2 cooperates with host CCR2-dependent recruitment of inflammatory monocytes and impairs early $CD8^+$ T cell response, and thereby delays viral clearance from organs (Daley-Bauer et al., 2012), whereas MCMV lacking MCK2 was cleared from organs more rapidly (Fleming et al., 1999; Wikstrom et al., 2013; Daley-Bauer et al., 2012).

1.10 Aim of the thesis

MCK2 has a dual function: It is a functional chemokine attracting monocytes and additionally it is part of a gH/gL/MCK2 envelope glycoprotein complex. It is not known whether the effect of MCK2 on immune modulation and viral dissemination is attributed to the chemokine activity of MCK2 or to its entry function as a part of the gH/gL/MCK2 entry complex or both. In order to understand and elucidate the role of MCK2, MCK2 mutant viruses have been cloned and used *in vitro* and *in vivo*. All *in vivo* studies on mice have nearly exclusively used MCK2 mutant viruses with a complete deletion of MCK2 (Saederup et al., 1999; Saederup et al., 2001; Stahl et al., 2015; Wikstrom et al., 2013; Daley-Bauer et al., 2014; Daley-Bauer et al., 2012; Farrell et al. 2019a; Farrell et al., 2016). Therefore, it is necessary to clone MCK2 mutant viruses, which are lacking only the chemokine function of MCK2 or the gH/gL complex function. This will enable us to discriminate between the contribution of each of MCK2 functions to the above-described phenotypes.

Objectives of this thesis were:

1- To investigate the role of the MCMV MCK2 chemokine and the role of the gH/gL/MCK2 entry complex in mediating early antiviral immune responses and viral dissemination.

2- To investigate the role of MCK2 in vaccination studies using MCMV vaccine vectors carrying different MCK2 mutations.

2. Materials

2.1 Devices

Instrument	Manufacturer
BD FACSCalibur™	BD Biosciences (Heidelberg, Germany)
BDK laminar flow system	Weiss Pharmatechnik GmbH (Sonnenbühl, Germany)
Beckman Optima L-80 XP Ultracentrifuge	Beckmann Coulter (Krefeld, Germany)
Bio-Rad PowerPAC 200 Power supply	Bio-Rad Laboratories (Hercules, USA)
Biosciences vacuubrand vacuum pump unit BVC21	Integra Biosciences (Hudson, USA)
Centrifuge Avanti J-26 XPI	Beckmann Coulter (Krefeld, Germany)
Chemiluminescence & Fluorescence imager Fusion FX7	Vilber Lourmat (Eberhardzell, Germany)
Counting Chamber 0,1 mm	Paul Marienfeld GmbH (Lauda-Königshofen, Germany)
CLARIOstar ® microplate reader	BMG Labtech (Ortenberg, Germany)
E-C Apparatus Minicell EC370M horizontal	Surplus Solutions (Woonsocket, Germany)
Electrophoresis Power Supply RCT basic	IKA® Werke (Staufen, Germany)
Eppendorf BioPhotometer 6131	Eppendorf (Wesseling-Berzdorf, Germany)
Eppendorf centrifuge 5424R	Thermo Fisher Scientific (Waltham, USA)
Eppendorf ThermoMixer C	Eppendorf (Wesseling-Berzdorf, Germany)
Eppi centrifuge mini	Carl Roth (Karsruhe, Germany)
FASTPREP® - 24	MP Biomedicals (USA)
Fluorescence microscope Olympus IX71	Olympus (Hamburg, Germany)
Gene Pulser Xcell™ Electroporation Systems	Bio-Rad Laboratories (Hercules, USA)
Gilson Pipetman®	Gilson (Middelton, USA)
HE99X Max agarose electrophoresis unit	GE Gealthcare Life Sciences (Chalfont St Giles, UK)
Heracell 150i Incubator	Thermo Fisher Scientific (Waltham, USA)
IKA Minishaker MS1	IKA (Staufen im Breisgau, Germany)
Incubator Memmert Model 200	Memmert (Schwabach, Germany)
Integra Biosciences™ Vacusafe™ Comfort Aspiration system	Integra Biosciences (Hudson, USA)
Integra Pipetboy 2	Integra Biosciences (Zizers, Switzerland)
Kern Balance 470	Kern & Sohn GmbH (Albstadt, Germany)
Kern Balance 510	Kern & Sohn GmbH (Albstadt, Germany)
Microliter Syringe	Carl Roth (Karsruhe, Germany)
Mini-Trans-Blot® cell	Bio-Rad Laboratories (Hercules, USA)

Mini-Protean® Tetra cell	Bio-Rad Laboratories (Hercules, USA)
Molecular Imager® Gel DocTM XR system	Bio-Rad Laboratories (Hercules, USA)
Multifuge 3 S-R centrifuge	Heraeus Group (Hanau, Germany)
Microwave Inverter	Sharp (Osaka, Japan)
NanoPhotometer® P330	Implen GmbH (Munich, Germany)
New Brunswick™Galaxy®170R CO_2 Incubator	Eppendorf (Wesseling-Berzdorf, Germany)
Olympus U-LH100HG Fluorescence light source	Olympus (Hamburg, Germany)
Olympus U-RFL-T Power Supply	Olympus (Hamburg, Germany)
pH meter 430	Corning (New York, USA)
Pharmacia Biotech EPS 600	Pharmacia Biotech (Uppsala, Sweden)
QuantStudio™ 3 Real-Time PCR System	Thermo Fisher Scientific (Waltham, USA)
Sonifier W-250	G. Heinemann Ultraschall- und Labortechnik (Schwäbisch Gmünd, Germany)
Stuart scientific roller mixer	Merck (Darmstadt, Germany)
T Gradient Thermocycler	Analytik Jena (Jena, Germany)
UV-Transilluminator UST-20-8RA	Biostep (Burkhardtsdorf, Germany)
VersaMax Tunable Microplate Reader	Molecular Devices (San José, USA)
Water bath Model 1002	Gesellschaft für Labortechnik (Burgwedel, Germany)
Zeiss Axiovert 40S Tissue culture microscope	Carl Zeiss Microscopy (Jena, Germany)

2.2 Consumables

Consumable	Manufacturer
Aluminium foil	Roth (Karlsruhe, Germany)
Cell scraper	Sarstedt (Nürnbrecht, Germany)
Cell strainer	Corning (New York, USA)
Combitips (10 ml, 5 ml)	Eppendorf (Wesseling-Berzdorf, Germany)
CryoPure tubes (1.6 ml)	Sarstedt (Nürnbrecht, Germany)
Gene Pulser® Cuvette (0.2 cm electrode)	Bio-Rad (Hercules, Germany)
Falcon™ Standard cell culture dishes	Corning (New York, USA)
Filter (0.45 µm, 0.22 µm)	Sartorius AG (Göttingen, Germany)
Filter pipet tips	STARLAB International GmbH (Hamburg, Germany)
Fine-Ject 26G X 1/ 2 cannulas	Henke-Sass Wolf GmbH (Tuttlingen, Germany)
HybondTM-ECL Nitrocellulose membranes	Amersham Biosciences (Freiburg, Germany)
Inoculation loop	Sarstedt (Nürnbrecht, Germany)
Millicell cell culture hanging inserts	Merck (Darmstadt, Germany)
No-filter pipet tips	STARLAB International GmbH (Hamburg, Germany)
PCR tubes	Biozym (Hessisches Oldendorf, Germany)
Petri dishes (10 cm)	Sarstedt (Nürnbrecht, Germany)
Photometer cuvettes	Brand (Wertheim, Germany)
SafeSeal reaction tubes (1.5 ml, 2 ml)	Sarstedt (Nürnbrecht, Germany)
Screw cap micro tubes	Sarstedt (Nürnbrecht, Germany)
Serological pipets (2 ml, 5 ml, 10 ml, 25 ml)	Sarstedt (Nürnbrecht, Germany)
Syringes (2 ml, 20 ml)	B.Braun (Melsungen, Germany)
Single use syringe (1ml)	B.Braun (Melsungen, Germany)
Ultracentrifugation tubes	Beckman Coulter GmbH (Krefeld, Germany)
TC plate (6-well, 24-well, 48-well, 96-well)	Sarstedt (Nürnbrecht, Germany)
Tubes (5, 15 ml, 50 ml)	Sarstedt (Nürnbrecht, Germany)
TC flask T75	Sarstedt (Nürnbrecht, Germany)
Whatman paper	Machery&Nagel (Düren, Germany)

2.3 Reagents

Chemical/Buffer	Manufacturer
1kb DNA Ladder	New England Biolabs (Ipswich,USA)
1-Thioglycerol	Sigma-Aldrich (Deisenhofen, Germany)
Ammonium chloride	Sigma-Aldrich (Deisenhofen, Germany)
Ammonium persulfate	Sigma-Aldrich (Deisenhofen, Germany)
Ampicillin	Sigma-Aldrich (Deisenhofen, Germany)
Arabinose	Sigma-Aldrich (Deisenhofen, Germany)
Bacillol AF	Paul Hartmann AG, Heidenheim, Germany
Bacto-Agar	BD Bioscience (Heidelberg, Germany)
Bacto™Yeast extract	BD Bioscience (Heidelberg, Germany)
Boric acid	Roth (Karlsruhe, Germany)
Bovine serum albumin (BSA)	BioLabs (Frankfurt am Main, Germany)
Brefeldin A Solution	BioLegend (San Diego, USA)
Bromophenol blue	Sigma-Aldrich (Deisenhofen, Germany)
Calcein-AM in DMSO	BioLegend (San Diego, USA)
Carboxymethyl cellulose sodium salt	Sigma-Aldrich (Deisenhofen, Germany)
Cell Stimulation Cocktail, PMA/Ionomycin	Biolegend (San Diego, USA)
Chloramphenicol	Sigma-Aldrich (Deisenhofen, Germany)
Cristal violet	Sigma-Aldrich (Deisenhofen, Germany)
Dulbecco's Modified Eagle Medium (DMEM)	Life Technologies (Darmstadt, Germany)
dNTPs	New England Biolabs (Ipswich,USA)
EDTA	Sigma-Aldrich (Deisenhofen, Germany)
Ethanol	Roth (Karlsruhe, Germany)
Ethidiumbromide solution	Roth (Karlsruhe, Germany)
FcR Blocking Reagent	MACS Miltenyi Biotec GmbH (Bergisch Gladbach, Germany)
Fetal calf serum (FCS)	PAN Biotech (Aidenbach, Germany)
FuGENE® HD Transfection Reagent	Promega (Mannheim, Germany)
Glycerol	Roth (Karlsruhe, Germany)
Glycin	Roth (Karlsruhe, Germany)
Hoechst 33258, Pentahydrate (Bis-Benzimide)	Thermo Fisher Scientific (Waltham, USA)
Hydrochloric acid	VWR International GmbH (Ismaning, Germany)
Isopropanol	Merk (Darmstadt, Germany)

Kanamycin	Life Technologies (Darmstadt, Germany)
L-Glutamine	Life Technologies (Darmstadt, Germany)
MEM (10x)	Life Technologies (Darmstadt, Germany)
MEM Non-Essential Amino Acid Solution	Life Technologies (Darmstadt, Germany)
Mercaptoethanol	Merck (Darmstadt, Germany)
Methanol	Sigma-Aldrich (Deisenhofen, Germany)
N, N, N', N'-Tetramethylethylendiamin (TEMED)	Roth (Karlsruhe, Germany)
OptiPRO Serum Free Medium	Life Technologies (Darmstadt, Germany)
Orange G	Fluka-Chemika (Buchs, Switzerland)
PageRulerTM Prestained Protein Ladder	Thermo Fisher Scientific (Waltham, USA)
Paraformaldehyde (PFA)	Sigma-Aldrich (Deisenhofen, Germany)
Penicillin-Streptomycin	Life Technologies (Darmstadt, Germany)
Phenol/Chloroform/Isoamyl alcohol	Carl Roth GmbH (Karlsruhe, Germany)
Phosphate buffered saline (PBS)	Life Technologies (Darmstadt, Germany)
Polyethylenimin (PEI)	Sigma-Aldrich (Deisenhofen, Germany)
Ponceau S solution	Sigma-Aldrich (Deisenhofen, Germany)
RPMI medium 1640 (1X)	Life Technologies (Darmstadt, Germany)
Saponin	Sigma-Aldrich (Deisenhofen, Germany)
SeaKem LE Agarose	Biozym Scientific (Hessisch Oldendorf, Germany)
Skim milk powder	Merck (Darmstadt, Germany)
Sodium chloride	Merck (Darmstadt, Germany)
Sodium dodecyl sulfate (SDS)	Sigma-Aldrich (Deisenhofen, Germany)
Sodium hydrogen carbonate	Life Technologies (Darmstadt, Germany)
TRIS	Carl Roth GmbH (Karlsruhe, Germany)
Triton X-100	Sigma-Aldrich (Deisenhofen, Germany)
Trypan Blue	Sigma-Aldrich (Deisenhofen, Germany)
Trypsin/EDTA 0.25%	Life Technologies (Darmstadt, Germany)
Trypton/Pepton from Casein	Carl Roth GmbH (Karlsruhe, Germany)
Tween-20	Sigma-Aldrich (Deisenhofen, Germany)
Gibco® Versene Solution	Life Technologies (Darmstadt,Germany
Glasgow-MEM BHK-21	Life Technologies (Darmstadt, Germany)
Power SYPR Green PCR Master Mix	Applied biosystems (Thermofisher UK)

2.4 Commercial kits

Kit	Manufacturer
QIAquick® gel Extraction kit	Qiagen (Hilden, Germany)
QIAquick® PCR Purification kit	Qiagen (Hilden, Germany)
Macherey-NagelTM NucleoBondTM Xtra Midi	Machery&Nagel (Düren, Germany)
SuperSignal™ West Pico PLUS Chemiluminescent Substrate	Thermo Fisher Scientific (Waltham, USA)
Mouse IFN -γ ELISA MAX ™ Deluxe Sets	BioLegend (San Diego, CA).
Mouse MCP-1 ELISA MAX ™ Deluxe Sets	BioLegend (San Diego, CA).
Verikine mouse interferon alpha ELISA kit	PBL Assay Science (Piscataway, NJ)
DNeasy Blood & Tissue Kits	Qiagen (Hilden, Germany)
Qiagen Plasmid Maxi kit	Qiagen (Hilden, Germany)

2.5 Enzymes for molecular biology

Restriction enzymes and their corresponding reaction buffers were purchased from NEB, Frankfurt am Main, DE.

2.6 Plasmids

Plasmid	Provided by
pEPkan-S	(Tischer et al. 2006)
pDrive_gB_PTHrP	Kindly provided by Prof Dr. Mattias Reddehase (Simon et al., 2005)
pFuse -hIgG1-Fc2	Invivogen (San Diego, USA)
pFuse MCK2	Laura Jochem (Bachelor thesis, 2012)
pFuse CC1 MCK2	Simone Boos (AG Adler)
Rpl8	Kindly provided by Prof. Dr.Heiko Adler (Ruiss et al., 2012)
gB-MHV68	Kindly provided by Prof. Heiko Adler (Ruiss et al., 2012)

2.7 Primers

Primers were synthesized by Metabion (Martinsried, DE).

Primer	Sequence
M74 del532 for	5´- TTT AAA ATA TTT GGC GGT GAT GTT ACT TTT CGG GGT GAT GAG GTC TCT CCA GGA TGA CGA CGA TAA GTA GGG- 3´
M74 del532 rev	5´- AGA GCC GCG ATT AAT GTC CGC TGT ATT CAA CGC GGA GAT CAG CCC TCC CGG GAG AGA CCT CAT CAC CCC GAA AAG TAA CAT CAC CGC CAA ATA TTT TAAA CAA CCA ATT AAC CAA TTC TGA TTAG - 3´
PTHrP for	5´- TGT TGG GAG CAG GTT TGGA - 3´
PTHrP rev	5´- CGT TTC TTC CTC CAC CAT CTG - 3´
M55 gB for	5´- TTG ACA CAC TCG GAC ATC GC - 3´
M55 gB rev	5´- AAT CCG TCC AAC ATC TTG TCG - 3´
rpL8 for	5´- CAT CCC TTT GGA GGT GGTA - 3´
rpL8 rev	5´- CAT CTC TTC GGA TGG TGGA - 3´
MHV68-gBqufor	5´- GGC CCA AAT TCA ATT TGC CT - 3´
MHV68-gBqurev	5´- CCC TGG ACA ACT CCT CAA GC - 3´

2.8 Peptides

Peptide	Sequence	Provided by
Scrambled control for M123/IE1	NFYPTLPHM	IPT Peptide Technologies GmbH (Berlin, Germany)
M123/IE1 MCMV	YPHFMPTNL	IPT Peptide Technologies GmbH (Berlin, Germany)
M45 peptide MCMV	HGIRNASFI	IPT Peptide Technologies GmbH (Berlin, Germany)
ORF6 peptide MHV-68	AGPHNDMEI	IPT Peptide Technologies GmbH (Berlin, Germany)

2.9 Antibodies

Antibody	Host	Source
mouse anti-MCMV ie1, (Croma 101)	Mouse	Kindly provided by Stipan Jonjic (University of Rijeka, Croatia) (Bantug et al., 2008)
Alexa Fluor 488-goat-anti mouse	Goat	Dianova (Hamburg, Germany)
FITC anti-mouse CD8a Antibody, Clone: 53- 6.7	Rat	Biolegend (San Diego, USA)
FITC Rat IgG2a, κ Isotype Ctrl Antibody, Clone: Rat RTK2758	Rat	Biolegend (San Diego, USA)
FITC anti-mouse CD4 Antibody, Clone: GK1.5	Rat	Biolegend (San Diego, USA)
Monoclonal anti-MCK-2 O4 Antibody	Mouse	Kindly provided by Stipan Jonjic (University of Rijeka, Croatia)
Monoclonal anti-human IgG (Fc-specific) Biotin, Clone: HP-6017	Mouse	Sigma Aldrich (St. Louis, USA)
Monoclonal α-HA, Clone: 3F10	Rat	Sigma Aldrich (St. Louis, USA)
Monoclonal mouse anti-gB Antibody (5F12)	Mouse	Astrid Karbach (PhD Dissertation)
Polyclonal anti-human IgG (Fc-specific) POX	Goat	Sigma Aldrich (St. Louis, USA)
Polyclonal α-mouse POX	Goat	Sigma Aldrich (St. Louis, USA)
Polyclonal α-rat POX	Donkey	Dianova (Hamburg, Germany)
PE anti-mouse IFN-γ Antibody; Clone: XMG1.2	Rat	Biolegend (San Diego, USA)
PE Rat IgG1, κ Isotype Ctrl Antibody, Clone: Rat RTK2071	Rat	Biolegend (San Diego, USA)

2.10 Cells and media

2.10.1 Bacteria

Bacterial strain	Genotype	Provided by
E.coli GS1783	DH10B [λc1857 (cro-bioA)<>araC-PBadI-Sce-I] galK^{+} gal 490	Gregory A. Smith (Northwestern University, Chicago, USA)

2.10.2 Eucaryotic cells

Cells	Description	Reference /ATCC No
Primary cells		
MEF	Mouse embryonal fibroblasts	Prepared from mouse embryos (BALB/c & C57BL/6)
Cell lines		
ANA-1	Mouse macrophage cell line	(Cox et al., 1989)
BHK-21	Baby hamster kidney fibroblasts	ATCC: CCL-10
D2SC1	Dendritic cell line	(Paglia et al., 1993)
J774 MΦ	BALB/c macrophage cell line	ATCC: TIB-67
NIH 3T3 fibroblasts	Swiss mouse embryo fibroblasts	ATCC: CRL-1658
HEK 293 kidney cells	Human kidney epithelial cells	ATCC: CRL-1573

2.10.3 Media for eucaryotic cells

Media	Used for
Glasgow-MEM BHK-21 5% FCS 5% Tryptose Phosphate Broth (TPB) 100 U/ml penicillin, 100 µg/ml streptomycin 2 mM L-Glutamine	**BHK-21**
Dulbecco's Modified Eagle Medium (DMEM) 10% FCS 100 U/ml penicillin, 100 µg/ml streptomycin	**NIH3T3**
Dulbecco's Modified Eagle Medium (DMEM) 10% FCS 100 U/ml penicillin, 100 µg/ml streptomycin	**MEF**
Iscove's Modified Dulbecco's Medium (IMDM) 5% FCS 100 U/ml penicillin, 100 µg/ml streptomycin 2 mM L-Glutamine 0.05 mM 2- Merceptoethanol	**D2SC1**

RPMI 1640 10% FCS 100 U/ml penicillin, 100 µg /ml streptomycin 2 mM L-Glutamine	**ANA-1**
RPMI 1640 10% FCS 100 U/ml penicillin, 100 µg /ml streptomycin 2 mM L-Glutamine 0.05 mM 2- Merceptoethanol	**Splenocytes**
RPMI 1640 2% FCS 100 U/ml penicillin, 100 µg /ml streptomycin 2 mM L-Glutamine	**PBMC**

2.11 Viruses

A- Mouse cytomegalovirus strain Smith was derived from infected laboratory mice's salivary glands (Smith, 1954). It was cloned as a bacterial artificial chromosome (BAC) called pSM3fr (Messerle et al., 1997; Wagner et al., 1999). Some years later, a frameshift mutation within the open reading frame (ORF) of MCK2 was repaired and the repaired BAC called pSM3fr-MCK-2fl (Jordan et al., 2011). All of the MCMV BACs used in this thesis were derived from pSM3fr-MCK-2fl.

B- Murine Gammaherpesvirus 68 (MHV-68): wildtype (clone G2.4) (Adler et al., 2000).

C- MCK2 mutant viruses

1- 131 stop mutant (MCMV $_{\text{no MCK2}}$): BAC-derived MCMV mutant was constructed in the Adler lab (Wagner et al. 2013). A stop cassette was inserted in the m131 domain of MCK2, which prevents the expression of the MCK2 protein.

2- 129 stop mutant (MCMV $_{\text{no complex}}$): A stop cassette was inserted in the m129 domain of MCK2 (Wagner et al. 2013), which prevents the formation of the gH/gL/MCK2 binding complex and results in a truncated protein which should still have the chemokine function of MCK2.

3- CC1 mutant (MCMV $_{\text{no chemokine}}$): This mutant has recently been cloned by Thomas Deiler during an internship in the Adler lab. A point mutation was introduced in the m131 domain of MCK2, exchanging a cysteine for glycine (AA 27).

4- 131 d stop: The 131 stop mutant contains a stop codon in m131 ORF, which allow the expression of 66 amino acid. Additional stop codon was introduced directly behind the start codon of the reading frame m131 in MCMV BAC (131 stop mutant) to ensure that no more MCK2 protein can be expressed.

D- MCMV vaccine vectors: MCMV vaccine vectors expressing ORF6 of murine gamma herpes virus 68 (MHV-68) as a vaccine antigen.

1- wt ORF6: An MCMV vaccine vector, which has recently been cloned by Ursula Rambold during her master project in the Adler lab, m128 ORF (IE2) from MCMV genome was deleted and replaced with ORF6-HA in BAC-cloned MCMV.

2- MCMV $_{\text{no chemokine}}$ ORF6: An MCMV vaccine vector, which has recently been cloned by Ursula Rambold during her master project in the Adler lab, m128 ORF (IE2) from MCMV genome was deleted and replaced with ORF6-HA in a BAC-cloned MCMV, then a point mutation of CC1 (explained above) was subsequently introduced.

3- MCMV $_{\text{no MCK2}}$ ORF6: An MCMV vaccine vector, m128 ORF from MCMV genome was deleted and replaced with ORF6-HA in a BAC-cloned MCMV (131 stop mutant), then 131 d stop mutation (explained above) was subsequently introduced.

4- MCMV $_{\text{no complex}}$ ORF6: An MCMV vaccine vector, which has recently been cloned by Ursula Rambold during her master project in the Adler lab, m128 ORF (IE2) from MCMV genome was deleted and replaced with ORF6-HA in a BAC-cloned MCMV, then 129 stop mutation (explained above) was subsequently introduced.

2.12 Software

Software	Manufacturer
BD CellQuestTM Pro	BD Bioscience (Heidelberg, Germany)
Flowing Software 2.5.1.	Perttu Terho (University of Turku, Finland)
Fusion 15.12f	Vilber Lourmat (Eberhardzell, Germany)
Prism	GraphPad Software (San Diego, USA)
Quantstudio	Thermo Fisher Scientific (Waltham, USA)
SnapGene®	GSL Biotech LLC (Chicago, USA)

3. Methods

3.1 Bacterial cell culture

Escherichia coli (*E.coli)* GS1783 were cultivated either on LB agar plates or in LB medium at 32°C. A temperature shift to 42°C results in activation of Red recombinases *exo*, *bet* and *gam* (Warming et al., 2005). The addition of specific antibiotics was required for selection of bacteria at different steps of cloning. Bacterial cultures were measured at optical density (OD) = 600 nm (OD600 of 1 corresponds to 1 × 10^8 cells/ml), in order to assess the growth of bacterial suspensions.

LB-medium (1 L)

10 g Bacto tryptone
5 g Bacto yeast extract
8 g NaCl

Antibiotics

Chloramphenicol (CAM): 25 µg/ml
Kanamycin (KAN): 50 µg/ml

LB-agar (500 ml)

7 g Bacto Agar
500 ml LB medium

3.1.1 Glycerol stocks

For storing bacteria, glycerol stocks were prepared by adding 500 µl of 50 % glycerol (in H_2O) to 500 µl of an overnight culture and stored at -80°C.

3.2 General molecular biology

3.2.1 Preparative Plasmid Midi Preparation

Large scale preparations (midi-preps) of plasmid DNA were performed. 200 ml of overnight culture was used to isolate plasmid DNA using the Macherey-NagelTM NucleoBondTM Xtra Midi Kit according to the manufacturer's protocol.

3.2.2 Determination of DNA concentration

The concentration of nucleic acids was measured using NanoPhotometer® according to the manufacturer's protocol (Implen GmbH). The absorption was measured at 260 nm. $OD_{260\ of}$ 1 corresponds to 50 µg/ml dsDNA.

3.2.3 Quantitative real-time PCR for viral genomes in mouse organs

Briefly, DNA was extracted from blood and spleen cells using DNeasy Blood & Tissue Kits and quantified by UV spectrophotometry and kept at 4°C. Quantification of viral and cellular genes was performed using the Quantstudio 3 real time PCR machine. Amplification was performed in 20 µl reaction volumes using a SYBR green kit. Absolute quantification of the desired genes was achieved by generating standard curves for plasmids harboring the same genes under investigation. PCR was performed with the following cycler conditions: an initial 2 minutes (min) at 50°C, then 15 min at 95°C for HotStarTaq DNA polymerase activation, followed by 50 cycles of 15 s at 94°C, 1 min at 60°C. Following amplification, a melting curve analysis of the PCR products was conducted by increasing the temperature to 95°C, cooling down quickly to 60°C for 1 min, and then slowly raising the temperature again to 95°C for 15 s. The calculations of the copy numbers were performed using Quantstudio software, depending on CT values of the standard curves.

3.2.4 Analysis of DNA

3.2.4.1 Restriction enzyme digestion

Digestions of DNA were performed using restriction endonucleases according to the manufacturer's instructions (NEB). Plasmid digestions were usually performed using 1 µg plasmid DNA in a volume of 20 µl. For digestion of BAC-DNA, 2 µg BAC-DNA or a complete BAC-mini preparation were digested with the respective enzyme and NEB buffer and incubated overnight at the recommended temperature.

3.2.4.2 Agarose gel electrophoresis

DNA fragments were separated by agarose gel electrophoresis. Samples were mixed with 10x DNA loading buffer before loading onto the gel. Ethidium bromide was added to visualize DNA fragments under UV-light. 1% TAE agarose gels were used for small gel analytical or preparative analysis. The settings for gel electrophoresis of small gels were 100 V for 40–60 min. BAC-DNA was separated in 0.8% agarose/TBE gels for restriction digest analysis. These gels were run for 3 h at 120 V.

50x TAE buffer, pH 7.3	10x TBE buffer, pH 8.3	10x DNA loading buffer
2 M Tris	900 mM Tris	50 mM Tris-HCL, pH 7.6
250 mM Na-acetate	900 mM boric acid	60 % (v/v) glycerol
50 mM EDTA	20 mM EDTA	2.5 mg/ml orange G

3.2.4.3 Isolation of DNA fragments from agarose gels

DNA fragments separated in agarose gels after gel electrophoresis were cut on a UV table (254 nm) using a scalpel and isolated from the agarose gel using the QIAquick® gel extraction kit (QIAGEN) according to the manufacturer's protocol.

3.3 BAC-mutagenesis

BAC (bacterial artificial chromosome) cloning is a technique used for mutagenesis and stable maintenance of large DNA fragments of up to 300 kbp using an *E.coli* F-plasmid (Shizuya et al., 1992) and was first applied for a herpes virus genome by (Messerle et al., 1997). Traceless mutagenesis which allows mutagenesis of viral genes without introducing additional changes in the genome was used to construct virus mutants. The traceless BAC-mutagenesis consists of two Red-recombination events and one cleavage step by the rare cutter *I-SceI* (Tischer et al. 2006). *E.coli* GS1783 is the bacterial strain used for traceless mutagenesis of BACs. The *E. coli* recABCD recombination system is disrupted in this strain of bacteria. However, the expression of recombinases is induced by a temperature shift to 42°C under the control of the temperature-sensitive phage repressor cl857 and the phage promotor pL (Warming et al., 2005; Lee et al., 2001; Yu et al., 2000). Firstly, touchdown PCR was used to amplify a kanamycin cassette and a flanking I-SceI restriction site from the plasmid pEPkan-S. The PCR primers are designed in a way to contain homologous sequences of the target BAC-DNA which should be mutated. The resulting PCR product will be introduced into the target BAC via a first homologous recombination event, which results in the deletion of BAC-DNA of interest and insertion of the kanamycin cassette. For induction of the second recombination step, the addition of L-Arabinose is essential for switching on the expression of *I-SceI* in *E.coli* GS1783. This enzyme cuts the sequence at the I-SceI cleavage site, thus facilitates the traceless removal of KanR (Figure 7).

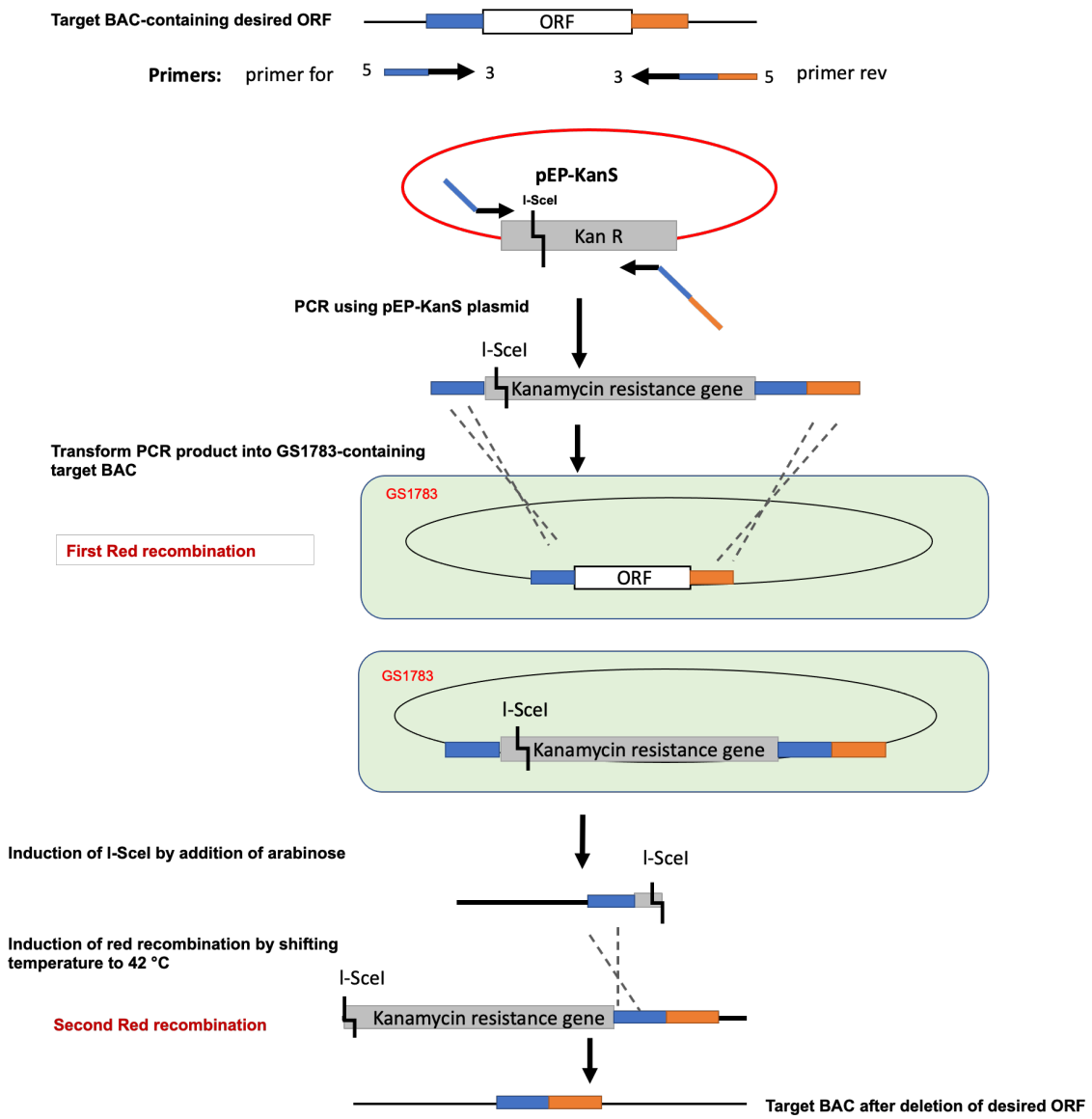

Figure 7: Schematic illustration showing the strategy of BAC traceless-mutagenesis for deletion of ORF of interest.
Colored rectangles represent identical sequences; black dotted lines indicate homologous recombination steps.

- **Protocol**

Firstly, *E.coli* GS1783 containing the BAC of interest was made electrocompetent (see 3.3.2). Afterwards, PCR product of recombinant fragment was electroporated into these electrocompetent bacteria and the first red recombination occurred. After electroporation, the bacterial cells were recovered by adding 1 ml LB medium and grown for 2 h at 32°C. Then, the bacteria were plated on LB agar plates supplemented with 50 µg/ml kanamycin and 25 µg/ml chloramphenicol. Positive clones which grew

on both of CAM and KAN were selected for BAC Mini Preparation (see 3.3.4) and checked by restriction digest analysis. For starting second recombination, 4 ml pre-warmed LB supplemented with 25 µg/mL CAM was inoculated with 100 µL pre-culture of KAN and CAM-positive clones. The bacteria were grown at 32°C for 2 h until the bacteria reach only early logarithmic phase. Thereafter, 2 ml pre-warmed LB medium supplemented with 25 µg/mL CAM and and 0.5% arabinose (final concentration) were added for induction of I- SceI expression, and the incubation of bacteria continued for additional 30 min at 32°C. Afterwards, the bacteria were transferred to a water bath with shaking for 15 min at 42°C to induce the expression of red recombination system. During this incubation step, the removal of the positive selection marker occurs. Then, the culture was returned back to 32°C and incubated for 3 h. Finally, bacteria were plated at 10^{-1} to 10^{-3} dilutions on freshly prepared agar plates with 25 µg/ml CAM and 0.5% arabinose and incubated overnight. After 24 h, colonies were picked from these plates and transferred to replica plates supplemented with both of 25 µg/ml CAM and 50 µg/ml KAN or only 25 µg/ml CAM. The next day, the clones which were CAM-KAN negative, but CAM-positive, were selected for BAC Mini Preparation and checked by subsequent restriction digest analysis. At the end, positive clones were chosen for BAC-Midi preparation (see 3.3.5) and sent to Sequiserve (Vaterstetten, Germany) for sequencing. The sequencing results were analyzed by SnapGene software.

3.3.1 Polymerase chain reaction (PCR)

The amplification of DNA with longer primers was conducted by touchdown PCR (Table 1). Touchdown PCR is one of PCR methods which aims to avoid amplification of non-specific sequences. It depends on using higher annealing temperature at the earliest steps then the annealing temperature is decreased incrementally after each cycle till a specified or “touchdown” annealing temperature is reached (Green & Sambrook, 2018).

Table 1: Touchdown PCR program.

	Step	Temperature	Time	Cycles
1.	initial-denaturation	95°C	5 min	
2.	denaturation (TD)	95°C	30 sec	
3.	annealing (TD)	62-45°C	30 sec	
4.	elongation (TD)	72°C	2 min	17 x back to **2**.
5.	denaturation	95°C	30 sec	
6.	annealing	45°C	45 sec	
7.	elongation	72°C	2 min	18 x back to **5**.
8.	final-elongation	72°C	5 min	
9.	end	4°C	hold	

3.3.2 Preparation of electrocompetent bacteria for BAC mutagenesis

Electrocompetent bacteria are required for introduction of foreign DNA by electroporation. 150 ml LB medium supplemented with CAM antibiotic (required for BAC selection) was inoculated with 3 ml overnight culture of GS1783 containing an MCMV BAC and grown at 32°C until an OD600 of about 0.5 was reached. Then, the culture was transferred to a water bath with 42°C for 15 min to induce expression of recombinases. All the next preparation steps were performed on ice using pre-cooled pipettes and solutions. Bacteria were cooled on ice for 20 min and then pelleted by centrifugation at 5,500 ×g for 10 min and subsequently washed for 3 times with 150 ml 10% glycerol. Afterwards, bacteria were pelleted again and resuspended in 1.5 ml 10% glycerol and snap frozen in liquid nitrogen as 70 µl aliquots and stored at -80°C.

3.3.3 Transformation of electrocompetent bacteria

DNA was introduced into electrocompetent bacteria (for BAC mutagenesis) by electroporation. 50- 300 ng DNA was added to electrocompetent bacteria which were pre-thawed on ice. The bacteria were transferred to a cuvette (Biorad; 0.2 µm in diameter) and the cuvette was kept on ice then the bacteria were electroporated using a gene pulser (2,5 kV, 400 Ω and 25 µF). This way, the genetic material could be introduced into the bacterial cells. After the electroporation, 1 ml of antibiotic-free LB

medium was added immediately. Afterwards, the bacteria were grown for 2 h at 32°C. 200 µl of bacterial suspension and the remaining 800 µl concentrated to 200 µl were plated on agar plates and incubated overnight.

3.3.4 Analytical BAC Mini Preparation

Buffers of the plasmid Maxi kit (Qiagen, Germany) were used for small scale BAC-DNA preparations (analytical BAC Mini-Preps), which was done as followed. 10 ml overnight culture was prepared with appropriate antibiotics for each clone. The next day, the bacterial cells were pelleted at 2,643 × g for 15 min at room temperature (RT). The supernatants were removed, and the pellets were resuspended in 300 µl resuspension Buffer (Qiagen, Germany), then 300 µl lysis buffer (Qiagen, Germany) was added and the samples were gently inverted several times, followed by addition of 300 µl of the neutralization buffer (Qiagen, Germany) to stop the action of lysis buffer, then the samples were incubated on ice for 5 min for complete precipitation of proteins and chromosomal DNA, followed by centrifugation at 18,407 × g at RT for 5 min. The supernatant-containing BAC-DNA was carefully transferred to a new tube and mixed with 1 ml phenol/chloroform/isoamyl alcohol (25/24/1). Samples were gently mixed by inverting several times and centrifuged 5 min at 18,407 × g at RT. The upper phase, which contains BAC-DNA was transferred to new tubes with 1 ml isopropanol. The BAC plasmids were precipitated at 18,407 × g for 20 min at RT. The pellets were washed with 1 ml ethanol to remove salt, then re-pelleted at 18,407 × g for 10 min at 4°C. After a short drying of the pellets, they were resuspended in 30 µl TE buffer (pH = 7.5). BAC-DNA was then analyzed by restriction digest analysis.

P1 resuspension buffer
50 mM Tris-HCl, pH 8
10 mM EDTA
100 µg/ml RNase I

P3 neutralization buffer
3 M KAc, pH 5,5

P2 lysis buffer
200 mM NaOH
1% (w/v) SDS

TE buffer pH (7.5)
10 mM Tris-HCl, pH 7.5
1 mM EDTA

3.3.5 Preparative BAC Midi Preparation

Overnight cultures in 200 ml volume were used to isolate BAC-DNA in a large scale (BAC-midi-preps), using a modified protocol of the Qiagen Maxi kit manufacturer's protocol. Buffer P1, Buffer P2 and Buffer P3 were used in 20 ml volume instead of 10 ml. BAC-DNA was then analyzed by restriction digest analysis.

3.4 Analysis of protein

3.4.1 Protein extracts

Cell extracts or extracts from virus stocks cells were prepared by lysis with 2x sample buffer. In cell extracts, DNA was disrupted by ultrasonication.

2x sample buffer

10% (w/v) SDS	6 ml
0.5 M Tris-HCl, pH 6.8	2.5 ml
α-Thioglycerol	1 ml
Glycerol	1 ml
Bromophenol Blue	0.01%

3.4.2 Protein separation using SDS-PAGE

The mobility of proteins in an electrical field depends mainly on its mass and charges. SDS incorporates into unfolded proteins and mask the intrinsic charges of proteins and adds to them negative charges, so the separation of proteins depends solely on size of the protein. Cell lysates in 2x sample buffer were heated for 5 min at 95°C. Proteins were separated on polyacrylamide gel electrophoresis (PAGE), and the electric voltage was adjusted to 100 V until the protein samples had passed through the stacking gel, then the voltage was increased to 140 V for 1 h. A protein standard (Pre-stained Protein Marker, Invitrogen) was also loaded in parallel with the samples to determine the molecular weight of the samples.

Table 2: Components of separating and stacking gel used for SDS-Polyacrylamide gels

Component	Separating gel	Stacking gel
ddH2O	2000 µl	1410 µl
Tris-HCl	1250 µl (1.5 M, pH 8.8)	630 µl (0.5 M, pH 6.8)
10% SDS	50 µl	25 µl
30% Acrylamide	1670 µl	420 µl
10% APS	50 µl	25 µl
TEMED	2.0 µl	1.5 µl

10x running buffer

Tris	25 mM
10% (w/v) SDS	10%
Glycine	250 mM

3.4.3 Western blot

After protein separation via SDS PAGE, the proteins were transferred to a nitrocellulose membrane in an electric field in order to detect specific proteins. Membranes and gels were incubated for 15 min in blotting buffer before transfer of the gel onto a nitrocellulose membrane. The blotting was performed for 1 h at 100 V. The transfer of proteins could be confirmed by staining the membrane with Ponceau Red. Afterwards, the membrane was blocked using blocking buffer for 1 h to avoid non-specific binding of protein. Then, the membrane was incubated with a primary antibody diluted in blocking buffer. The incubation with the primary antibody was conducted overnight at 4°C on a roller mixer. The next day, membrane was washed five times (5 min/each) with TBST and then incubated with horseradish peroxidase-conjugated secondary antibody diluted in blocking buffer for 2 h at RT. After washing the membrane again for five times with TBST, the membrane was transferred to TBS buffer. The kit SuperSignal™ West Pico PLUS Chemiluminescent Substrate was used for visualization of the protein bands according to manufacturer's instruction and the signal was detected by Fusion FX7 Imager at 425 nm.

Blotting buffer	**TBST buffer**	**Blocking buffer**
25 mM Tris	150 mM NaCl	TBST
192 mM glycine	10 mM Tris-HCl	5% skimmed milk
20% methanol (v/v)	0.2% Tween-20	

TBS buffer

150 mM NaCl
10 mM Tris-HCl

3.4.4 Quantification of proteins by Enzyme-Linked Immunosorbent Assay (ELISA)

Sandwich Enzyme-Linked Immunosorbent Assay (ELISA) is an assay, which used for quantification of proteins. Fc fused proteins were quantified using ELISA. Firstly, a Neutravidin coated 96-well plate was washed three times with wash buffer. Then, 100 µl of diluted biotinylated capture antibody (10 µg/ml) were added to each well and incubated for 1 h at RT. Afterwards, the wells were washed three times with wash buffer (200 µl/well). The Fc fused samples were previously diluted 1:2, 1:4 and 1:8 in the respective medium, then added (100 µl/well). In parallel, the standard was also diluted to 6.00, 3.00, 1.50, 0.75, 0.38 and 0.19 µg/ml and added (100 µl/well). The samples and standard were incubated for 30 min at RT, followed by three times washing with washing buffer (200 µl/well). Afterwards, the peroxidase-conjugated secondary antibody was diluted 1:3000 in wash buffer, added (100 µl/well) and incubated for 30 min in dark. Then the wells were washed three times with wash buffer, followed by adding the TMB substrate (100 µl/well). After 15-30 min incubation period, the peroxidase substrate was oxidized, producing a blue-coloured end-product. 10% phosphate acid was added (100 µl/well) as reaction stop solution. Absorbance was measured at 450 nm using an ELISA reader. The concentrations of Fc fused proteins were quantified using the standard curve.

Wash buffer, pH 7.2

25 mM Tris
150 mM NaCl
0.1% BSA
0.05% Tween-20

3.5 Mammalian cell culture

3.5.1 Cultivation of mammalian cells

All of the mammalian cell lines were cultivated at 37°C, 6 or 8% CO_2, in a humidified cell culture incubator. For maintenance of the cells, sub-culturing was regularly performed. The general procedures of sub-culturing involved washing of the cells once with PBS, then detachment of the cells from plates or flasks by adding a 25% trypsin/EDTA solution for 3-5 min at 37°C. The trypsin reaction was stopped by adding adequate amount of the respective medium with FCS. Then, the cells were resuspended and reseeded into new plates or flask containing fresh medium and incubated at 37°C. In order to count the cell numbers in a cell suspension, a Neubauer cell counting chamber was used. The cell suspension was mixed with trypan blue to discriminate between live and dead cells

3.5.2 Freezing of cells

For long-term storage, cells were grown to 90% confluency, harvested and pelleted at 300 xg for 5 min at RT. The pelleted cells were resuspended with precooled freezing medium. 1 ml aliquots were dispensed into cryo tubes and slowly cooled down to 80°C. After 48 h, cells were transferred to a liquid nitrogen tank.

Freezing medium

70% cell-type specific media
20% FCS
10% DMSO

3.5.3 Thawing of cells

For thawing the cells, frozen cells were rapidly thawed at 37°C, pelleted and washed with appropriate medium to remove DMSO. Then, the cells were resuspended in cell-type specific medium and transferred to appropriate cell culture dishes.

3.5.4 Preparation of primary murine embryonic fibroblast cells

Primary murine embryonic fibroblast cells (MEF) were prepared from 14 day old BALB/c mouse embryos. The uterus with embryos was transferred to a petri dish. The embryos were then isolated from amnion and placenta and transferred to a new petri dish. The internal organs and brain were removed, then the embryos were cut with a scalpel and tweezers into small pieces on ice. Afterwards, the cutted pieces were

transferred to an Erlenmeyer beaker with glass beads and filled with 30 ml EDTA/trypsin in PBS (1:1) dilution, pH 7.4. The tissue suspension was incubated for 1 h at 37°C with stirring. During the last 30 min of incubation, additional 30 ml EDTA/trypsin in PBS was added. Afterwards, the tissue suspension was resuspended and transferred to a wire mesh, which was placed on an Erlenmeyer beaker to get rid of big tissues pieces. Then, the cell suspension was collected and centrifuged at 311 xg for 5 min at RT to pellet the cells, followed by washing with DMEM medium supplemented with 10% FCS, L-glutamine and Pen/Strep. Thereafter, the cells were filtered using 100 µm cell strainers to remove cell clumps. Then, the filtered cells were counted and adjusted to 2-3 x 10^7 cells per 15 cm plate, or at least one 15 cm dish for each embryo. The cells were cultured for 1 day. On day 2, the cells were washed 3x with PBS to remove non adherent cells and fresh medium was added. The cells were incubated until they reached 80% confluency (4-5 days). Then, the cells were frozen for long term storage.

3.5.5 Transfection of cells using PEI

Polyethyleneimine (PEI) is widely used as an effective transfection reagent, which is capable of condensing DNA into positively charged particles, which can enter the cell by endocytosis (Longo et al., 2013). The transfection with polyethyleneimine was used to transfer DNA into eukaryotic cells. HEK 293 cells were seeded into 10 cm dishes one day before transfection. The transfection mixture was prepared in a 1.5 ml tube: for each 10 cm dish, 400 µl Opti-MEM medium, 60 µl PEI and 24 µg of the plasmid were mixed and incubated for 40 min at RT. Then, the transfection mixture was added dropwise to the cells, followed by a 3 h incubation period then exchanged with Opti-MEM serum-free medium.

3.5.6 Migration assay

The migration assay was performed to test the capacity of the cells to migrate in response to a stimulus through cell culture inserts with a specific pore size. The migrated cells were measured using the cell-permeable dye calcein-AM, which is converted to a green, fluorescent calcein after hydrolysis by intracellular esterases in viable cells. Therefore, a florescent signal is produced and can be measured. J774 cells (mouse macrophages) were harvested using versene (EDTA solution) and centrifuged for 5 min at 311 xg to pellet the cells, then the cells were resuspended in

DMEM supplemented with 0.2% BSA, counted. Cell culture inserts were placed into 24 well plate, and divided the well of 24 well plate into lower chamber and upper chamber. Chemokine samples under investigation were added in 1.3 ml volume to the lower chamber of the wells, while 1 x 10^5 cells were added to the upper chamber. The chambers were incubated for 4 h at 37°C. In order to be able to determine the number of migrated cells, a standard curve was generated at the same time, and two-fold serial dilutions of the cells starting from 1 x 10^5 cells were prepared. Then, 100 µl of each dilution were added on a black 96-well plate and incubated at 37°C for 4 h. At the end of the incubation period, the cell culture inserts were removed from 24 well plates, and the fluid and cells on the upper side of the insert was removed with a cotton swab. The migrated cells in 24 well plates and the cells of the standard curve on 96 well plates were pelleted at 311 xg for 5 min at RT. The supernatants were sucked off, then 600 µl of 8 µM calcein-AM in versene were added to the migrated cells in 24 well plates and the cell cultured inserts were returned back to their corresponding wells. In addition, 100 µl of the 8 µM of calcein-AM was added to each well in 96 well plate. The cells were incubated for 45 min at 37°C. In order to remove cells sticking to the membrane of the cell culture inserts, their membranes were washed four times with the liquid of the wells. Then, (4x) 100 µl aliquots of each sample were transferred to the black 96-well plate and the fluorescence measured (excitation: 483-14, emission: 530-30). The number of migrated cells was calculated from the standard curve readings.

3.5.7 Fluorescence-activated cell sorting (FACS) of cells

1- Surface staining

Surface staining was performed on U-bottom 96 well plates. The cells were pelleted at 311 xg for 5 min at 4°C, then resuspended in 50 µl FACS buffer containing 1 µl of Fc block and incubated for 10 min on ice. Thereafter, the cell surfaces were stained with antibodies to surface markers or their respective control isotypes for 30 min on ice and in the dark, followed by washing with 150 µl FACS buffer. Afterwards, the cells were pelleted and resuspended in 150 µl of 1% paraformaldehyde/PBS and measured using BD FACSCalibur™ machine. The data was analyzed using Flowing Software 2.5.1.

FACS buffer 2% FCS in PBS

2- Intracellular staining for infected cells

For intracellular staining of viral IE1 protein in MCMV-infected cells, cells were harvested using trypsin, resuspended in the appropriate medium, pelleted, then transferred to 1.5 ml tubes for further procedures. The cells were pelleted again at 425 xg for 5 min at RT, the supernatant was aspirated, and the cells were fixed using 500 µl 1% PFA/PBS for 10 min at RT. Starting from here, all following steps were performed on ice. After fixation of the cells, they were pelleted at 425 xg for 5 min at 4 °C and washed twice with 1 ml washing buffer. Then, the cells were incubated with 100 µl of the first antibody (mouse anti-ie antibody croma 101) diluted (1:100) in staining buffer for 30 min on ice. After that, the cells were washed with 1 ml washing buffer and centrifuged at 425 xg, 5 min at 4°C. Then, the supernatant was aspirated, and the cells were stained with 100 µl of the secondary antibody (anti-mouse Fluor 488-coupled antibody) diluted (1:1000) in staining buffer. The samples were again incubated for 30 min on ice, then washed with 1 ml washing buffer and pelleted at 425 xg for 5 min at 4°C. Finally, the pelleted cells were resuspended with 400 µl 1% PFA/PBS and measured using BD FACSCalibur™ machine. The data was analyzed using Flowing Software 2.5.1.

Wash buffer 0.03% saponin in PBS

Staining buffer 0.3% saponin in PBS, 1% BSA

3- Intracellular cytokine staining (ICS)

Intracellular cytokine staining was performed on $1x10^6$ cells/ well in U-shaped 96 well plates for *ex vivo* peptide-stimulated splenocytes or splenocytes which were cocultured with infected MEF. All procedures were performed at 4°C. The cells were pelleted at 311 xg for 5 min at 4°C, then resuspended with 50 µl FACS buffer containing 1 µl of Fc block and incubated for 10 min on ice. Thereafter, the cells were surface stained with anti-CD8 (1:200 in FACS buffer), anti-CD4 (1:100 in FACS buffer) antibodies or control isotypes for 30 min on ice and in the dark, followed by washing with 150 µl FACS buffer. Then, the cells were fixed using 150 µl of 1% PFA for 10 min at RT, pelleted and washed with 150 µl of washing buffer. The samples were then resuspended in permeabilization buffer containing anti-IFN γ antibodies (1:100) for 30 min on ice and dark, washed again with 150 µl of washing buffer, pelleted,

resuspended with 1% PFA in PBS and subjected to flow cytometry (BD FACSCalibur™). The data was analyzed using Flowing Software 2.5.1.

FACS buffer 2% FCS in PBS

Permeabilization buffer 0.1% saponin in PBS, 10% FCS

Wash buffer 0.03% saponin in PBS

3.6 Virological methods

3.6.1 Virus reconstitution from BAC-DNA

To reconstitute infectious virus from BAC-cloned MCMV genomes, the DNA was transfected into MEF cells using the transfection reagent FuGene HD. One day before transfection, MEF cells were seeded on 6-well plates. The reconstitution was performed in duplicate for each BAC-DNA. Briefly, 1.5 µg BAC-DNA was mixed with 100 µl OptiMEM and then 6 µl of Fugene HD reagent was added. The mixture was carefully mixed and incubated for 40 min at RT. After the incubation period, the transfection mixture was added dropwise to the cell culture supernatant. After 24 h cultivation, the cells were washed with PBS, trypsinized, transferred to a 10 cm dish, and cultivated until plaques appeared. The cells were checked daily for plaque formation. When a complete cytopathogenic effect (CPE) was reached, the supernatants were harvested.

3.6.2 Virus production in MEF cells

Cells were seeded one day before infection, to achieve about 80% - 90% confluence. Virus inocula were diluted in DMEM medium containing 10% FCS and applied to the cells in small volume, e.g., 4 ml on a 10 cm plate. The cells were co-incubated with the inocula for 1.5 h at 37°C, then washed three times with medium to remove the inocula and supplied with fresh medium and incubated at 37°C. Sometimes centrifugal enhancement was used to enhance the infection efficiency. For centrifugal enhancement, cells with virus were centrifuged at 863 xg for 30 min at RT, then incubated for 1 h at 37°C, followed by a medium change.

3.6.3 Virus harvest

After a complete CPE was observed, cell culture supernatants were harvested from the infected cells and centrifuged at 2643 xg for 15 minutes at RT, in order to remove the cell debris. Then, the supernatants were frozen at -80°C.

3.6.4 Virus stock production

1- MCMV virus stock:

A virus inoculum was prepared, prior to the production of an MCMV virus stock. To do that, 10 cm dishes of MEF cells were infected and incubated at 37°C until a complete CPE was reached, supernatants and infected cells were detached by scraping and stored at -80°C. For starting virus stock preparation, NIH3T3 cells from four-15 cm dishes, which were 100% confluent, were trypsinized, pelleted and resuspended with the virus inoculum. Then, 16 dishes (15 cm) were seeded with the virus inoculum-NIH3T3 cell mixture. After complete cell lysis (usually 4-5 days post-infection), the supernatants were harvested and cleared from cellular debris at 5403 xg at 4°C for 15 min. Afterwards, virus particles were pelleted at 25364 xg for 3 h at 4°C. Pellets were resuspended in 1.5 ml of VSB overnight at 4°C. The next day, a precooled douncer was used for resuspension of the pellet by douncing 20 times. Thereafter, the resuspended pellet was carefully layered on a sucrose cushion composed of 10 ml cold VSB buffer + 15% Sucrose in an ultracentrifugation tube, avoiding mixing of the layers. The virus on this sucrose cushion was centrifuged for 70 min at 53,837 xg, 4 °C (Beckman OptimaTM L-80 XP Ultracentrifuge, Rotor: SW32 Ti). The supernatant was discarded, and the pellet was washed twice with 10 ml ice cold VSB to remove any leftovers of sucrose. Then, the pellet was covered with 1.5 ml VSB buffer and kept overnight at 4°C on ice to soften the pellet. The next day, the pellet was resuspended by pipetting on ice, and the suspension was cleared at 956 xg for 3 min at 4°C. The supernatant was then transferred to a new tube and centrifuged for a second time, followed by aliquoting of the resulting supernatant. The virus stock was kept at -80°C.

VSB buffer (pH 7.8)	Tris-HCL	50 mM
	KCl	12 mM
	EDTA	5 mM

2- MHV-68 virus stock:

For production of an MHV-68 virus stock, BHK-21 cells were seeded in four T75 culture flasks. The next day, the cells in each flask were infected with 50 µl MHV-68 virus stock, diluted in 6 ml BHK-21 medium and co-incubated for 1 h. After this incubation period, the virus supernatant was removed, and new medium was added. The cells were incubated for 4 days until a complete CPE occurred. The cells and supernatants were harvested. Cells were pelleted at 1349 xg for 10 min at 4°C and the pelleted cells were resuspended in 1 ml medium, followed by two cycles of freezing and thawing and centrifuged again at 1349 xg for 10 min at 4°C. The produced supernatants from the cells were aliquoted and kept at -80°C.

3.6.5 Virus growth curves

Multi-step growth curves were performed, to assess the kinetic of virus growth on MEF cells. MEF cells were seeded in 24-well plates (6×10^4 cells per well) and the cells were incubated for 24 h at 37°C. Afterwards, the cells were infected at multiplicity of infection (MOI) of 0.2. The infection was performed for 1.5 h, then the cells were washed 6 times with 1 ml medium per well to remove any leftovers from the inoculum. After the last wash step, 1 ml medium was added to each well and the infected cells were incubated at 37°C for up to 5 days. The virus supernatants were harvested after 24 h, 48 h, 72 h, 96 h and 120 h, cleared from cells and cell debris by centrifugation at 2643 xg for 15 min at 4°C. Then, the supernatants were frozen at -80°C and virus titer was determined by the TCID50 method.

3.6.6 Titration of the virus using a TCID50 assay

Virus titers were determined using a tissue culture infectious dose (TCID50) assay, which was performed on MEF cells in 96-well plates. One day before the titration, MEF cells were seeded. MCMV virus was 10-fold serially diluted from 10^{-1} to 10^{-8}. 100 µl of each dilution were added in quadruplicates. The cells were incubated for 5-6 days, then stained with 1x cristal violet for 10 min at RT and washed with water. After drying of the plates, plaque positive wells were counted under the microscope and the $TCID_{50}$ values were calculated following the Reed and Muench (1938) method.

10x crystal violet	Formaldehyde/PBS	10%
	Crystal violet	1%

3.6.7 Titration of the virus using a plaque assay

Plaque assay is another method which is used to determine the number of plaque-forming unit (PFU) of infectious viruses.

3.6.7.1 Titration of MCMV

MEF were seeded in 48-well plates one day before titration. MCMV virus was 10-fold serially diluted from 10^{-1} to 10^{-8} (1 ml volumes), 200 µl of each dilution were added in triplicates onto MEF cells for 1 h at 37°C. Then, a methylcellulose overlay was added to prevent supernatant-driven virus spread. The infected cells were incubated for three days at 37°C, then stained with crystal violet, and plaques were counted to calculate the virus titer in plaque forming units (PFU) per ml. The calculation is based on the publication of Dulbecco and Vogt (1954). The virus titers were calculated according to the following formula:

Viral Titer (PFU/ml) = number of plaques X dilution X Input factor

Input factor = 1ml /0.2ml = 5

Methyl cellulose overlay medium (MEM)	Carboxymethylcellulose sodium salt	3.75 g
	dd H2O	388 ml
	FCS	25 ml
	10x MEM	50 ml
	Glutamine	5 ml
	MEM nonessential amino acids	2.5 ml
	Pen/Strep	5 ml
	$NaHCO_3$	24.7 ml

3.6.7.2 Titration of MHV-68

A plaque assay was also used to determine the number of infectious MHV-68 particles. BHK-21 cells were seeded in 24-well plates (40000 cells/well). The next day, ten-fold serial dilutions of samples (10^{-1} to 10^{-8}) were prepared in a volume of 1 ml. 900 µl of each dilution were added onto BHK-21 cells for 90 min. Afterwards, the virus solutions were removed and 2 ml of prewarmed overlay medium (0.75% methylcellulose) was added to the cells, then incubated for 4 days. Afterwards, the cells were stained with crystal violet (300 µl/well) for 15 min. After the staining, the cells were washed with water and dried at RT, then the plaques were counted. The virus titers were calculated according to the following formula:

Viral Titer (PFU/ml) = number of plaques X dilution X Input factor

Input factor = 1ml /0.9ml = 1.1

Methyl cellulose overlay medium (BHK-21)	Glasgow -MEM BHK-21	440 ml
	FCS	25 ml (5%)
	Tryptose phosphate	25 ml (5%)
	Pencillin /Streptomycin	5 ml (1%)
	L-Glutamin	5 ml (1%)
	Carboxymethylcellulose sodium	3.75 g (0.75%)

3.6.8 Infection of monocytes

ANA-1 and D2SC1 were seeded the day before the infection to reach about 80% confluency. Then, the cells were detached with versene, pelleted and counted. Afterwards, the cells were transferred to 1.5 ml tubes and infected with virus supernatants/stocks at an MOI of 1. The infection was performed for 2 h at 37°C, with a periodical sniping of the tubes every 30 min. Then, the cells were transferred to 6 well plates. After 24 h, the efficiency of infection was monitored by intracellular staining of MCMV protein IE1 using FACS analysis.

3.7 *In vivo* experiments

3.7.1 Mice

Mouse husbandry was conducted under specific-pathogen-free environment according to the Federation of European Laboratory Animal Science Associations protocols (FELASA) at the Max von Pettenkofer-Institute, Munich. Experiments were performed in accordance with German animal care and ethics legislation and with the approval of the responsible animal welfare authority. Inbred BALB/c and C57BL/6 (6 weeks), female mice were purchased from Janvier (France). Mice were housed in individually ventilated cages and all of the applications were performed under a sterile hood. Mice were killed using CO2 asphyxiation.

3.7.2 Infection of mice

1- Intraperitoneal infection

MCMV or MCMV vaccine vectors were intraperitoneally injected in a final volume of 150 µl PBS. Mice were injected into the peritoneum using 26 G 1 /2 cannula: mouse was restrained appropriately in the head-down position and injected in the lower right quadrant of the abdomen.

2- Intranasal infection

MHV-68 was intranasally administrated. Before the intranasal infection, the mice were anesthetized by intraperitoneal injection of Ketamin (80 mg/kg)/ Xylazin (10 mg/kg). Then, the mice were infected intranasally with 20 µl of virus diluted in PBS, by application of the fluid to the nostrils of the mouse. Then, the mouse was put on heating pad for 3-4 min and regular breathing was monitored all of the time. The mouse was returned back to the cage after recovery from anesthesia.

3.7.3 Preparation of organ homogenates

To determine virus titers or cytokine levels in organs, organs had to be homogenized. Organs of mice killed by CO_2 were transferred to 2 ml tubes under sterile conditions, and placed in dry ice until storage at -80°C. For preparation of organ homogenates, the organs were thawed and then placed on ice. Before homogenization, organs were weighed. Afterwards, the organs were placed in Fasrprep-24 tubes. Each tube was supplemented with one bead and filled with 500 µl of MEF medium or BHK-21 medium. For mechanic homogenization of organs, FASTPREP®-24 instrument was used.

Then, the organ homogenates were transferred to 15 ml falcon tubes and the volume was completed to 3 ml (spleen, lungs, salivary glands) or 10 ml (liver). Afterwards, the samples were centrifuged at 863 xg for 15 min at 4°C to remove bigger tissue parts. The samples for titration and cytokine measurement were taken from the supernatants and kept at -80°C.

3.7.4 Titration of viral titers in organs

Organ homogenates (spleen, lungs, salivary glands, and liver) of MCMV-infected mice were titrated on MEF cells. MEF were seeded on 48-well plates (200 µl/well). 400 µl of organ homogenate was used to start a serial 1:5 dilution. Then, 200 µl of each dilution were added to the cells (in duplicate wells). Infection was done using centrifugal enhancement. Then, the supernatants were sucked off and 500 µl of prewarmed methylcellulose was added. The cells were incubated for 3 days at 37 °C, then stained with crystal violet, and the number of the plaques were counted. Titers were calculated according to the following formula:

Viral titers in different organs: Number of plaques X dilution X input factor

Input factor is 15 in spleen, lungs and salivary glands, and 50 in case of liver. Titers were finally calculated per gram organ. Organ homogenates infected with MHV-68 were titrated on BHK-21 cells as in 3.6.7.2.

3.7.5 Quantification of cytokines and chemokines by ELISA

IFN-γ, CCL2 and IFN-α were measured in the spleen using commercial sandwich ELISA kits following the manufacturer's instructions. Standard curves for each cytokine were generated (in duplicate) using the standard set of cytokines, provided in each kit (Mouse IFN-γ ELISA MAX ™ Deluxe Sets, Mouse MCP-1 ELISA MAX ™ Deluxe Sets, Verikine mouse interferon alpha ELISA kit).

3.7.6 Infectious center assay

To determine the number of MCMV-infected leukocytes in the peripheral blood, an infectious center assay was performed. Blood samples were taken from the chest cavities of mice killed with CO_2 and collected in Eppendorf tube-containing 0.5 M EDTA as anti-coagulant agent. For separation of leukocytes from whole blood, the non-coagulated blood was transferred to 15 ml falcon tubes containing 1 ml 8mM EDTA in PBS.

Then, erythrocytes were lysed by mixing the blood suspension with 5 ml ACK lysis buffer, followed by 5 min incubation at RT. Then, 5 ml of RPMI medium were added to stop the lysis buffer, followed by centrifugation at 216 xg for 5 min. The supernatant was sucked off carefully, the pellet resuspended in 300 µl of RPMI medium, and then the cells counted. In order to avoid counting of leftovers of erythrocytes, PBS 2% HAC (acetic acid) was added to the trypan blue stain. This eliminates remaining erythrocytes. The leukocytes were then added to 12-well plates with MEF cells seeded a day before (2×10^5/well). For that, the supernatants were sucked off and the separated leukocytes were added and distributed in two wells (1ml/well), for each mouse. After 14hr, the supernatant was sucked off and 1.5 ml of methylcellulose were added. The cells were incubated for additional 2 days at 37°C then stained with crystal violet and the number of plaques counted.

ACK Lysis buffer	NH_4Cl	0.15 M
(pH 7.2-7.4)	$KHCO_3$	1.0 M
	EDTA	0.1 mM

3.7.7 Isolation of mouse splenocytes

Spleens were transferred to PBS/2%FCS and kept on ice. For further applications, single cells suspensions from spleens were prepared. The spleens were transferred to cell strainers (100 µm pore size) on top of 50 ml falcon tube. The spleens were mashed carefully with the plunger of 2 ml syringe. Afterwards, the spleen cells were pelleted at 216 xg for 5 min at RT and the supernatant was discarded. In order to get rid of the erythrocytes, the pellet of the cells was resuspended with 3 ml ACK lysis buffer for 5 min then 10 ml of RPMI medium (10% FCS, L-glutamine and Pen/Strep, 0.05 mM 2-Merceptoethanol) was added to stop the lysis reaction. The splenocytes were pelleted again, washed twice with 10 ml medium and counted.

3.7.8 Stimulation of splenocytes by peptides

For *ex vivo* stimulation of splenocytes, the splenocytes cells were adjusted to a concentration of $1x10^7$/ml and seeded in 96-well U-bottom plates (100 µl/well). The stimulant peptide was added to the cells at a final concentration of 1 µg/mL and incubated for 1 h. As a positive control, cells were stimulated with a cell activation cocktail containing PMA (50 ng/ml) plus ionomycin (1000 ngl/ml). After 1 h, Brefeldin

A Solution (1 µl/ml) was added to each well as an inhibitor of protein secretion via the Golgi apparatus. Afterwards, the stimulation time was continued for further 5 h, then the PMA/Ionomycin cocktail removed and exchanged with splenocytes medium, and the plates were kept at 4°C until FACS staining.

3.7.9 Stimulation of splenocytes by infected cells

MEF cells were seeded in flat 96-well plates (1.2×10^4/well) and the next day, the cells were infected with MHV68 at an MOI of 0.2 and the infection was enhanced by centrifugation at 863 xg for 30 min. The next day, the splenocytes cells were added directly to the infected MEF cells in flat 96-well plates (1×10^6 cells/well). Afterwards, the cells were co-incubated for 1 h. Then, Brefeldin A Solution (1 µl/ml) was added, and the incubation time was continued for additional 5 h. After that, the splenocytes were transferred from the flat 96-well plate to U-shaped 96-well plates for FACS staining.

3.7.10 *Ex vivo* Reactivation assay

Latently MHV-68 infected splenocytes can reactivate the virus after contact with NIH3T3 cells. A reactivation assay was performed to determine the frequency of latently infected cells. NIH3T3 cells were seeded in 96-well plates a day before (7.5×10^3 cells) in 200 µl/well. Spleen cells were threefold serially diluted, starting at a concentration of 1.5×10^5 cells/well, and plated on NIH3T3 cells in 96-well plates (100 µl/well), 24 wells for each dilution. After 7 and 14 days, NIH3T3 cells in the plates were screened microscopically for a viral cytopathic effect (CPE). The other half of the dilutions were frozen and thawed twice to mechanically destroy intact spleen cells, and applied to NIH3T3 cells according to the above scheme, in order to differentiate between latently infected cells and infectious virus in the samples.

The percentage of CPE-positive wells per dilution was calculated using the following formula:

(CPE positive wells latent virus - CPE positive wells lytic virus) x 100/24

3.8 Statistical analysis

All statistics analysis were performed with Prism 6.0 software (GraphPad, CA). Normally distributed datasets were analyzed by one-way ANOVA with Tukey post-test. Datasets with skewed distributions were analyzed with the nonparametric test, Mann-Whitney U test. P values < 0.05 were considered statistically significant and shown as * in the figures; ** $p < 0.01$; *** $p < 0.001$.

4. Results

4.1 Characterization of MCMV MCK2 mutants *in vitro*

4.1.1 Description of MCK2 mutants

MCMV encodes a viral CC chemokine called MCK2, which results from splicing of the two MCMV open reading frames (ORFs) m131 and m129 (MacDonald et al. 1999) (Figure 8). Like the HCMV UL128 gene product, MCMV MCK2 has a dual function: As CC chemokine, it can for example attract monocytes and activate them and additionally, MCK2 is part of the gH/gL/MCK2 envelope glycoprotein complex promoting infection of macrophages with MCMV (Wagner et al., 2013). Studies with MCMV mutants lacking MCK2 demonstrated a role of MCK2 in viral dissemination and in immunomodulation of the host's antiviral immune response (Saederup et al., 2001; Stahl et al., 2015; Wikstrom et al., 2013; Daley-Bauer et al., 2014; Daley-Bauer et al., 2012; Farrell et al. 2019; Jordan et al., 2011; Wagner et al., 2013; Farrell et al., 2016). To date, it is not known whether dissemination and immunomodulation are driven by the chemokine activity of MCK2 or by its entry function or by both.

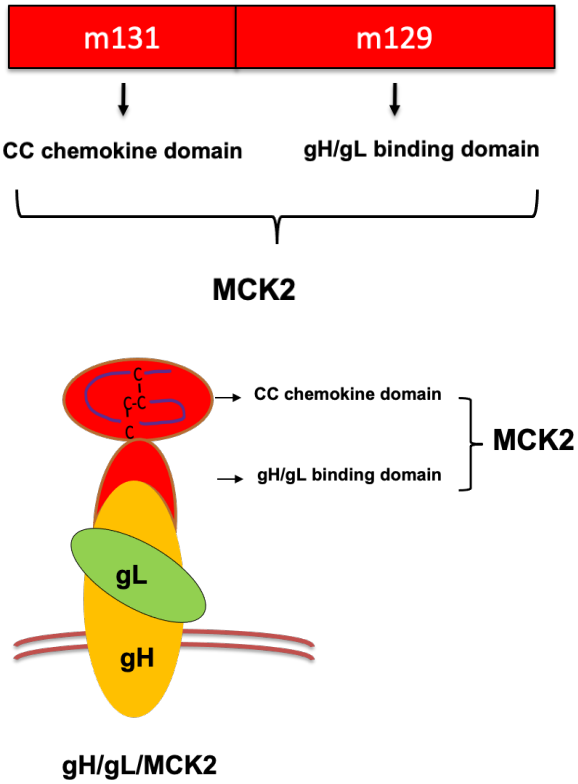

Figure 8: Schematic presentation of MCK2, indicating the CC chemokine domain and the gH/gL binding domain of MCK2.

In order to investigate the role of MCK2 and discriminate between the chemokine function and the entry function of MCK2, a set of MCMV mutants expressing different MCK2 mutations is required. All of MCK2 mutants used in the thesis are illustrated in Figure 9 and were generated on the backbone of pSM3fr-MCK-2fl (Jordan et al., 2011), designated as MCMV wildtype (wt). At the beginning of my thesis, the following MCK2 mutants were available:

1- 131 stop mutant (MCMV $_{\text{no MCK2}}$): an MCK2 mutant, which has been cloned by inserting a stop cassette in the m131 domain of MCK2, that prevents the expression of the complete MCK2 protein. The 131 stop mutant has been characterized *in vitro* and *in vivo,* and showed for example low titers in salivary glands, and impaired macrophage infection (Wagner et al. 2013; Lemmermann et al. 2015).

2- 129 stop mutant (MCMV $_{\text{no complex}}$): an MCK2 mutant, which has been cloned by inserting a stop cassette in the m129 domain of MCK2 (Wagner et al. 2013), that prevents the formation of the gH/gL/MCK2 complex and results in a truncated protein which should still have the chemokine function. The 129 stop mutant has been characterized and also showed a low capacity to infect macrophages and low titers in salivary glands (Jordan et al. 2011; Wagner et al. 2013).

An MCK2 mutant, which lacks the chemokine function, but retains its entry function was missing at the beginning of the thesis. Saederup et al., 2001, generated an MCK2 mutant called CC mutant, by introducing a point mutation in the m131 domain of MCK2, exchanging two cysteines for glycine (AA 27, 28), assuming that this would eliminate the chemokine activity of MCK2, since these cysteines form disulfide bonds, which are necessary for chemokine function (Clark-Lewis et al., 1995; Rajarathnam et al., 1999). Yet, a profound characterization of this mutant was lacking.

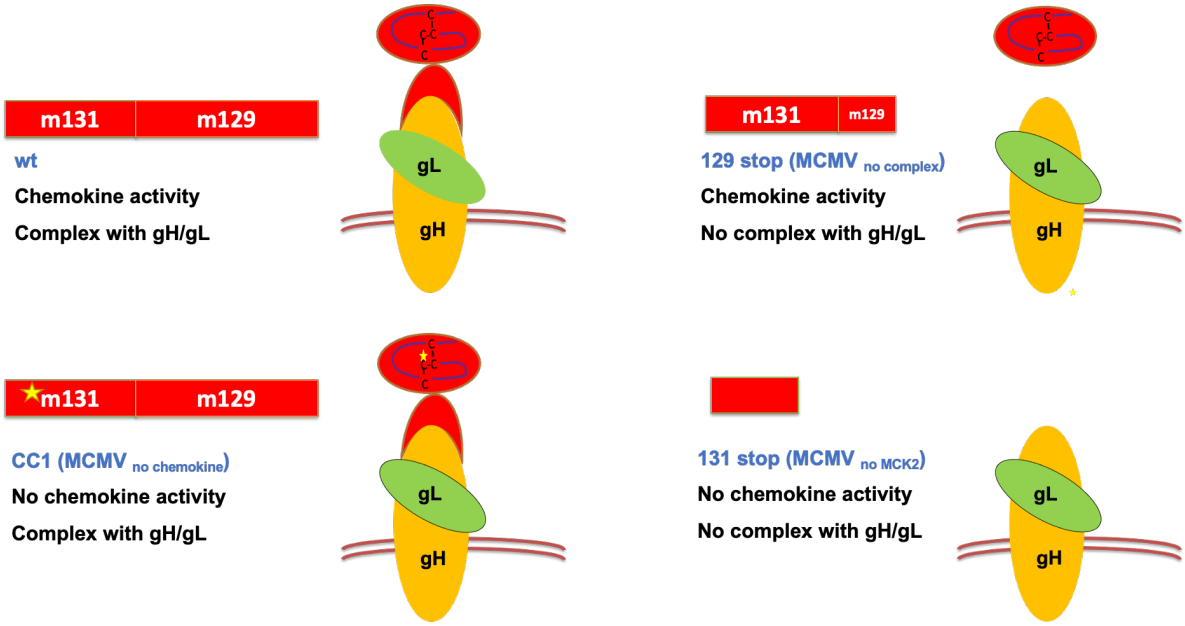

Figure 9: Schematic presentation of MCK2 mutants.

4.1.2 An MCK2 mutant lacking the chemokine function, but still able to form the gH/gL/MCK2 complex

In an attempt to generate an MCK2 mutant, which lacks the chemokine function, a new MCK2 mutant designated CC1 has been generated in the AG Adler. For that, a point mutation was introduced in the m131 domain of MCK2, exchanging the cysteine (TGT) at position 27 for glycine (GGT) (Figure 10). This CC1 mutation was expected to abolish the chemokine activity of MCK2, as the conserved CC motif forms disulfide bonds, which are crucial for the chemokine function (Clark-Lewis et al., 1995; Rajarathnam et al., 1999). Additionally, this subtle mutation should not disturb the protein structure to a degree that MCK2 loses its entry function and cannot form a complex with gH/gL. The starting point of my thesis was focusing on characterization of the CC1 MCK2 mutant and comparing it with the previously characterized MCK2 mutants.

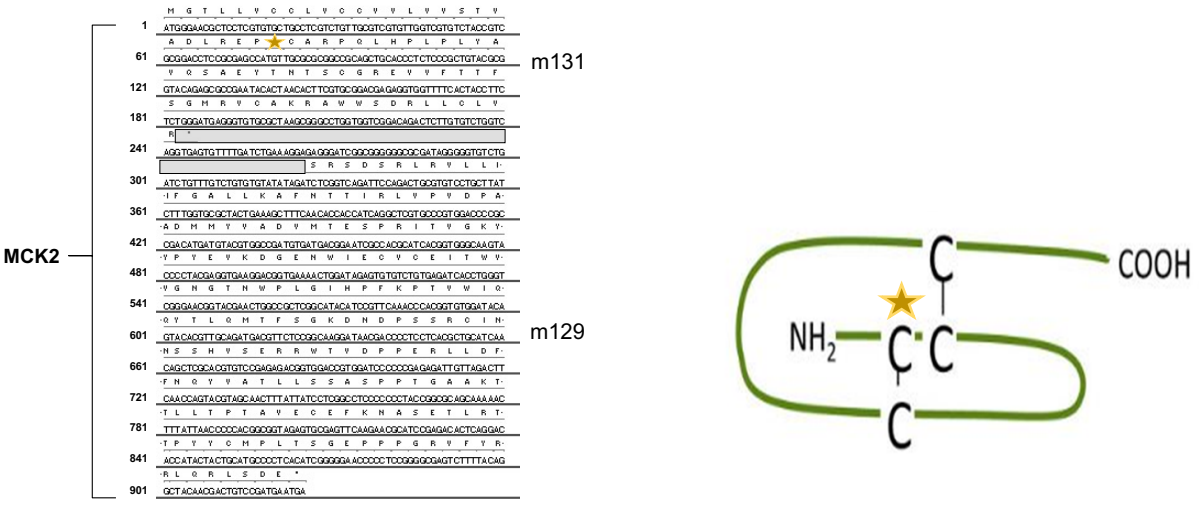

Figure 10: Sequence of MCK2, indicating ORF m131 and ORF m129, * indicates the mutated cysteine in the CC1 MCK2 mutant.

4.1.2.1 Expression of CC1 MCK2

To study the expression of CC1 MCK2, extracts of MEF cells infected with wt MCMV and different MCK2 mutant viruses were analyzed by Western blot. Additionally, the expression of CC/MCK2 protein (mutation in AA 27, 28) (Saederup et al., 2001) was also tested to compare it with the expression of CC1 MCK2 protein (mutation in AA 27). In the Western blot, wt MCK2 has been shown before to appear as several bands due to different levels of glycosylation (MacDonald et al. 1999). In virions, only the most glycosylated band can be detected (Wagner et al. 2013) (Figure 11a). In extracts of infected cells, similar bands were detected for wt MCK2 and CC1 MCK2 mutant protein (Figure 11b). An α-MCK2 (04) antibody was used for detection. This antibody recognizes an epitope in the 129 ORF, which is deleted by the stop cassettes in 129 stop and 131 stop viruses. Therefore, no bands were detected in 131 stop and 129 stop proteins. The expression of MCK2 protein was also analyzed in virions produced by infected NIH3T3 cells. Supernatant virus of wt and MCK2 mutants were resuspended with sample buffer and subjected to SDS-PAGE and Western blot. The detection of MCK2 expression was also performed using α-MCK2 (04) antibody, and in parallel the expression of gB was also investigated to normalize the input of virions. The Western blot shows the expression of CC1 MCK2 and wt MCK2 in these extracts, suggesting that both are integrated in virions very likely as complexes with gH/gL. In contrast, the CC/MCK2 protein ran at a different size in extracts of infected cells and was not detected in extracts of virions (Figure 11c).

This implies that the CC mutant was not able to integrate in virions, very likely because it cannot form a complex with gH/gL. In summary, the expression of the CC1 MCK2 protein in Western blot implies that CC1 MCK2 can form a complex with gH/gL and is equally glycosylated as wt MCK2.

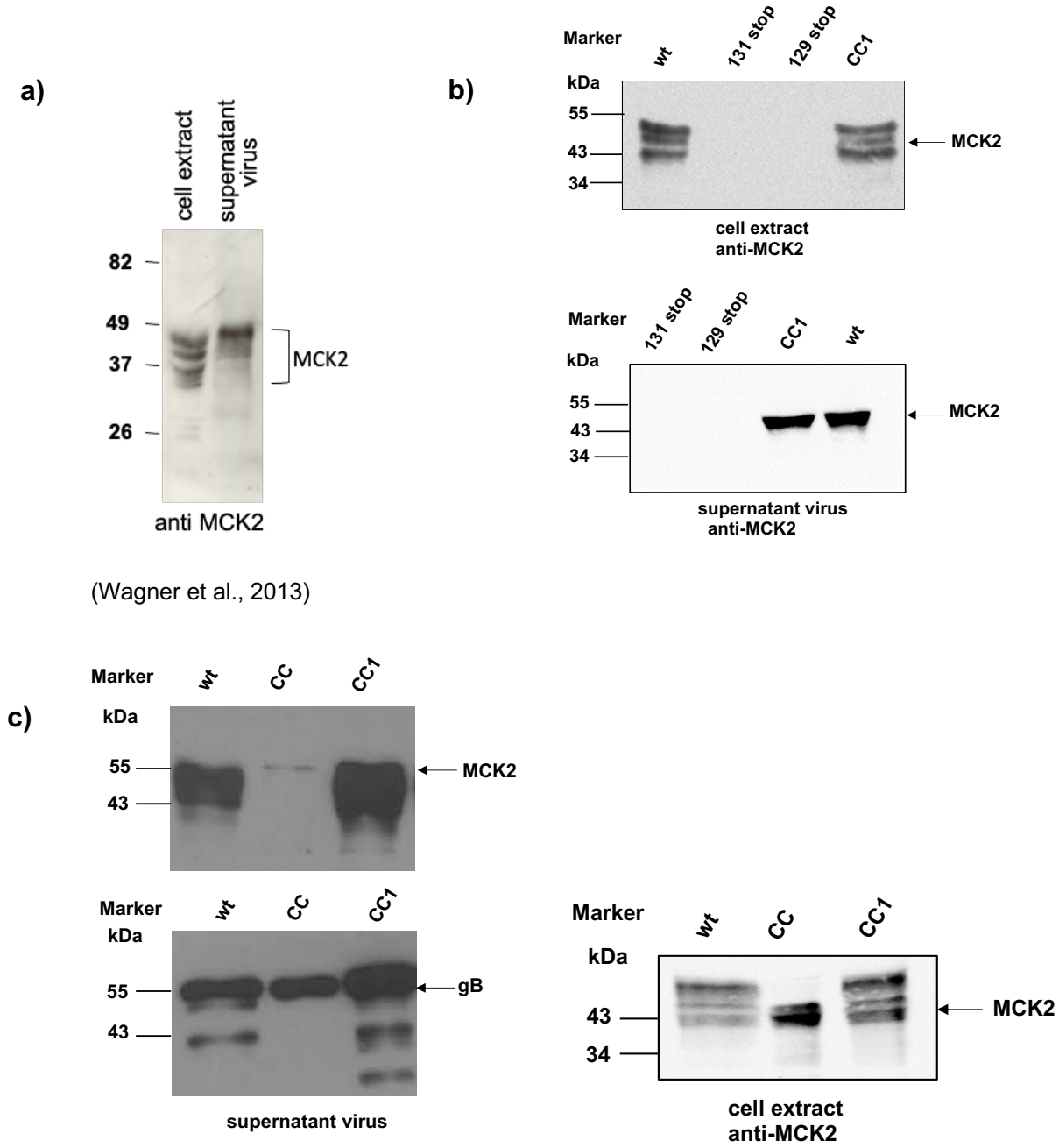

(Wagner et al., 2013)

Figure 11: Expression of MCK2 in infected cells and virions.
a) Expression of MCK2 in cell lysate of infected MEF and supernatant virus produced by infected NIH3T3 (Wagner et al., 2013); b) MCK2 protein expressed by wt MCMV, MCMV 131 stop, MCMV 129 stop, MCMV CC1 in the cell lysate of infected MEF and supernatant virus produced by infected NIH3T3. Primary antibody: mouse α-MCK2 04 (1:1000); Secondary antibody: Polyclonal α-mouse POX (1:1000); c) MCK2 protein expressed by wt MCMV, MCMV CC and MCMV CC1 in the cell lysate of infected MEF and virions. gB expression was detected using mouse α-gB MCMV (5F12).

4.1.3 Validation of the CC1 MCK2

4.1.3.1 Generation of a CC1 Δ m74 MCMV

The infection of MCMV is secured by the entry complexes gH/gL/gO and gH/gL/MCK2. The deletion of one of these entry complexes, would make the entry of MCMV strictly dependent on the other entry complex. To provide evidence that CC1 MCK2 still maintains its entry function as a part of gH/gL/MCK2, a second mutation was generated in MCMV genome carrying the CC1 mutation, to remove gO (m74) of the gH/gL/gO complex. The deletion of gO would make the entry of the CC1 mutant strictly dependent on gH/gL/MCK2. If CC1 MCK2 retained its entry function, a double mutant CC1/delta m74 (CC1 ΔgO) should still be able to grow in culture. Traceless mutagenesis was used to delete 532bp of the m74 ORF, resulting in an N-terminal deletion of 164 amino acids. The strategy is depicted in Figure 12.

First Red-Recombination: Replacement of m74 ORF in the CC1 BAC by KanR

Primer's design is crucial for the ORF deletion by traceless mutagenesis. The primer sequences were designed in a way to contain homologous sequences flanking the m74 region to be deleted, and sequences binding the pEPkan-I-SceI plasmid (Figure 12a). Traceless mutagenesis is based on two red recombination steps. In the first red-recombination of the BAC-mutagenesis, an MCMV genome cloned as a BAC and containing a CC1 mutation was used. KanR was inserted in the CC1 BAC (from here on called "CC1 BACmid"), replacing parts of the m74 ORF by homologous recombination. The homologous recombination in the first recombination step resulted in a removal of the N-terminus of gO, and introduction of the selection marker (KanR) and a flanking I-SceI restriction site. The successful recombination was assessed by restriction digest analysis using *NsiI* restriction enzyme. In successful recombined CC1 BACmid with KAN cassette, the *1 band was cut into two *2 and *3 (Figure 13).

Second Red-Recombination: Removal of KanR from CC1/KanR

The second red-recombination was performed with two clones. It was induced by adding L-arabinose and shifting the growth temperature to 42 °C, which induce the expression of I-SceI restriction enzyme in GS1783 bacteria and recombinases, respectively. As a result, the homologous recombination in the second red recombination led to a traceless removal of KanR (Figure 12b). BACmids were then analysed by using *NsiI* restriction enzyme (Figure 13).

Then, BAC-DNA was sequenced to confirm the deletion of gO and generation of CC1 Δ gO. The sequenced BAC-DNA was transfected into MEF cells and infectious virus could be reconstituted. If CC1 MCK2 did not form a functional gH/gL/MCK2 complex, the reconstitution of virus would not have been possible.

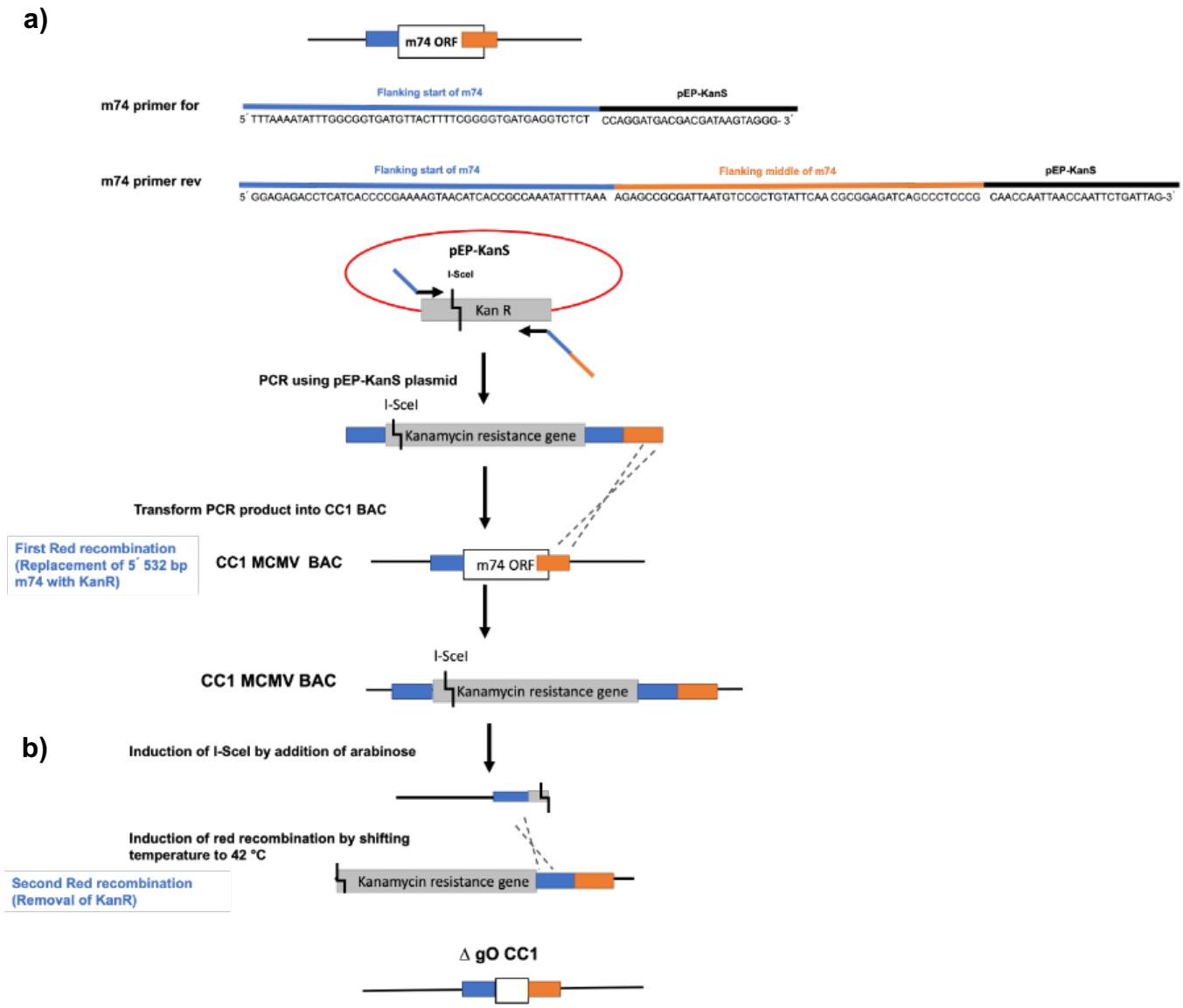

Figure 12: Schematic illustration showing the two recombination steps of traceless mutagenesis to generate CC1 Δ gO. a) KanR was amplified using m74 primer for and m74 primer rev, which contain homologous sequences flanking the m74 region. The PCR product was transformed into GS1783 bacteria contains an MCMV BAC with a CC1 mutation; b) The second recombination was induced by adding L-arabinose and shifting the growth temperature to 42 °C, which induce the expression of I-SceI and recombinases, respectively to remove KanR.

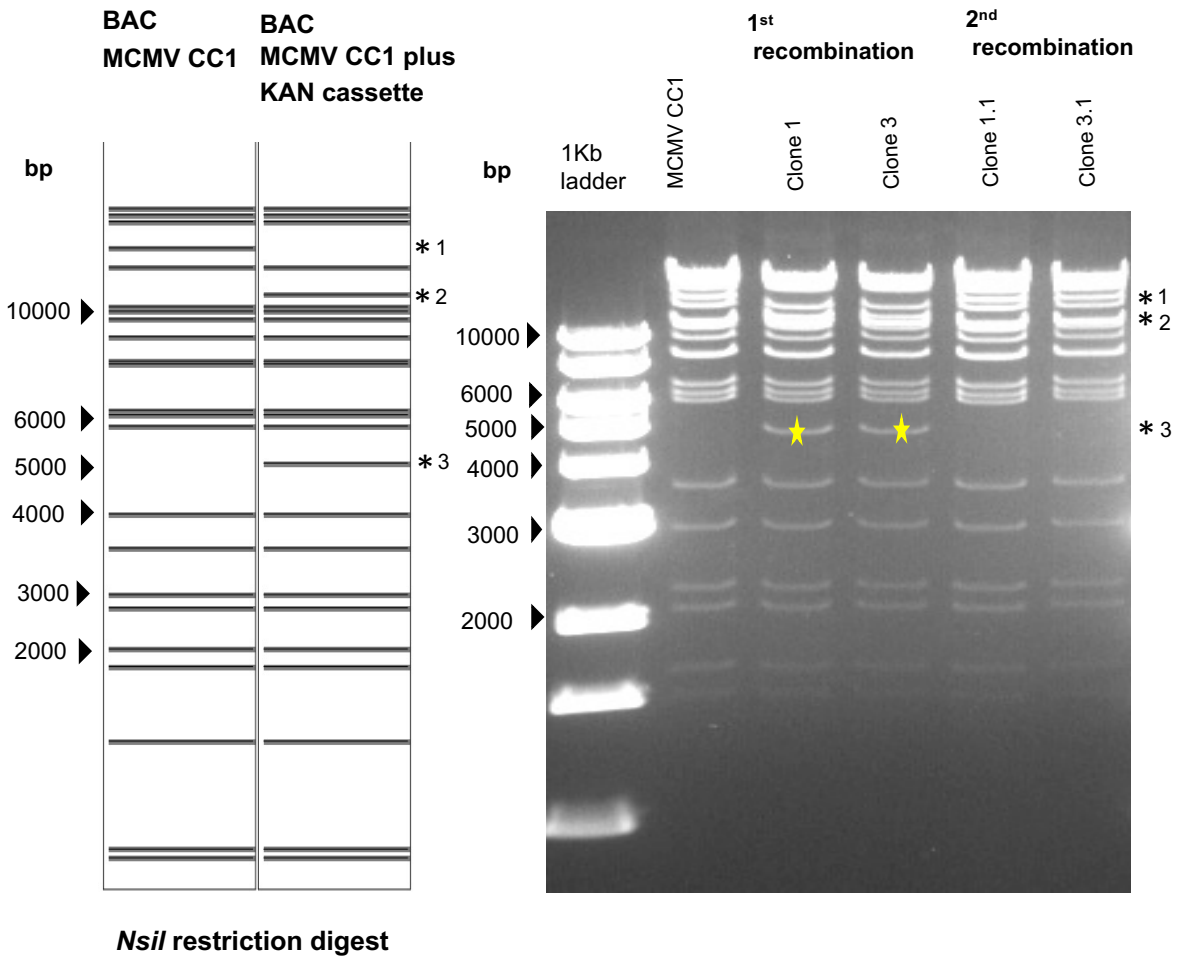

Figure 13: **Restriction analysis of BAC DNA during BAC mutagenesis.**
BAC Midis were digested after first and second red-Recombination with *NsiI* (0.8% agarose gel, 120V, 3 h), * indicates the bands of interest.

4.1.3.2 Growth of the MCMV double mutant CC1 Δ gO in fibroblast culture

MCMV infection of cells is promoted by gH/gL/gO and gH/gL/MCK2 complexes. Growth of MCMV mutants lacking gO (Δ gO) results in an attenuated growth pattern, due to a loss of particle infectivity in Δ gO MCMV. The residual growth depends on gH/gL/MCK2 (Scrivano et al. 2010; Wagner et al. 2013). If the entry function of the CC1 mutant was still intact, CC1 Δ gO mutant should grow like Δ gO. A multi-step growth curve was performed to investigate the growth kinetics of wt MCMV, Δ gO MCMV, and CC1 Δ gO MCMV in fibroblasts (MEF). MEF were infected at an MOI of 0.2. Then virus supernatants were collected every 24 h for five days and viral titers were determined by the $TCID_{50}$ method. The growth of CC1 Δ gO on MEF culture showed a comparable growth pattern to the growth of Δ gO (Figure 14), indicating that

the CC1 mutation does not impair the entry function of gH/gL/MCK2. If the point mutation in CC1 had affected the entry function of MCK2, the growth of CC1 Δ gO would have been different than the growth of Δ gO.

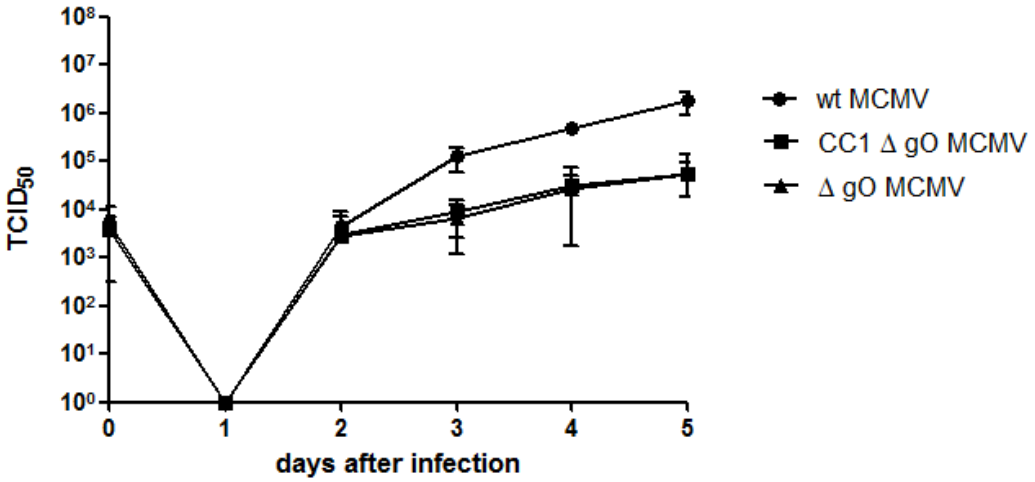

Figure 14: Multi-step growth curve of MCMV double mutants CC1 Δ gO, Δ gO, and wt MCMV. MEF cells were infected with wt, CC1 Δ gO and Δ gO MCMV at an MOI of 0.2. Virus supernatants were harvested every 24 h for five days. Viral titers in these supernatants were determined by the $TCID_{50}$ method. Shown are means +/- SD of three independent experiments.

4.1.4. Evaluation of the chemokine activity of the CC1 MCK2 protein

4.1.4.1 Production of MCK2 recombinant proteins

In order to verify that the CC1 mutant has lost its chemokine activity, a migration assay was performed using J774 macrophages. Recombinant Fc fusion MCK2 proteins, wt MCK2 and CC1 MCK2 cloned a pFuse-hIgG1-Fc2 vector were produced in HEK 293 cells. To do that, HEK 293 cells were transfected with pFuse-hIgG1-Fc2 plasmids expressing the whole reading frame of wt MCK2 and CC1 MCK2. After 48 hours, supernatants from the transfected cells were collected and the supernatant proteins were precipitated, followed by Western blot analysis to confirm the expression of the Fc fusion proteins. As a control, supernatant from cell transfected with pFuse-hIgG1-Fc2 vector was used. Wildtype MCK2 and CC1 MCK2 proteins showed protein bands with comparable sizes around 72 kDa, as shown in Figure 15, which matches with the expected size, since hIgG1-Fc has 26 kDa and MCK2 45 kDa. Fc fusion proteins were also quantified using sandwich ELISA.

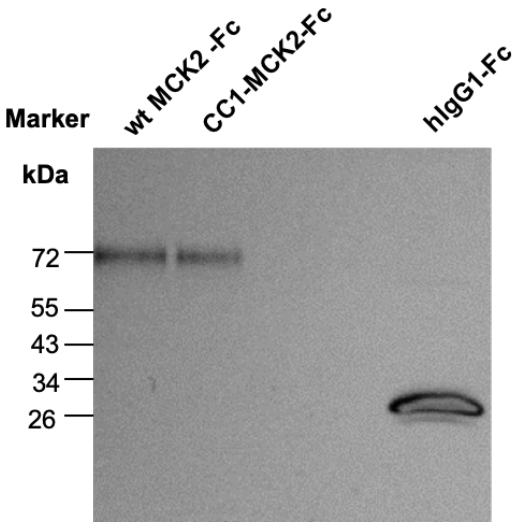

Figure 15: Recombinant MCK2 protein production and quantification.
HEK 293 cells were transfected with pFuse-hIgG1-Fc2 vector expressing wt MCK2 or CC1 MCK2 or a vector control (pFuse-hIgG1-Fc2). After 48 h, the supernatants were harvested from transfected cells and the proteins were precipitated and analyzed by Western blot; A polyclonal anti-human IgG-POX antibody (1:100) (Sigma) was used.

4.1.4.2 Migration assay

After quantification of MCK2 and CC1 MCK2 proteins using an ELISA based on detection of Fc fusion proteins, equal amounts of proteins were used to analyze the chemokine function of MCK2 and CC1 MCK2. The experimental design of the migration assay used is illustrated in Figure 16. Cell culture inserts with a small pore size (5 µm) were chosen to allow J774 MΦ to migrate in response to chemoattractant proteins, but not to fall through the pores. Cell culture inserts containing J774 MΦ cells were added to wells containing supernatants of HEK 293 cells transfected with pFuse-wt MCK2 or pFuse-CC1 MCK2. As a negative control, supernatants from cell transfected with pFuse-hIgG1-Fc2 vector was used. The cells were incubated for 4 h at 37 °C, and during this period the cells could migrate through the membrane of the insert, in response to the chemoattractant activity of the samples. The migrated cells were labelled with calcein-AM and the fluorescence signals measured (excitation: 483-14nm, emission: 530-30nm). For calculation of the exact number of migrated cells, standard curves of different numbers of J774 cells, which were treated equally as the migrated cells were prepared and measured in parallel. As shown in Figure 17, the CC1 MCK2 induced less migration than wt MCK2, suggesting that the CC1 MCK2 protein lost its chemokine activity.

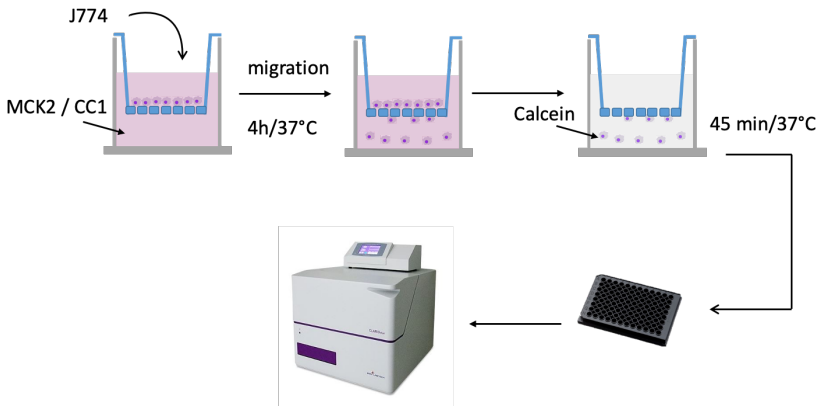

Figure 16: Experimental design of migration assay.
Cell culture inserts containing 1 x 10^5 J774 cells were placed to wells containing supernatants of MCK2 proteins. The cells were incubated for 4 h and the migrated cells were labelled with calcein-AM.

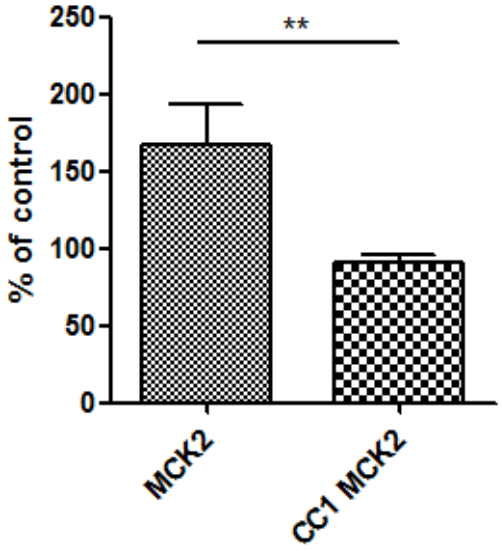

Figure 17: Migration assay to show the chemokine activity of wt MCK2 and CC1 MCK2 protein.
Supernatants containing MCK2 proteins, produced from transfected HEK 293 cells were used in 1 µg/ml concentration as chemotactic stimulus. Supernatant of mock-transfected HEK 293 cells was used as a control. Means +/- SD of three independent experiments are shown. Unpaired student's t-test was performed for statistical analysis (** denotes $p<0.01$).

4.1.5 Analysis of virus growth of MCK2 mutant viruses in fibroblast cultures

Virus growth in cell culture is dependent on entry, replication and spread capacities. It has been shown that HCMV with a mutation in the UL131 gene of the pentameric complex grew differently in fibroblast cultures than wildtype virus (Wang and Shenk 2005; Adler et al. 2006). Multi-step growth curves were performed to evaluate the growth kinetics of the CC1 MCK2 mutant and compare it with other MCK2 mutants. MEF were infected with wt MCMV, CC, CC1, 129 stop, and 131 stop mutants of MCMV

at an MOI of 0.2, and the growth of viruses was monitored for 5 days by harvesting of the virus supernatant every 24 h. Viral titers were determined by the $TCID_{50}$ method for all of the collected samples in parallel. The results demonstrate that 131 stop and 129 stop mutants showed higher titers of virus in the supernatant than wt MCMV (Figure 18). Notably, the CC1 MCK2 mutant grew like wt MCMV, indicating that the CC1 mutant grow on fibroblasts with the same kinetics as wt MCMV. The CC/MCK2, which was used in another study (Saederup et al., 2001) grew like the 131 stop mutant, confirming the data from Western blots, which indicated that this mutant behaves like a 131 mutant and cannot form a functional gH/gL/MCK2 complex.

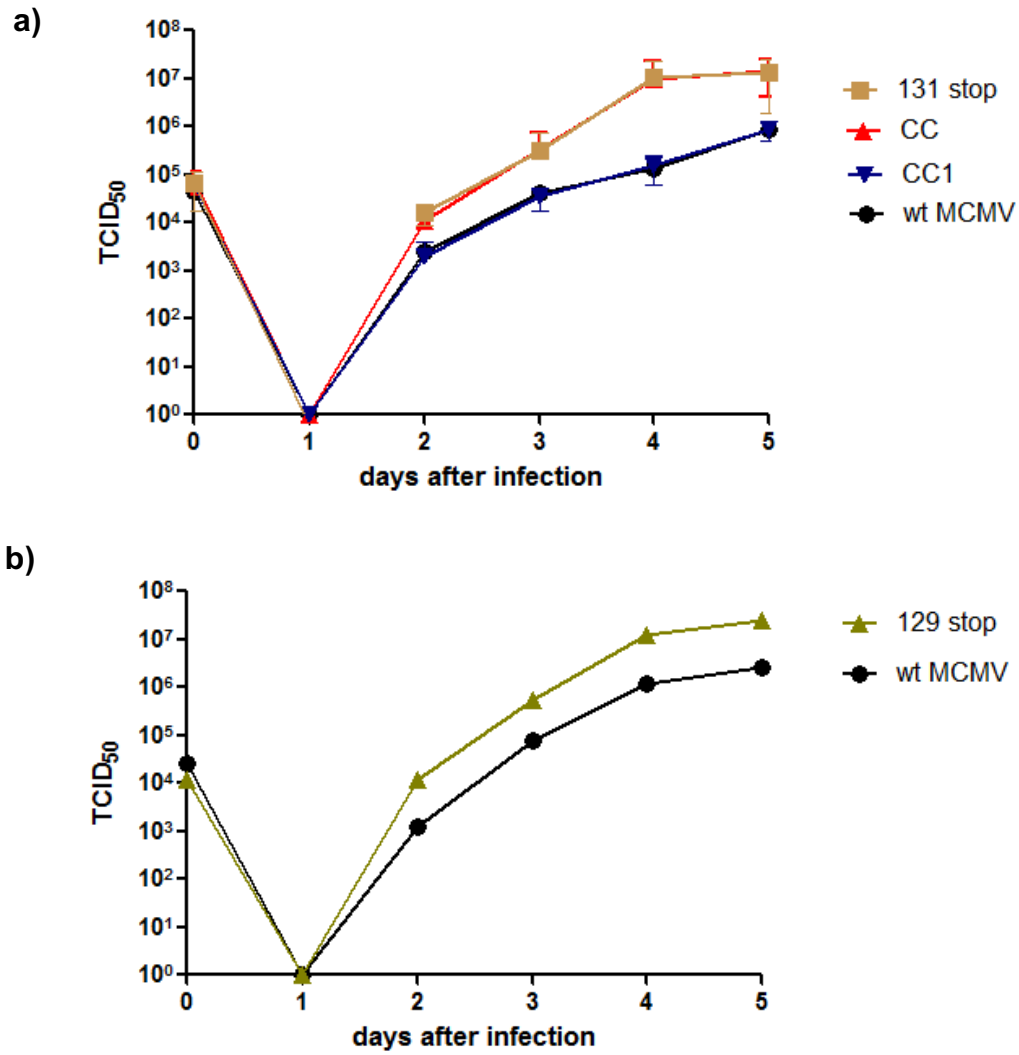

Figure 18: Multi-step growth curve of different MCK2 mutant viruses on fibroblasts.
a) MEF cells were infected with wt MCMV and different MCK2 mutant viruses at an MOI of 0.2. Virus supernatants were periodically harvested every 24 hr. Viral titers were determined by the $TCID_{50}$ method for all of the collected samples in parallel. Shown are means +/- SD of three independent experiments; b) MEF cells were infected with wt MCMV and 129 stop viruses at an MOI of 0.2, virus supernatants were harvested every 24 hr. Shown is one representative experiment.

4.1.6 MCK2 and viral cell tropism

From now on, wt MCMV will called "**wt**", CC1 mutant "**MCMV $_{\text{no chemokine}}$**", 129 stop mutant "**MCMV $_{\text{no complex}}$**" and 131 stop mutant "**MCMV $_{\text{no MCK2}}$**".

MCMV has a broad cell tropism, including its tropism for hematopoietic cells like dendritic cells or macrophages (Krmpotic et al., 2003). It has been shown that infection of macrophages was impaired after infection with MCMV MCK2 mutants, either lacking the complete MCK2 or no longer able to form the gH/gL/MCK2 complex (Wagner et al. 2013). Using the above described MCK2 mutants, these studies were extended and the contribution of MCK2 to infection of monocytes was investigated. ANA-1, a mouse macrophage cell line established from bone marrow cells of C57BL/6 mice (Cox et al., 1989) and D2SC1, an immortalized dendritic cell line, were infected with wt and the above mentioned MCK2 mutants at an MOI of 1 for 2 h. The next day, the infection capacity was evaluated by determining the percentage of infected ANA-1 and D2SC1 cells using intracellular FACS staining for MCMV IE1 protein. As shown in Figure 19, infection of ANA-1 and D2SC1 cells with MCMV lacking MCK2 or unable to form the gH/gL/MCK2 complex was highly impaired. In contrast, infection of the cells with wt MCMV or MCK2 mutant lacking only the chemokine function, showed a comparable infection efficiency. This suggests that reduced infection of macrophages and dendritic cells correlated with a loss of the gH/gL/MCK2 complex.

In summary, the characterization of MCK2 mutants *in vitro* showed that, the MCK2 mutant lacking only the chemokine function behaves like wt MCK2, with regard to entry and infection of fibroblasts, macrophages and dendritic cells.

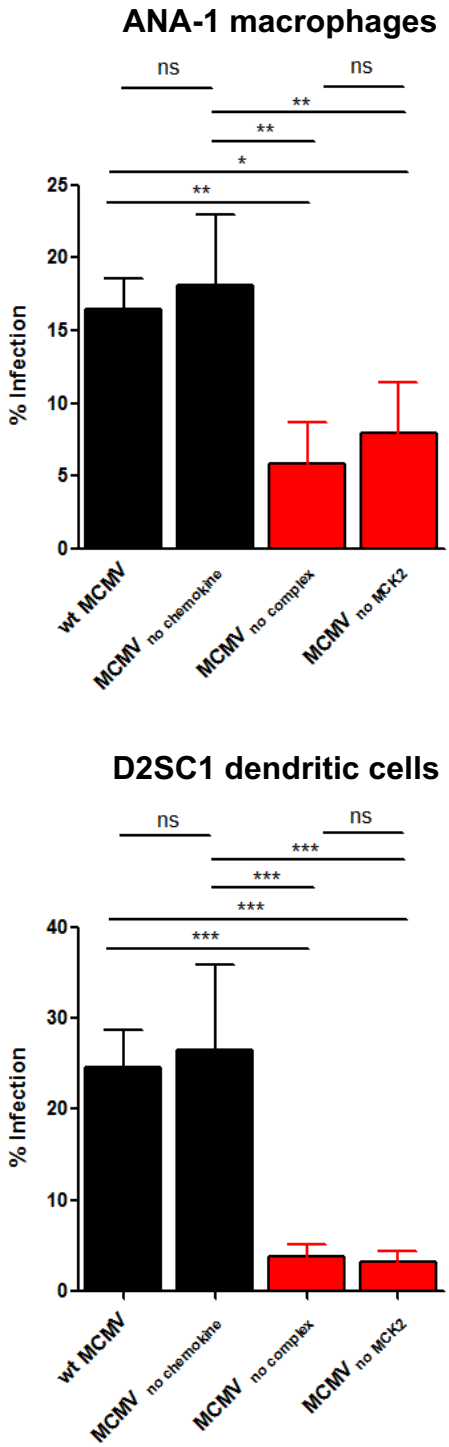

Figure 19: Comparison of the infection capacity of wt MCMV and different MCK2 mutant viruses for monocytes.

ANA-1 and D2SC1 cells were infected with wt MCMV and different MCMV MCK2 mutants at an MOI of 1. After 24 h, the number of infected cells were determined by intracellular FACS analysis specific for MCMV ie1 protein. Shown are means +/- SD of three independent experiments. One-way ANOVA with Tukey post-test was performed for statistical analysis (n.s. denotes $p>0.05$; * denotes $p<0.05$; ** denotes $p<0.01$; *** denotes $p<0.001$). Black bars indicate MCK2 mutants, which form the gH/gL/MCK2 complex, red bars indicate MCK2 mutants, which no longer form the gH/gL/MCK2 complex.

4.2 The role of the MCK2 chemokine and the role of the gH/gL/MCK2 entry complex in the MCMV infection *in vivo*

Investigation of aspects of virus infection like dissemination and interference with host immune responses can only be studied *in vivo*. It has been reported before that MCK2 contributes to MCMV dissemination and immunomodulation of the host's immune response (Saederup et al., 2001; Stahl et al., 2015; Wikstrom et al., 2013; Daley-Bauer et al., 2014; Daley-Bauer et al., 2012; Farrell et al. 2019a; Jordan et al., 2011; Wagner et al., 2013; Farrell et al., 2016). It has not been determined whether dissemination and regulation of the immune response is shaped by the chemokine activity of MCK2 or its entry function as part of the gH/gL/MCK2 complex or by both. In order to address this question, infection of BALB/c mice with MCMV was used as a model. BALB/c mice were chosen because they are more susceptible to MCMV infection, since BALB/c mice lack the NK cell receptor Ly49H. Thus, they are unable to mount a massive NK cell response. Consequently, the clearance of MCMV infection in BALB/c mice depends mainly on the adaptive immune response, in particular $CD8^+$ T cells (Reddehase et al., 2002; Schleiss, 2013). Additionally, BALB/c mice have been widely used in many of MCK2 studies (Fleming et al., 1999; Saederup et al., 2001; Jordan et al., 2011; Daley-Bauer et al., 2012; Wikstrom et al., 2013; Farrell et al., 2016; Farrell et al., 2019a).

BAC-derived wildtype murine cytomegalovirus and the above described MCK2 mutants were propagated in NIH3T3 cells and purified on a sucrose cushion as described in materials and methods (3.6.4). Virus titers were determined by a plaque assay on MEF cells. Female inbred BALB/c mice (6 weeks) were housed in individually ventilated cages in pathogen-free environment. The mice were infected intraperitoneally (i.p.) with 2×10^5 PFU of wt MCMV or MCMV MCK2 mutants in 150 µl volume of PBS. The mice were sacrificed at different timepoints after infection, and the organs were harvested (Figure 20).

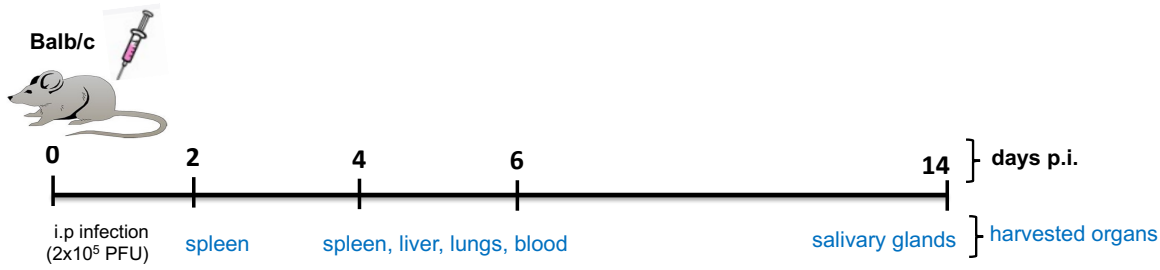

Figure 20: Schematic illustration of the *in vivo* experimental design.
BALB/c mice were infected i.p. with 2 × 10^5 PFU of wt MCMV or MCMV MCK2 mutants. The mice were sacrificed at the indicated timepoints, and the organs were harvested.

4.2.1 The role of MCK2 in MCMV dissemination *in vivo*

4.2.1.1 Viral dissemination to salivary glands

After infection of mice with MCMV, virus disseminates from primary sites of infection to distal organs like salivary glands via recruitment of monocytic peripheral blood leukocytes (Collins et al., 1994; Stoddart et al., 1994; Daley-Bauer et al., 2014). It has been shown that infection of mice with MCMV lacking MCK2, results in lower titers in the salivary glands, than in mice infected with wt MCMV (Fleming et al., 1999; Saederup et al., 2001; Jordan et al., 2011). The efficient infection of salivary glands in mice infected with wt MCMV could be driven by the chemokine activity of MCK2 and recruitment of monocytes, or gH/gL/MCK2-dependent infection of monocytes cells, which act as vehicles to disseminate the infection to the salivary glands. Therefore, the contribution of MCK2 to infection of salivary glands was investigated. BALB/c mice were infected i.p. with 2 × 10^5 PFU of wt MCMV or MCK2 mutants, and at day 14 post-infection (p.i.), salivary glands were harvested, homogenized and the titers were determined by a plaque assay. Figure 21 shows that mice infected with wt MCMV or MCMV $_{\text{no chemokine}}$, which can form the gH/gL/MCK2 entry complex showed 2 logs higher titers in the salivary glands than MCK2 mutants, which are unable to form the gH/gL/MCK2 entry complex. This suggests that MCMV infection of salivary glands is promoted by the gH/gL/MCK2 complex and independent of the chemokine function of MCK2. It has recently been reported that both MCK2-negative MCMV and wt MCMV are equally effective in seeding the initial infection in salivary glands at day 5 p.i. (Farrell et al., 2019a).

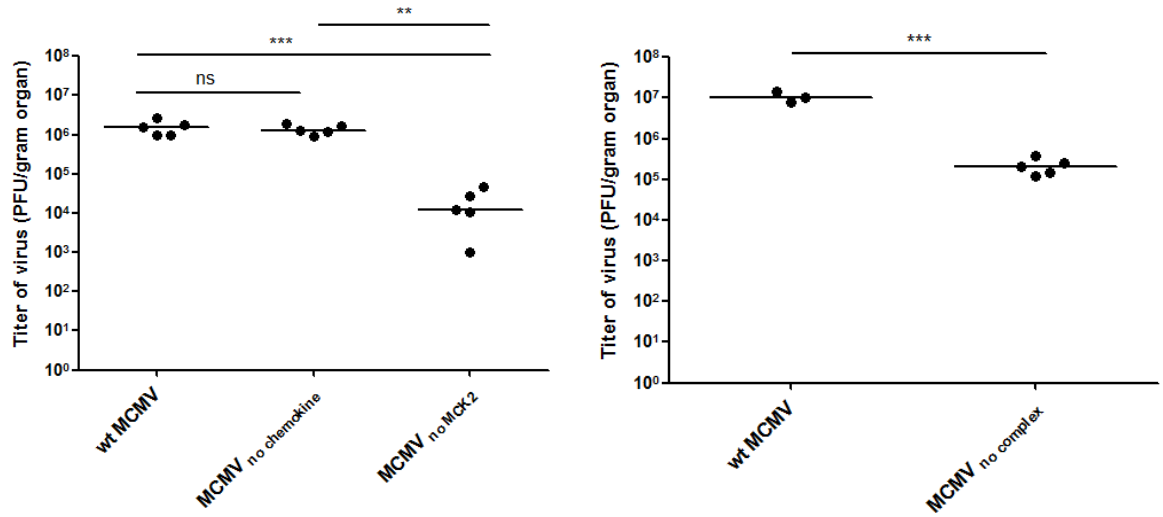

Figure 21: Dissemination of MCMV to the salivary glands is gH/gL/MCK2 complex-dependent. BALB/c mice were infected with 2 × 10^5 PFU of wt MCMV or MCK2 mutants. The mice were sacrificed at day 14 (p.i.) and the salivary glands were harvested and homogenized. Virus titers were determined by a plaque assay on MEF. Viral titers are expressed as PFU/g organ. Each symbol represents an individual mouse, and the bars represent the median. The data are from three independent experiments. One-way ANOVA with Tukey post-test was performed for statistical analysis (n.s. denotes p>0.05; ** denotes p<0.01; *** denotes p<0.001).

4.2.1.2 Infection of peripheral blood leukocytes

Blood-borne myeloid cells are infected during acute MCMV infection (Collins et al., 1994; Farrell et al., 2019a). It has been shown that the number of infected peripheral blood leukocytes is lower in mice infected with MCMV lacking MCK2 mutant at day 5 p.i. than in wt MCMV infections (Saederup et al., 1999; Saederup et al., 2001). In contrast, recent studies suggested that there is no difference between the numbers of infected leukocytes in blood infected with wt MCMV and those infected with MCMV lacking MCK2 (Farrell et al., 2016; Farrell et al., 2019a). The infection of leukocytes with wt MCMV or different MCK2 mutants was studied to address this discrepancy. BALB/c mice were infected i.p. with 2 × 10^5 PFU of wt MCMV or MCK2 mutants, and at day 4 p.i. non-coagulated blood samples were harvested and used for extraction of DNA from leukocytes. MCMV genomes were quantified by real time PCR. Absolute quantification of viral genes was performed using the plasmid pDrive_gB_PTHrP, which harbors the sequence of MCMV M55/gB and the sequence of the cellular gene mouse parathyroid hormone-related protein-encoding gene (PTHrP) needed to normalize for cellular DNA. The data are presented as viral genome copy numbers relative to the copy number of PTHrP.

No statistically significant differences could be observed between wt MCMV and MCK2 mutants in infection of leukocytes (Figure 22a). These findings contradict (Saederup et al. 1999, 2001) studies, but confirm the data of (Farrell et al., 2016; Farrell et al., 2019a) studies. To make sure that this contradiction is not due to the assay used, the same assay was used as in (Saederup et al., 1999, 2001) studies. After collection of non-coagulated blood samples at day 4 p.i., peripheral blood leukocytes (PBL) were isolated, counted and cocultured with MEF cells. After 14 hours, the cells were overlaid with carboxymethylcellulose. Infected leukocytes get activated after contact with fibroblasts and infect MEF cells, and accordingly plaques were formed. Two days later, the cells were stained with crystal violet and the number of the plaques were counted and thus the percentage of infected leukocytes calculated. Again, the numbers of infected PBL cells were comparable for wt MCMV and MCK2 mutants (Figure 22b), suggesting that the infection of leukocytes during acute MCMV infection is MCK2-independent. The data from the two assays contradict (Saederup et al., 1999, 2001) studies, but are in consistence with (Farrell et al., 2016; Farrell et al., 2019a).

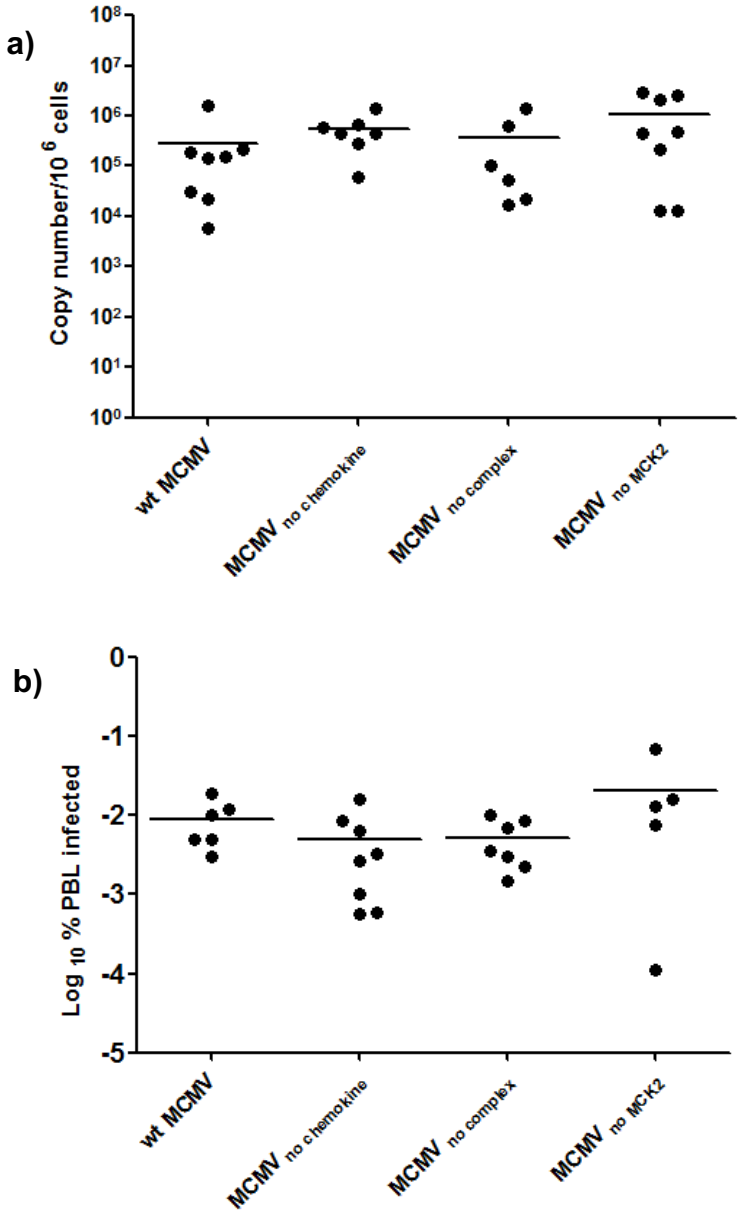

Figure 22: Infection of PBL with wt MCMV or MCK2 mutants.
BALB/c mice were infected i.p. with wt MCMV or MCK2 mutants and non-coagulated blood was collected at day 4 p.i. a) DNA was extracted from leukocytes and qPCR was performed to amplify both of gB and PTHrP genes. The data are from three independent experiments; b) PBL were isolated and subjected to an infection center assay on MEF cells. The data are from two independent experiments. Each symbol represents an individual mouse, the horizontal lines show means.

4.2.2 Effect of MCK2 on virus virulence and pathogenesis

Acute MCMV infection results in splenomegaly, which occurs in mice as a result of extramedullary hematopoiesis (EMS) (Jordan et al., 2013; Leung et al., 1991; Lucia & Booss, 1981). The role of MCK2 in the development of splenomegaly after MCMV infection was investigated. BALB/c mice were infected i.p. with 2 × 10^5 PFU of wt MCMV or MCK2 mutants and the mice were killed at days 0, 2, 4, and 6 p.i. and spleens weighed. As shown in Figure 23, the weights of the spleens in all groups increased over the course of early infection. Interestingly, mice infected with the MCMV $_{\text{no MCK2}}$ mutant exhibited slightly, but significantly bigger spleens at days 4 p.i, when compared to wt MCMV-infected mice. Statistical analysis was evaluated using one-way ANOVA with Dunnett test and the spleens weights of mice infected with wt MCMV was considered as a control group.

To evaluate the virulence of MCK2 mutant viruses, the weights of mice were monitored over 5 days. All groups with the exception of the MCMV $_{\text{no MCK2}}$ mutant showed a slight weight loss (about 5%) between day 2 and 4 (Figure 24). Interestingly, MCMV $_{\text{no MCK2}}$ showed weight increase like expected for non-infected mice. Original weights were restored for all groups at day 5. The data indicate that MCK2 may be involved in host-virus interaction and pathogenesis, thus the absence of MCK2 expression might reduce the virulence of MCMV infection on mice.

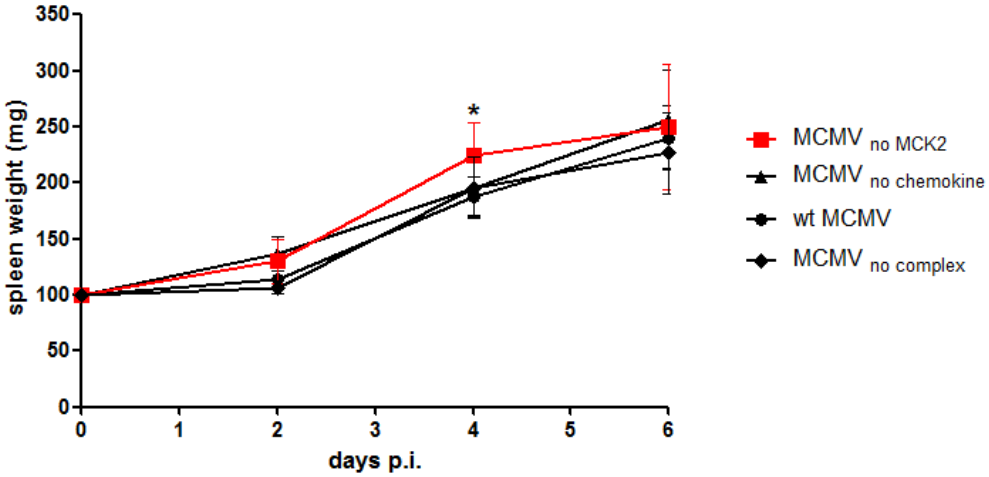

Figure 23: Spleen weight after infection with different MCK2 mutants.
BALB/c mice were infected i.p. with 2 × 10^5 PFU of wt MCMV or MCK2 mutants. The mice were sacrificed at day 0, 2, 4 and 6 p.i. and the spleens were harvested, and weights of spleens were determined. Spleen weight is shown as means ±SD of (6-9) mice per group. The data were pooled from two independent experiments. Statistical analysis was assessed by one-way ANOVA with Dunnett test (* denotes $p<0.05$).

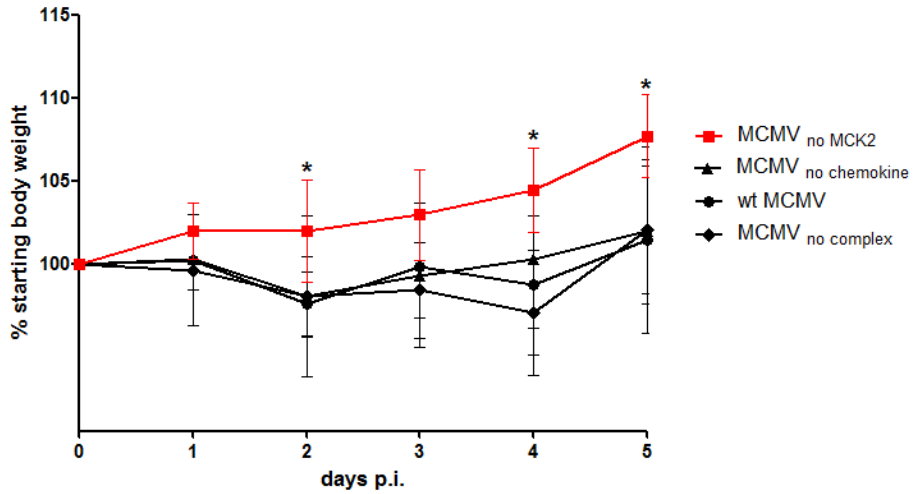

Figure 24: Monitoring of weight loss after infection with different MCK2 mutants.
BALB/c mice were infected i.p. with 2 × 10^5 PFU of wt MCMV or MCK2 mutants. Mice were weighed daily over 5 days. The weights of mice are expressed as percentage of original weight. Weight loss is shown as means ±SD of (6-9) mice per group. The data were pooled from two independent experiments. Statistical analysis was assessed by one-way ANOVA with Dunnett test (* denotes $p<0.05$).

4.2.3 Investigating the immunomodulatory activity of MCK2

It has been reported that MCK2 shapes the innate and adaptive immune responses early after the infection. MCK2 expression is associated with eliciting higher production of IFN-α during the early stage of viral infection (Wikstrom et al. 2013). Furthermore, the immunomodulatory activities of MCK2 result in an inhibition of early $CD8^+$ T cell response specific for IE1 and a delay of virus clearance within the host (Daley-Bauer et al., 2012; Wikstrom et al. 2013). It is not known whether these immunomodulatory activities are driven by the chemokine function of MCK2 or its entry function as a part of the gH/gL/MCK2 entry complex or both.

4.2.3.1 The role of MCK2 in virus clearance

Contradictory observations have been reported for the role of MCK2 in the early clearance of MCMV infection from organs. (Saederup et al., 2001) observed that MCMV infection was equally cleared from liver and spleen after infection of BALB/c with wt MCMV or MCMV lacking MCK2, and no differences were detected between wt MCMV and MCK2-negative MCMV. In contrast, it has been shown that infection of BALB/c mice with MCK2-negative MCMV was cleared more rapidly from liver and spleen at day 5 p.i. (Fleming et al., 1999) or spleen at day 6 p.i. (Wikstrom et al. 2013), or lung and spleen at day 5 p.i. (Daley-Bauer et al., 2012), compared to delayed

clearance after infection with wt MCMV. Therefore, it was of interest to test the clearance of MCMV infection from organs using the complete set of MCMV MCK2 mutants. The potential role of MCK2 in the early clearance of MCMV infection from organs was investigated. BALB/c mice were infected i.p. with 2×10^5 PFU of wt MCMV or MCK2 mutants. At day 4 and 6 p.i., mice were sacrificed, and spleens, livers and lungs harvested. Before titration, spleen, liver and lung homogenates were prepared. Then, the samples were titrated on MEF cells using a plaque assay.

Similar viral titers in the spleens (Figure 25a) and livers (Figure 25b) were observed at day 4 in all groups, then the infection with wt MCMV or MCK2 mutants was controlled equally at day 6 and the viral titers in the spleens and livers decreased, without any differences between wt MCMV and MCK2 mutants. Consequently, the data suggest that clearance of MCMV infection from spleen and liver is MCK2-independent. These results are in contradiction with previous studies (Fleming et al., 1999; Daley-Bauer et al., 2012; Wikstrom et al., 2013), which showed an earlier clearance of infection from spleen infected with MCK2-negative MCMV, although not consistently.

Viral titers in lungs are shown in Figure 25c. Viral titers of the MCMV $_{\text{no MCK2}}$ mutant were significantly reduced at day 6 p.i, compared to day 4. Additionally, also the viral titers of the MCMV $_{\text{no chemokine}}$ mutant decreased in lungs at day 6 p.i., however it was not significant. In contrast, there was no significant difference between viral titers of wt MCMV in lungs at day 4 and day 6, and the titers of the MCMV $_{\text{no complex}}$ mutant in the lungs even increased at day 6 p.i. This implies that infection with the MCMV $_{\text{no MCK2}}$ mutant was controlled much better in lungs at day 6 p.i., suggesting that MCK2 may contribute to the virulence of MCMV infection in lungs.

To sum up, the role of MCK2 in the early clearance of infection from organs was investigated here for the first time using a complete set of MCK2 mutants, including the MCK2 mutant, which lacks only the chemokine function of MCK2. The data here conclude that early clearance of MCMV infection from lungs is mediated by MCK2, whereas MCK2 is redundant for the clearance of MCMV infection from spleen and liver.

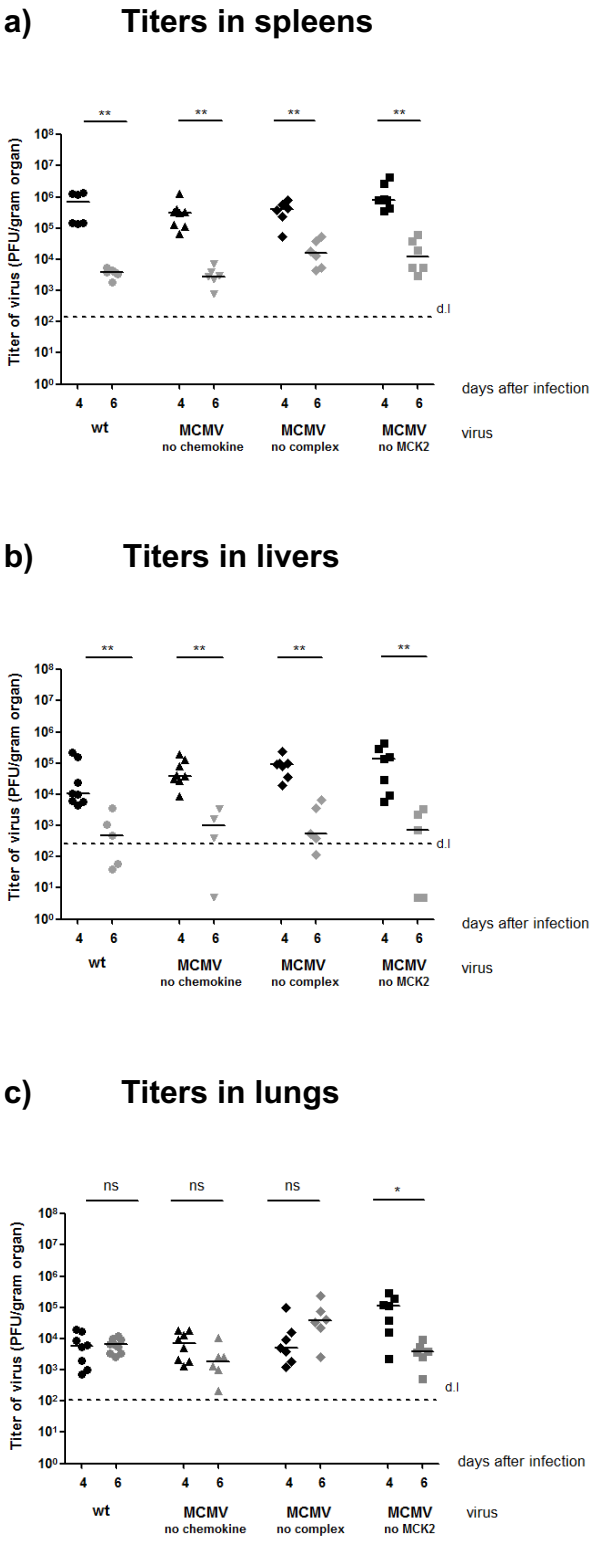

Figure 25: Viral clearance in organs after infection of mice with MCK2 mutants.
BALB/c mice were infected i.p. with 2 × 10^5 PFU of wt MCMV or MCK2 mutants. Mice were sacrificed at day 4 and 6 p.i., and spleens, livers and lungs were harvested and homogenized. The titers were determined by a plaque assay on MEF. Viral titers are expressed as PFU/g organ, each symbol represents an individual mouse, and the bars represent the median, dashed lines show the detection limit (d.l). The data are from two independent experiments. Mann-Whitney test was performed for statistical analysis (n.s. denotes p>0.05; * denotes p<0.05; ** denotes p<0.01).

4.2.3.2 MCK2 and the early anti-MCMV CD8$^+$ T cell response

4.2.3.2.1 IE1-specific CD8$^+$ T cell responses

It has been reported that infection of BALB/c mice with MCK2-negative MCMV results in an enhanced immediate early 1 (IE1)-specific CD8$^+$ T cell response at day 4 (Wikstrom et al. 2013) and day 7 p.i. (Daley-Bauer et al. 2012). To find out whether the differences observed in viral clearance from lungs (Figure 25c) are reflecting differences in CD8$^+$ T cell responses, the early CD8$^+$ T cell response was studied. Stimulation of CD8$^+$ T cells with an IE1-peptide was used. The H2L^d-restricted peptide (sequence: YPHFMPTNL) from IE1 of MCMV is one of the best characterized T-cell epitopes of MCMV (Reddehase, 2002; Volkmer et al., 1987; Andrews et al., 2008). BALB/c mice were infected with 2 × 10^5 PFU of wt MCMV or MCK2 mutants, spleens were harvested at day 4 p.i. and processed for single-cell suspensions. 1 × 10^6 splenocytes cells /well were stimulated with m123/IE1 peptide of MCMV in 1 µg/mL concentration. Cells were stimulated also with IE scrambled peptide (Sequence: NFYPTLPHM) as a negative control. After 1h, Brefeldin A Solution (1 µl/ml) was added for each well and the cells were incubated for further 5 h. In order to determine the percentage of IFN-γ producing CD8$^+$ T cells, the cells were stained for anti-CD8$^+$ surface marker, followed by intracellular staining for IFN-γ. The samples were measured using BD FACSCalibur^{TM} (BD Biosciences) and the analysis of the data was performed with the Flowing Software 2.5.1, gating strategy shown in Figure 26. Interestingly, infection of mice with the MCMV $_{\text{no chemokine}}$ or MCMV $_{\text{no MCK2}}$ mutants elicited higher percentage of IFN-γ-producing CD8$^+$ T cells, compared to wt MCMV or the MCMV $_{\text{no complex}}$ mutant (Figure 27). The data reveal that enhanced early CD8$^+$ T cell responses were detected only in mice infected with MCK2 mutants, which lack the chemokine function, suggesting an inhibitory effect of the chemokine activity of MCK2 on early CD8$^+$ T cell responses.

Taking together, the early clearance of infection from lungs infected with MCK2 mutants lacking chemokine function (Figure 25c) was correlated with an enhanced IE1-specific CD8$^+$ T cell response. This implies that early clearance of infection from lungs was driven by an elevated early CD8$^+$ T cell response.

These results are in consistence of previous studies (Wikstrom et al., 2013; Daley-Bauer et al. 2012), confirming the elevated early $CD8^+$ T cell response in mice infected with MCMV $_{no\ MCK2}$. Additionally, the data here provide the first evidence that the interaction between MCK2 and early $CD8^+$ T cell response during acute MCMV infection is driven by the chemokine function of MCK2.

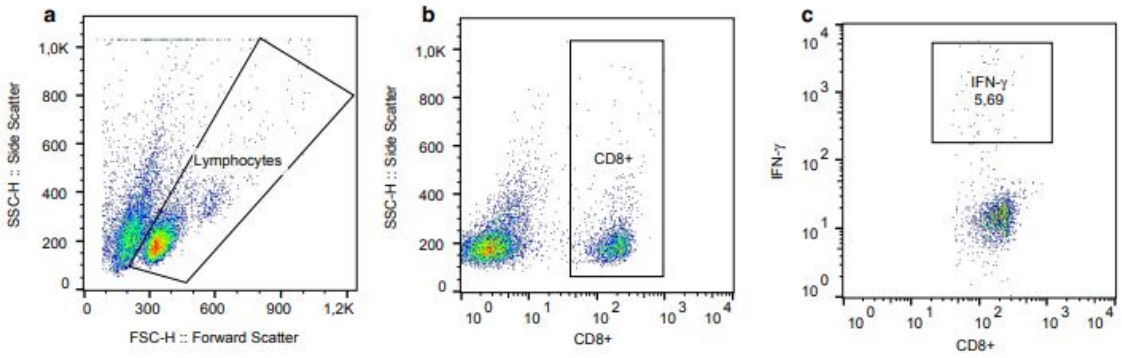

Figure 26: Gating strategy for IFN-γ positive $CD8^+$ T cells in splenocytes after stimulation with IE1 peptide. Lymphocytes were selected based on forward scatter height (FSC-H) and side scatter (SSC-H) (panel a). $CD8^+$-positive cells (b) were analyzed for intracellular IFN-γ (c).

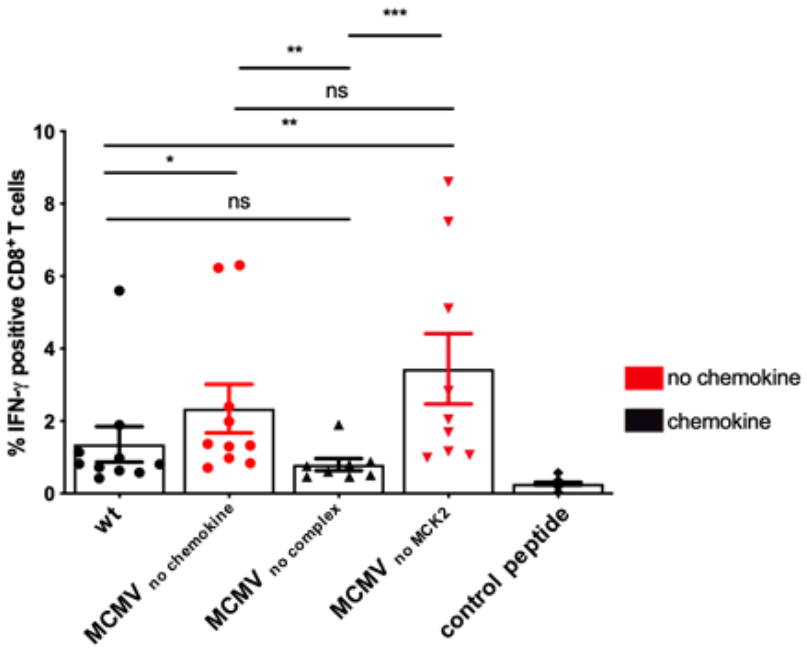

Figure 27: Enhanced IE1-specific CD8⁺ T cell response after infection with MCMV mutants lacking the MCK2 chemokine activity.
BALB/c mice were infected i.p. with 2 × 10^5 PFU of wt MCMV or MCMV MCK2 mutants. The mice were sacrificed at day 4 p.i. and spleens were harvested. Single-cell suspensions were prepared, 1 × 10^6 splenocytes cells /well were stimulated with IE1-peptide or scrambled peptide (control peptide) or PMA/Ionomycin as a positive control for 6 h. The cells were surface stained with an anti-CD8⁺ antibody for 30 min, followed by Intracellular staining for IFN-γ and the samples were measured by FACS. Three independent experiments were performed, and results were pooled (n=8-10 mice/group) and shown as group means +/- SEM. Each symbol represents one mouse. Mann-Whitney test was performed for statistical analysis (n.s. denotes p>0.05; * denotes p<0.05; ** denotes p<0.01; *** denotes p<0.001).

4.2.3.2.2 M45-specific CD8⁺ T cell response

It was of interest to investigate other MCMV-specific CD8⁺ T cell responses. The M45-derived peptide (Sequence: HGIRNASFI) is an epitope triggering a conventional MCMV-specific CD8⁺ T response with a peak at day 7 p.i. after MCMV infection in C57BL/6 mice (Munks et al., 2006; Dekhtiarenko et al., 2013).

Infection of C57BL/6 mice were chosen as most of M45 epitopes are identified for $H2L^b$-restriction. C57BL/6 mice were infected i.p. with 5×10^5 PFU of wt MCMV or MCK2 mutants. Spleens were harvested at day 8 p.i., the splenocytes were stimulated with M45 peptide for 6 h. Stimulation with M45 peptide resulted in a high M45-specific $CD8^+$ T cell response in all groups (Figure 28). Notably, the highest M45-specific $CD8^+$ T cell response was detected in mice infected with the MCMV $_{\text{no MCK2}}$ mutant, which was significantly higher than those in mice infected with wt MCMV. Again, the MCMV $_{\text{no MCK2}}$ infection showed an elevated stimulation, but this time no pattern was detected for a chemokine-dependency of increased T cell responses.

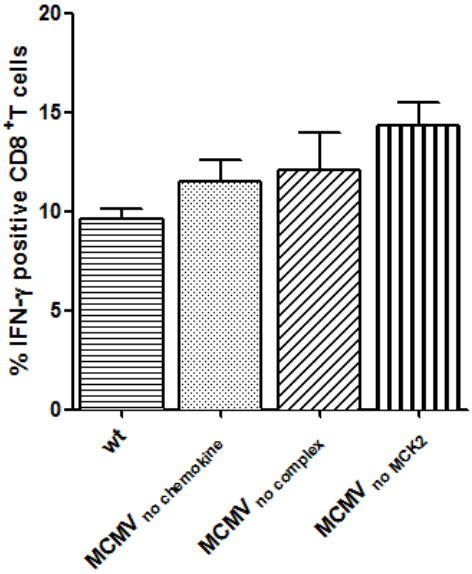

Figure 28: M45-specific $CD8^+$ T cell response after infection of mice with wt MCMV and MCMV MCK2 mutants.
C57BL/6 mice were infected i.p. with 5×10^5 PFU of wt MCMV or MCK2 mutants. The mice were killed at day 8 p.i. and spleens were harvested. Single-cell suspensions were prepared, splenocytes were stimulated with M45 peptides (1 µg/mL) for 6 h. Cells were stained with anti-$CD8^+$, followed by intracellular staining for IFN-γ and the samples were measured by FACS. Two independent experiments were performed, and results were pooled (n=5-6 mice /group) and shown as group means +/- SEM. One-way ANOVA with Tukey post-test was performed for statistical analysis.

4.2.3.3 MCK2 and induction of cytokines

4.2.3.3.1 Interferon alpha (IFN-α)

Cytokine production during MCMV infection can have pivotal effects on the course of infection (Dalod et al., 2003; Heise & Virgin, 1995; Robbins et al., 2007; Wikstrom et al., 2013).

Production of type I interferon as one of the first lines of host defense, is believed to have a protective role in MCMV infection (Gil et al., 2001; Steinberg et al., 2009). It has been shown that infection of mice with wt MCMV is associated with high levels of interferon alpha (IFN-α) production at 40 h p.i., in contrast to low levels of IFN-α after infection with MCK2-negative MCMV (Wikstrom et al., 2013). To investigate the contribution of MCK2 to IFN-α production, BALB/c mice were infected i.p. with 2×10^5 PFU of wt MCMV or MCK2 mutants. After 42 h, the mice were sacrificed, the spleens harvested, homogenized, and the titers determined by a plaque assay on MEF. In addition, IFN-α was measured in the supernatants of spleen homogenates using a commercial ELISA kit (PBL Assay Science, Piscataway, NJ). The amounts were calculated per spleen. The levels of IFN-α in non-infected mice were also measured. The data demonstrate that viral titers in spleens were comparable in all groups (Figure 29, left panel). Infection of mice with wt MCMV induced the highest levels of IFN-α and all groups of MCK2 mutants showed a reduction in IFN-α production (Figure 29, right panel), however no significant differences were detected.

(Wikstrom et al., 2013) reported that viral titers of MCK2-negative MCMV in spleens were higher than wt MCMV, in the context of lower IFN-α production at 40 h p.i., indicating that higher titers in spleens infected with MCK2-negative MCMV is a consequence of lower IFN-α production. Here, viral titers in spleens were comparable in mice infected with wt MCMV or MCK2 mutants. Spearman rank correlation analysis revealed that also here there is a direct a correlation between spleen titers and IFN-α production at 42 h p.i. The correlations were strong for wt MCMV (r=1), MCMV $_{\text{no complex}}$ (r=1) and MCMV $_{\text{no MCK2}}$ (r=0.9). While a moderate correlation of r=0.5 was detected for MCMV $_{\text{no chemokine}}$. The high titers of wt MCMV in spleens induced the production of high levels of IFN-α, high titers of the MCMV $_{\text{no MCK2}}$ and MCMV $_{\text{no complex}}$ mutants elicited also high levels of IFN-α, but in a lower range than those induced by wt MCMV infection. More mice would have been needed to detect the significant differences between wt MCMV and MCK2 mutants.

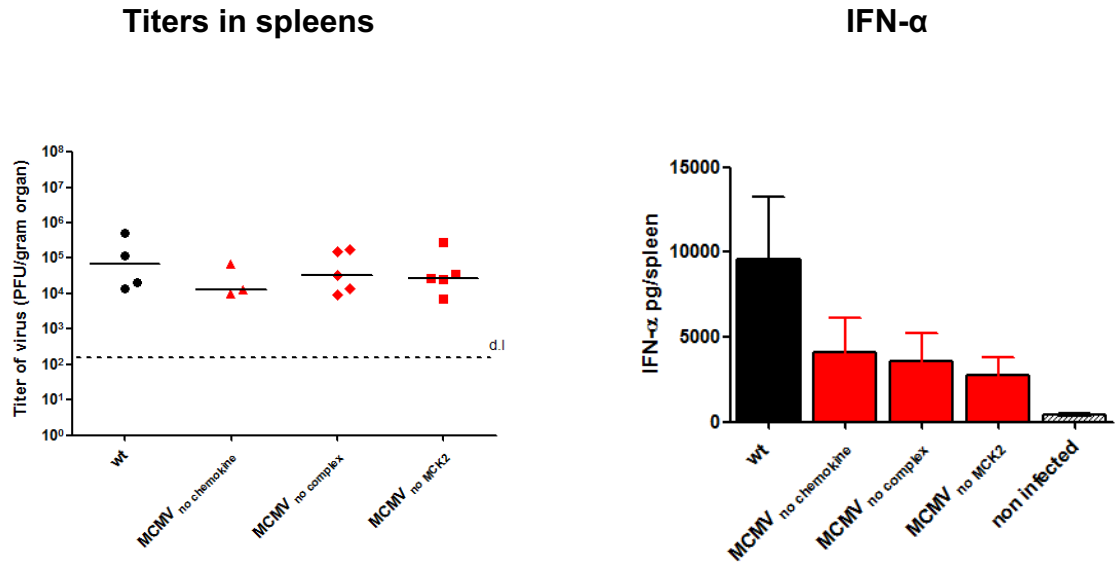

Figure 29: IFN-α production after infection of mice with different MCK2 mutants.
BALB/c mice were infected i.p. with 2 × 10^5 PFU of wt MCMV or MCK2 mutants. The mice were sacrificed after 42 h, and spleens were harvested and homogenized. The titers were determined by a plaque assay on MEF, viral titers are expressed as PFU/g organ. IFN-α concentrations were measured by a commercial ELISA kit. The concentrations are plotted as mean+/- SEM (n= 3-5 mice/group) from two independent experiments. Mann-Whitney test was performed for statistical analysis. Black bar indicates wt MCMV (intact MCK2), red bars indicate MCK2 mutants.

4.2.3.3.2 IFN-γ and CCL2

Interferon gamma (IFN-γ) has been shown to control MCMV infection and inhibit lytic MCMV replication (Gribaudo et al., 1993; Lucin et al.,1994; Krmpotic et al., 2003). Monocyte chemoattractant protein-1 (MCP-1 or also called CCL2) is considered to play a role in tissue inflammation and is produced in response to infection. It can attract inflammatory monocytes to enter inflamed tissue (Geissmann et al., 2003; Wikstrom et al., 2013; Daley-Bauer et al. 2012). It has been reported that infection of mice with wt MCMV induced higher levels of IFN-γ (at day 5 p.i.) and CCL2 (at day 4 and 5 p.i.), compared to lower levels of IFN-γ and CCL2 production after infection with MCK2-negative MCMV (Wikstrom et al., 2013).

Here, the effect of MCK2 on IFN-γ and CCL2 production was studied to find out which role of MCK2 may affect IFN-γ or CCL2 induction. BALB/c mice were infected i.p. with 2 × 10^5 PFU of wt MCMV or MCK2 mutants. At day 4 and 6 p.i., mice were sacrificed, and spleens harvested. Local production of IFN-γ and CCL2 was subsequently examined. IFN-γ and CCL2 were measured in the supernatants of spleen homogenates using a commercial ELISA kit (Biolegend, San Diego, CA).

The amounts were calculated per spleen (3000 µl spleen homogenate), the level of IFN-γ and CCL2 in non-infected mice were also measured. The data demonstrate that BALB/c mice infected with wt MCMV showed higher IFN-γ production at day 4 and day 6 than mice infected with MCK2 mutants (Figure 30a). CCL2 production in spleens (Figure 30b) also showed higher levels of CCL2 on day 4 after wt MCMV infection than after infection with MCK2 mutants, followed by a decline on day 6. All MCK2 mutants induced the same levels of CCL2 at day 4 and 6. Only for wt MCMV, there is a correlation between viral titers in spleens (at day 4 and 6) (Figure 25a) and IFN-γ and CCL2 levels, but for MCK2 mutants, IFN-γ and CCL2 levels were low on both days. The data confirm (Wikstrom et al., 2013) study, showing the higher production of IFN-γ and CCL2 in mice infected with wt MCMV, compared to MCMV lacking MCK2.

To sum up, IFN-α, IFN-γ and CCL2 levels induced by infection with wt MCMV were always higher than those induced by MCK2 mutants. Moreover, no differences were detected between MCK2 mutant lacking the chemokine function, and those lacking the gH/gL/MCK2 complex, suggesting that both chemokine and entry functions of MCK2 are required for higher IFN-α, IFN-γ and CCL2 productions. Thus, the production of these cytokines might be influenced by both chemokine activity and infection of immunoregulatory cells producing theses cytokines.

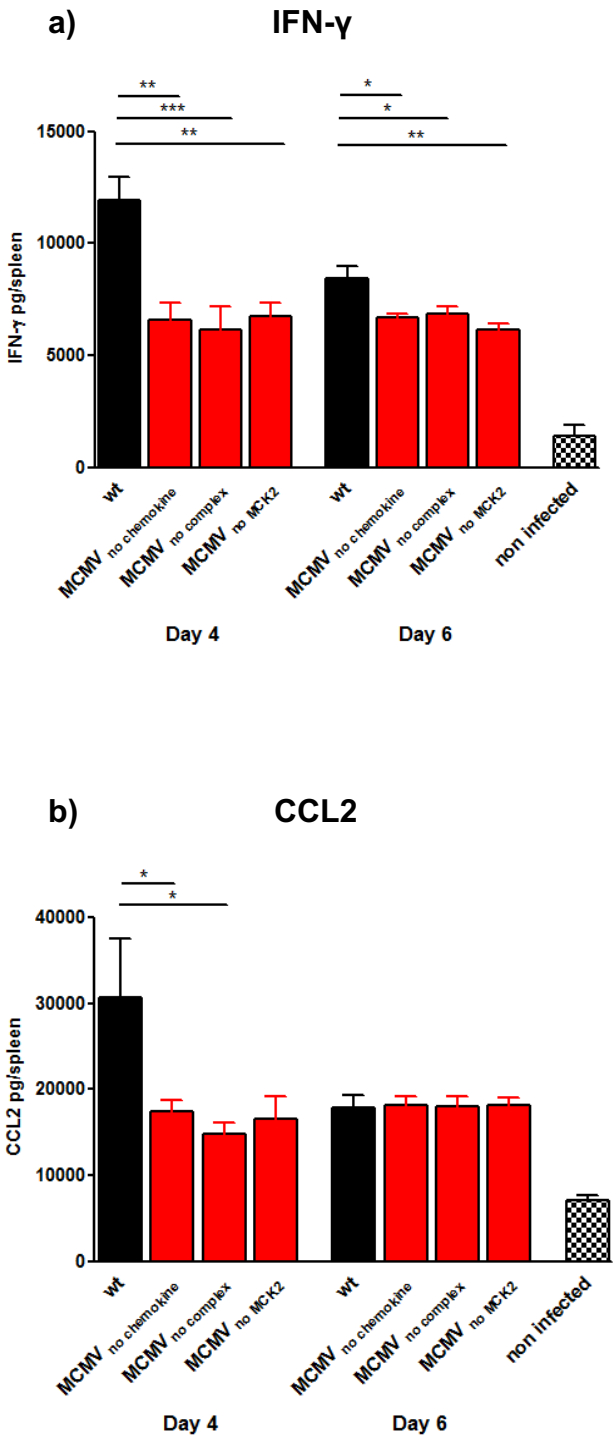

Figure 30: IFN-γ and CCL2 production in spleens after infection with different MCK2 mutants. BALB/c mice were infected i.p. with 2 × 10^5 PFU of wt MCMV or MCK2 mutants. The mice were killed at day 4 and 6 p.i. and spleens were harvested and homogenized. a) viral titers in spleens; b) IFN-γ production; c) CCL2 production. The concentrations are plotted as means +/- SEM (n= 6-8 mice/group) from two independent experiments. One-way ANOVA with Tukey post-test was performed for statistical analysis (* denotes $p<0.05$; ** denotes $p<0.01$; *** denotes $p<0.001$). Black bars indicate wt MCMV (intact MCK2), red bars indicate MCK2 mutants.

As differences in viral titers in the lungs were observed for the different MCMV mutants (Figure 25c), IFN-γ and CCL2 levels were also measured in lung homogenates. At days 4 and 6 p.i., the lungs were harvested and IFN-γ and CCL2 were measured in the supernatants of lung homogenates using a commercial ELISA kit (Biolegend, San Diego, CA). The concentrations were calculated per 100 mg lungs. As shown in Figure 31, the production of IFN-γ (Figure 31b) and CCL2 (Figure 31c) in lung tissues directly correlated with the titers in the lungs at days 4 and 6 (Figure 31a), independent of the virus used. These observations are in contrast to what was observed in the spleen cytokines, since cytokines levels in the lungs correlate with infection levels.

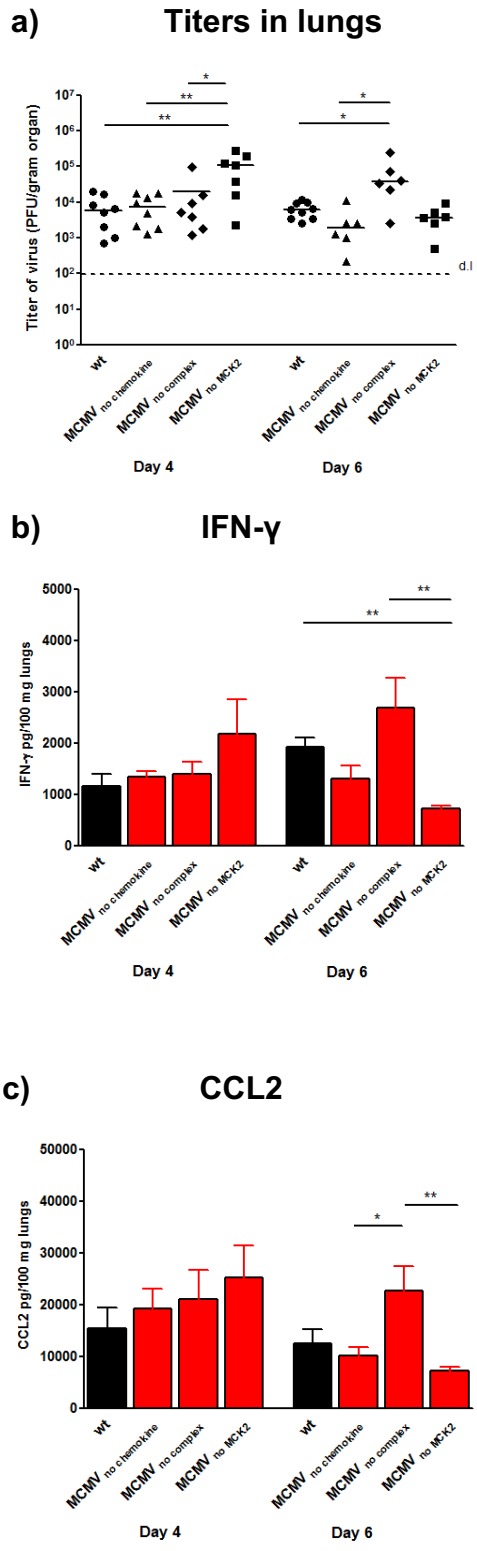

Figure 31: IFN-γ and CCL2 production in lungs after infection with different MCK2 mutants.
BALB/c mice were infected i.p. with 2 × 10^5 PFU of wt MCMV or MCMV MCK2 mutants. The mice were killed at day 4 and 6 p.i. and lungs were harvested and homogenized. a) viral titers in lungs; b) IFN-γ production; c) CCL2 production. The concentrations are plotted as means +/- SEM (n= 6-8 mice/group) from two independent experiments. For titers in lungs, one-way ANOVA with Tukey post-test was performed for statistical analysis. For IFN-γ and CCL2, Mann-Whitney test was performed for statistical analysis (* denotes $p<0.05$; ** denotes $p<0.01$). Black bars indicate wt MCMV (intact MCK2), red bars indicate MCMV MCK2 mutants.

4.2.4 The role of MCK2 in MCMV latency

The herpesvirus latency stage is characterized by the existence of viral genomes in infected cells in the absence of virus production. After persistent infection of MCMV in the salivary glands, MCMV establishes latent infection in different organs like spleen, liver, and lungs (Pollock & Virgin, 1995; Kurz et al., 1997; Reddehase et al., 2002). To study the role of MCK2 in establishment of MCMV latency in the spleen, C57BL/6 mice were infected i.p. with 5 × 10^5 PFU of wt MCMV or MCK2 mutants. The mice were killed at day 59 p.i. and spleens were harvested and processed for preparation of splenocytes. DNA was extracted from the splenocytes, and real time PCR was performed, in order to quantify the gB gene from MCMV in parallel with the cellular gene PTHrP, to normalize for cellular DNA. The data were presented as viral genome copy numbers relative to the copy number of PTHrP. As shown in Figure 32, no significant difference was detected between viral genomic loads in mice infected with wt MCMV and those in MCK2 mutants. These results indicate that MCK2 has no impact on MCMV latency in the spleen.

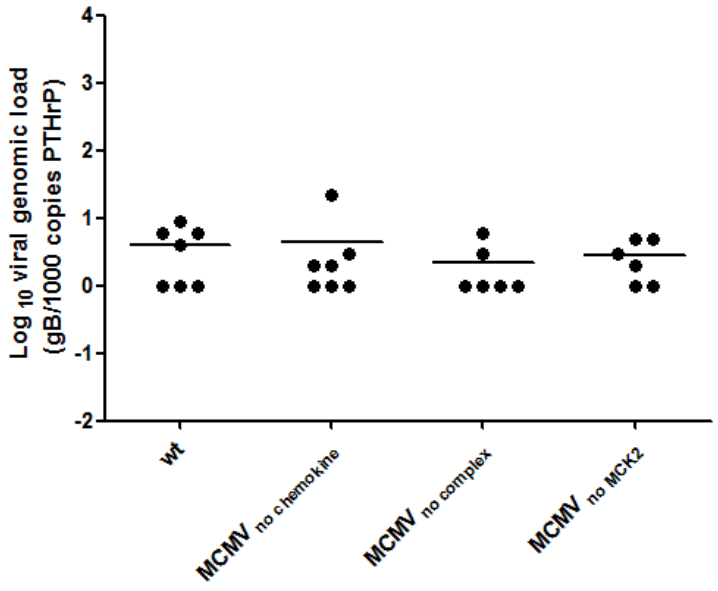

Figure 32: MCMV latency in the spleen after infection with different MCK2 mutants.
C57BL/6 mice were infected i.p. with 5 × 10^5 PFU of wt MCMV or MCMV MCK2 mutants. The mice were sacrificed at day 59 p.i., the spleens were collected followed by preparation of splenocytes. DNA was extracted from splenocytes, and qPCR was performed to amplify both of gB and PTHrP genes. The data are from three independent experiments. Each symbol represents an individual mouse, the horizontal lines show means.

4.3 Investigating the role of MCK2 in vaccination with MCMV vaccine vectors

4.3.1 Generation of MCMV vaccine vectors

The characterization of MCK2 mutants *in vivo* highlighted the role of the chemokine function of MCK2 in the early $CD8^+$ T cell response. Additionally, early cytokine production after infection was mediated by both the MCK2 chemokine and the gH/gL/MCK2 complex. A question which arises is whether the differences observed for MCK2 mutations *in vivo*, play a role when MCMV is used as a vaccine vector.

Mice infected with murine γ-Herpesvirus 68 (MHV-68) is widely used as a model to study the human gamma herpes viruses Epstein-Barr virus and Kaposi's sarcoma herpesvirus (Simas and Efstathiou 1998; Virgin IV and Speck 1999; Weinberg et al. 2004). MHV-68 ORF6 codes for a single-stranded DNA binding protein and is known for its ability to induce $CD8^+$ T cell responses in C57BL/6 mice (Gredmark-Russ et al., 2008). Therefore, ORF6 was chosen as a vaccine antigen to be inserted into MCMV vaccine vectors. ORF6 has recently been used in a vaccination study in mice using modified vaccinia ankara virus (MVA). This offers the unique opportunity to directly compare two viral vectors, MCMV and MVA. The MCMV immediate early 2 protein (ORFm128) is expressed during the early phase of MCMV replication and encodes a non-essential viral protein. Thus, m128 (IE2) can be deleted without any effect on virus replication *in vitro* and *in vivo* (Cardin et al., 1995). The cloning strategy was therefore based on deletion of MCMV IE2 and replacing it with MHV-68 ORF6 using traceless BAC-mutagenesis. Only m128 ORF was removed, in order to enable the expression of ORF6 vaccine antigen under the transcriptional control of m128 promotor (Dekhtiarenko et al. 2013; Zheng et al. 2019). The different MCK2 mutations (no chemokine, no complex and no MCK2) were subsequently introduced (Figure 33). Finally, these viruses were reconstituted and amplified. A construct carrying only the m128 deletion was generated as a control vector and designated MCMV Δm128. The cloning of these vaccine vectors was performed by students in the AG Adler.

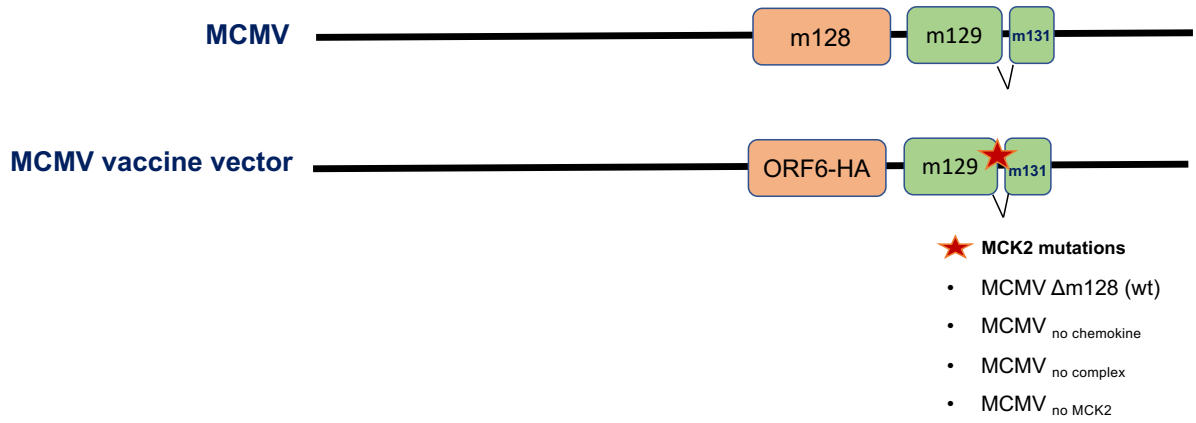

Figure 33: Schematic diagram for MCMV vaccine vectors.
Traceless-BAC mutagenesis was used to delete m128/IE2 from MCMV and replaced with ORF6 of MHV-68, thereafter, MCK2 mutations were introduced.

4.3.1.1 ORF6 expression by MCMV vaccine vectors

To detect ORF6 protein by Western blot, a human influenza hemagglutinin (HA) tag was added to the C-terminus of ORF6 during BAC mutagenesis. To verify the expression of ORF6 by the MCMV vectors, MEF were infected with MCMV Δm128 ORF6 (wt ORF6), MCMV $_{\text{no chemokine}}$ ORF6, MCMV $_{\text{no MCK2}}$ ORF6, and MCMV $_{\text{no complex}}$ ORF6. The extracts of the infected cells were lysed with sample buffer and the proteins were separated by SDS-PAGE, and subsequently analyzed by Western blot. As shown in Figure 34, all extracts of cells infected with ORF6 vectors showed a band at around 130 kDa, which matches the expected size of 124 kDa for ORF6-HA.

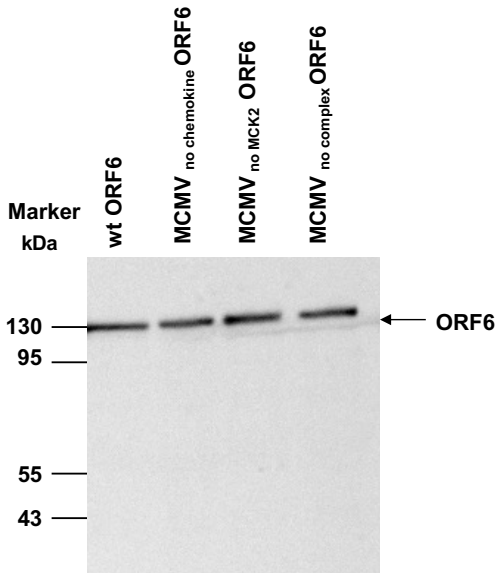

Figure 34: MCMV vaccine vectors express ORF6.
Detection of ORF6-HA protein in cell lysates of MEF infected with wt ORF6, MCMV $_{\text{no chemokine}}$ ORF6, MCMV $_{\text{no MCK2}}$ ORF6 and MCMV $_{\text{no complex}}$ ORF6 by Western blot analysis. Membranes were stained with monoclonal rat α-HA antibody, and the proteins detected with a polyclonal donkey α-rat-POX antibody (Dianova).

4.3.2 Design of the vaccination experiments

After intranasal infection of mice with MHV-68, virus replicates in the lungs, followed by trafficking of infection to secondary lymphoid organs, and latency establishment in B cells, dendritic cells and macrophages in the spleen (Flaño et al., 2000; Flaño et al., 2005). The protective efficiency of MCMV vaccine vectors against MHV-68 infection was investigated. C57BL/6 mice were infected i.p. with 5×10^5 PFU of MCMV vaccine vectors (wt ORF6, MCMV $_{\text{no chemokine}}$ ORF6, MCMV $_{\text{no complex}}$ ORF6, MCMV $_{\text{no MCK2}}$ ORF6) or MCMV Δm128 (as infection control). A group of mice was also injected with PBS (as a negative mock control). A group of mice was sacrificed at day 8 p.i., and spleen harvested. At day 42 p.i., the mice were infected intranasally (i.n.) with 5×10^4 PFU of MHV-68. Mice were either sacrificed at day 6 post-challenge, and lungs and spleens harvested or at day 17 post-challenge, and spleens and blood harvested, as illustrated in Figure 35.

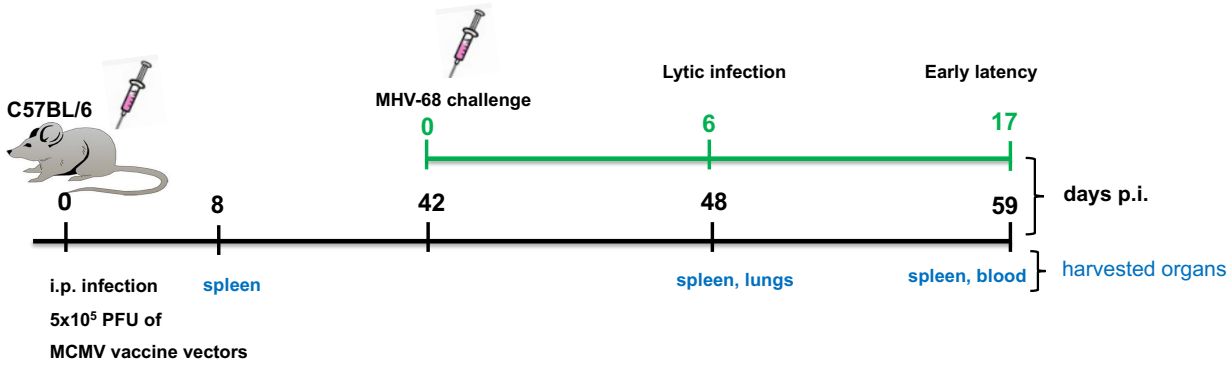

Figure 35: Schematic illustration of the design of the vaccination experiments analyzing lytic and latent infection.
C57BL/6 mice were vaccinated i.p. with 5 × 10^5 PFU of MCMV vaccine vectors or injected with PBS. A group of mice was sacrificed at day 8 p.i., and spleen harvested. At day 42 p.i., the mice were challenged i.n. with 5 × 10^4 PFU of MHV-68. At day 6 post-challenge, the mice were sacrificed, and spleens and lungs were harvested. At day 17 post-challenge, spleens and blood were harvested.

4.3.3 $CD8^+$ T cell responses elicited by MCMV vaccine vectors

4.3.3.1 ORF6-specific $CD8^+$ T cell responses at day 8 p.i.

ORF6 of MHV-68 is capable of inducing a strong $CD8^+$ T cell response in H-2^b haplotype C57BL/6 mice (Gredmark-Russ et al., 2008). Proof-of-concept experiments were performed to look for an ORF6-specific $CD8^+$ T cell response after infection with ORF6-expressing vectors. For that, C57BL/6 mice were infected i.p. with 5 × 10^5 PFU of MCMV vaccine vectors (wt ORF6, MCMV $_{\text{no chemokine}}$ ORF6, MCMV $_{\text{no complex}}$ ORF6, MCMV $_{\text{no MCK2}}$ ORF6), MCMV Δm128, as a control or injected with PBS (Figure 35). At day 8 p.i., spleens of infected mice were harvested, and single-cell suspensions were prepared. Splenocytes cells were seeded onto 96-well plates and stimulated with ORF6 $_{487\text{-}495}$ peptide (Sequence: AGPHNDMEI). All ORF6-expressing vectors elicited an ORF6-specific $CD8^+$ T cell response (Figure 36). Interestingly, all MCK2 mutants elicited a higher ORF6-specific $CD8^+$ T cell response than the wt vector, while MCMV $_{\text{no chemokine}}$ induced the highest response. As expected, no stimulation was detected after infection with control vector MCMV Δm128.

In summary, the data confirmed that all ORF6 MCMV vaccine vectors elicited ORF6-specific $CD8^+$ T cell responses at day 8 p.i.

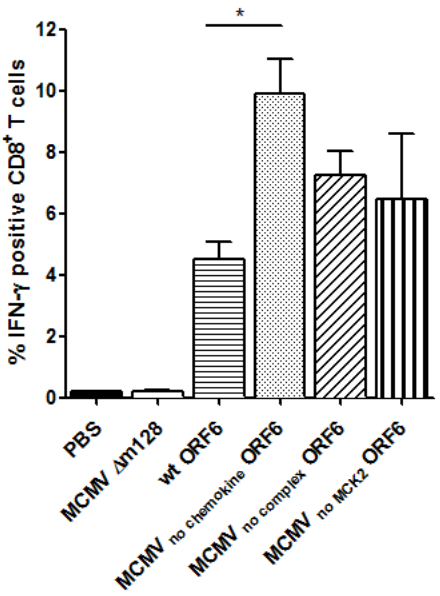

Figure 36: MCMV vaccine vectors elicited ORF6-specific CD8⁺ T cell response.
C57BL/6 mice were injected i.p. with 5 × 10^5 PFU of MCMV vaccine vectors or PBS. The mice were sacrificed at day 8 p.i. and spleens harvested. Single-cell suspensions were prepared and splenocytes stimulated with ORF6 peptide (1 µg/mL) for 6 h. Cells were stained with anti-CD8⁺, followed by an intracellular staining for IFN-γ and the samples were measured by FACS. Two independent experiments were performed, and results were pooled (n=5-6 mice /group) and shown as group means +/- SEM. One-way ANOVA with Tukey post-test was performed for statistical analysis (* denotes $p<0.05$).

4.3.3.2 ORF6-specific CD8⁺ T cell responses in vaccinated mice after challenge with MHV-68

CD8⁺ T cells play a pivotal role in controlling MHV-68 infection, which is essential to limit lytic infection or to inhibit reactivation from latency (Dutia et al., 1997; Weck et al., 1997). Therefore, CD8⁺ T cell responses were monitored in immunized mice after MHV-68 challenge. CD8⁺ T cell responses elicited by the ORF6 vaccine antigen and the kinetic pattern of ORF6-specific CD8⁺ T cell response were investigated in immunized mice at day 6 and day 17 after challenge with MHV-68. A group of control mice were vaccinated with wt ORF6 but were not challenged with MHV-68, to detect the ORF6-specific CD8⁺ T cell response elicited by the MCMV vector alone. At day 6 and 17 after MHV-68 infection, high levels of ORF6-specific CD8⁺ T cell responses could be detected, and the differences observed for MCMV vaccine vectors at day 8 after immunization disappeared (Figure 37).

ORF6-specific CD8$^+$ T cell response levels observed at day 6 and 17 after MHV-68 challenge (corresponding to day 48, 59 after vaccination with MCMV vaccine vectors) were similar to primary ORF6-specific CD8$^+$ T cell responses induced at day 8 after infection with MCMV vaccine vectors (Figure 36). Interestingly, ORF6-specific CD8$^+$ T cell responses elicited by wt ORF6 in non-challenged mice were also high (Figure 37, right panel, control). This suggests that ORF6-specific CD8$^+$ T cell responses elicited by MCMV vaccine vectors do not contract until day 59 p.i. An ORF6-specific CD8$^+$ T cell response triggered by the natural MHV-68 infection in mice injected with PBS or immunized with empty vector (MCMV Δm128), showed an increase between day 6 and day 17 post- challenge.

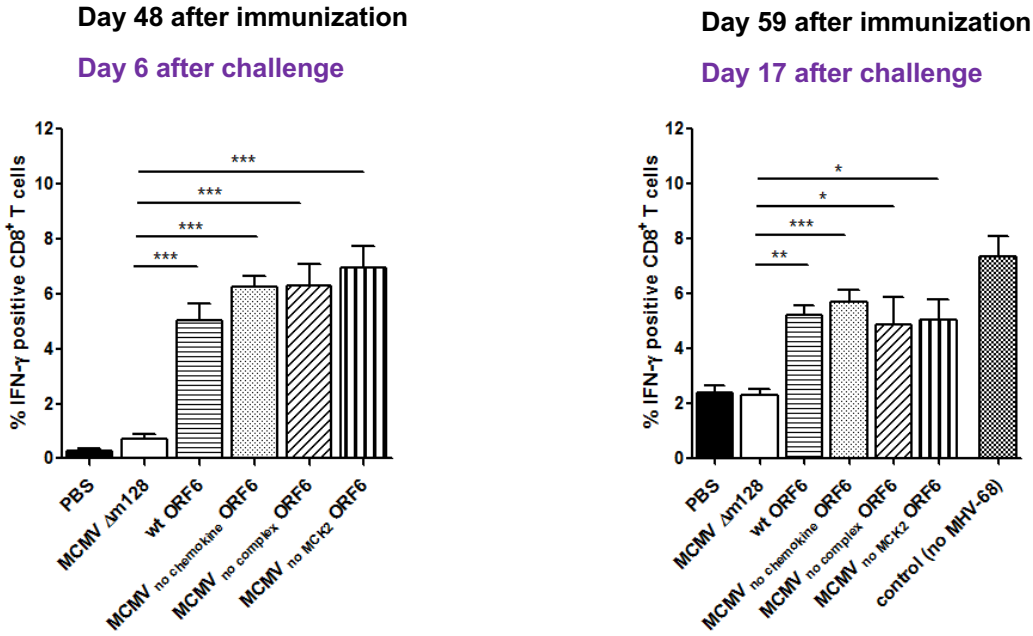

Figure 37: Kinetic of ORF6-specific CD8$^+$ T cell response during the lytic and latent infection of MHV-68.
C57BL/6 mice were vaccinated i.p. with 5 × 10^5 PFU of MCMV vaccine vectors or injected with PBS. After 42 days, the mice were infected i.n. with 5 × 10^4 PFU of MHV-68. The mice were killed at day 6 or day 17 post-challenge, the spleens were harvested. Splenocytes were stimulated with ORF6 peptide (1 µg/mL) for 6 h. The cells were surface stained with an anti-CD8$^+$ antibody, followed by intracellular staining for IFN-γ and the samples were measured by FACS. Three independent experiments were performed, and the results were pooled (n=5-7 mice /group) and shown as group means +/- SEM. One-way ANOVA with Tukey post-test was performed for statistical analysis (* denotes $p<0.05$; ** denotes $p<0.01$; *** denotes $p<0.001$).

4.3.3.3 MHV-68-specific CD8$^+$ T cell responses in vaccinated mice after challenge with MHV-68

Another question to be answered was how the immunization of mice with different MCMV vectors would affect the anti-MHV-68 T cell response in general.

For this purpose, MHV-68-infected cells were used for *ex vivo* stimulation of splenocytes at day 17 post-challenge. MEF prepared from C57BL/6 mice were infected with MHV-68 at an MOI of 0.2. The next day, the infected MEF-cells were used to stimulate splenocytes. The splenocytes were also stimulated with non-infected MEF as a control. Stimulation with MHV-68-infected cells, reveals the T cell response to all MHV-68 T cell antigens. It was observed that $CD8^+$ T cell responses were downregulated in all mice which were vaccinated with MCMV vectors, however the differences were not significant due to the wide spread of values (Figure 38a). In contrast, the $CD4^+$ T cell response was diminished only for ORF6 MCMV vaccine vectors (Figure 38b). $CD4^+$ T cell responses were measured for 2-3 mice in one experiment and have to be considered as a preliminary experiment.

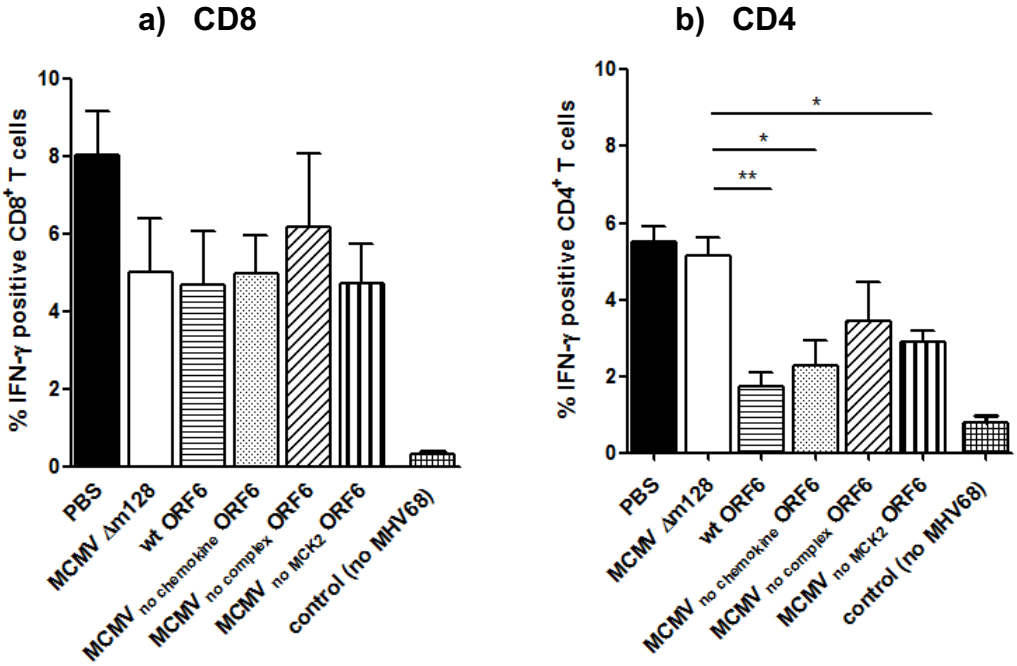

Figure 38: MHV-68-specific $CD8^+$ and $CD4^+$ T cell responses in splenocytes of MCMV vaccinated mice.

C57BL/6 mice were vaccinated i.p. with 5×10^5 PFU of MCMV vaccine vectors or injected with PBS. After 42 days, the mice were infected i.n. with 5×10^4 PFU of MHV-68. The mice were killed at day 17 post-challenge, the spleens were harvested. a) For $CD8^+$ T cell response, three independent experiments were performed, and results were pooled (n=6-7 mice /group); b) For $CD4^+$ T cell response, the data were from one preliminary experiment (n=2-3 mice /group) and shown as group means +/- SEM. Mann-Whitney test was performed for statistical analysis (* denotes $p<0.05$; ** denotes $p<0.01$).

4.3.4 Control of lytic MHV-68 infection

Protection from lytic MHV-68 infection was studied to look whether the immunized mice would be protected from lytic infection of MHV-68 in the lungs, and whether this protection could be correlated with ORF6-specific $CD8^+$ T cell responses.

To do that, lungs of vaccinated mice were harvested at day 6 post-challenge and the titers in the lungs determined using a plaque assay on BHK-21 cells. As shown in Figure 39, viral titers in lungs were reduced by about 2 logs in mice vaccinated with MCMV vaccine vectors, when compared to vaccination with the control vector (MCMV Δm128) or the mock control (PBS). Protection was independent of MCK2.

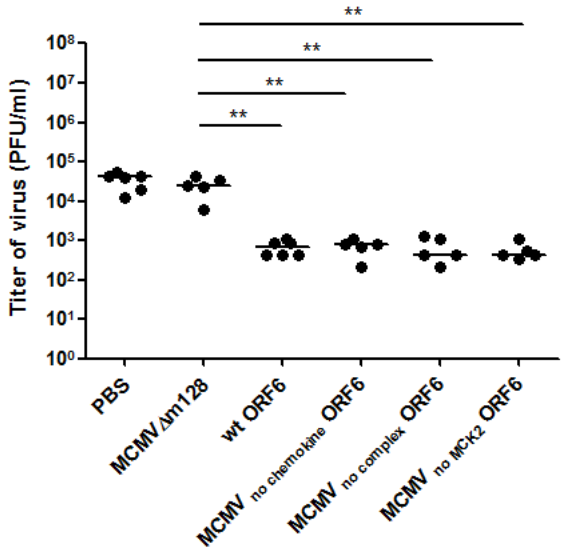

Figure 39: Reduction of lytic MHV-68 infection in the lung after immunization with MCMV vaccine vectors.

C57BL/6 mice were vaccinated i.p. with 5×10^5 PFU of MCMV vaccine vectors or injected with PBS. After 42 days, mice were infected i.n. with 5×10^4 PFU of MHV-68. At day 6 post-challenge, lungs were harvested, and the titers determined by plaque assay on BHK-21 cells. Viral titers are shown for individual mice, each symbol represents an individual mouse and the bar represent the median. The data are from three independent experiments. One-way ANOVA with Tukey post-test was performed for statistical analysis (** denotes $p<0.01$).

4.3.5 Control of latent MHV-68 infection

4.3.5.1 Splenomegaly after immunization with MCMV vaccine vectors

Latency of MHV-68 is associated with splenomegaly, which is a consequence of a virus-induced increase in numbers of B and T cells and establishment of latency in B cells, dendritic cells, and macrophages in the spleen (Flaño et al., 2000; Flaño et al., 2005). The peak of splenomegaly is at day 14 post infection (Sunil-Chandra et al., 1992; Flaño et al., 2000).

For all immunizations, the degree of splenomegaly was analyzed at day 17 after MHV-68 challenge, the time of establishment of early MHV-68 latency. To do that, C57BL/6 mice were vaccinated i.p. with 5 × 10^5 PFU of MCMV vaccine vectors or injected with PBS. A control group was infected with wt ORF6 without challenge with MHV-68, to determine the degree of splenomegaly caused by the MCMV vector alone. 42 days after vaccination, mice were challenged i.n. with 5 × 10^4 PFU of MHV-68 and the control group was not challenged. At day 17 post-challenge, spleens were taken, and the weights of spleens were determined. As shown in Figure 40, the spleens weights of mice vaccinated with MCMV vaccine vectors (wt ORF6, MCMV $_{\text{no chemokine}}$ ORF6, MCMV $_{\text{no complex}}$ ORF6, MCMV $_{\text{no MCK2}}$ ORF6) were about 2-fold lower than the spleens weights of mice injected with PBS or infected with MCMV Δm128. The weight reductions were comparable for all MCMV-ORF6 vaccinated mice. Spleen weights of mice vaccinated with MCMV $_{\text{no chemokine}}$ ORF6 appeared a bit more reduced, but the difference was not significant.

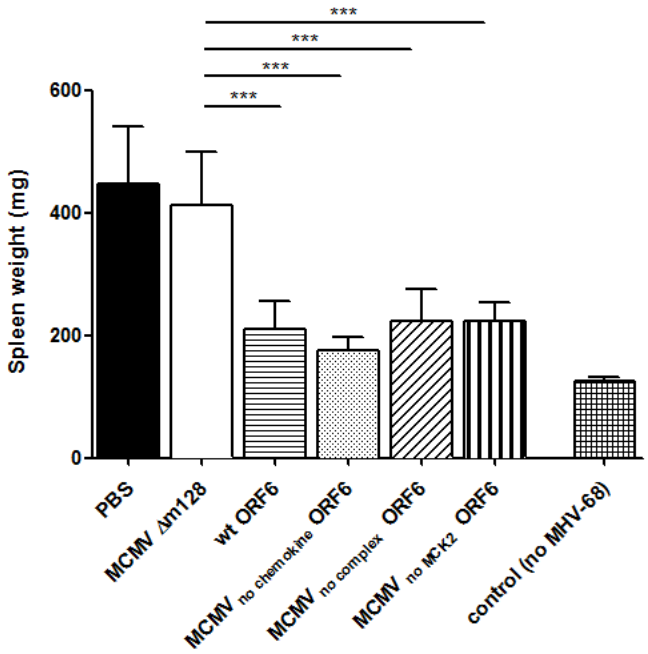

Figure 40: Spleen weights in MHV-68 latent phase of vaccinated mice.
C57BL/6 mice were vaccinated i.p. with 5 × 10^5 PFU of MCMV vaccine vectors or injected with PBS. After 42 days, the mice were anaesthetized and challenged i.n. with 5 × 10^4 PFU of MHV-68. The mice were killed at day 17 post-challenge, the spleens were harvested, and the weights of spleens were measured. Three independent experiments were performed, (n=5-7 mice /group) and are shown as group means +/- SD. One-way ANOVA with Tukey post-test was performed for statistical analysis (*** denotes $p<0.001$).

4.3.5.2 Determination of latently infected splenocytes in the spleen at day 17 of MHV-68 infection

In addition to spleens weights, also DNA load in spleen or reactivation of latently infected splenocytes are parameters to quantify latency. Latently infected spleen cells can reactivate and re-enter the lytic phase. The reactivation can be triggered *ex vivo* by contact with fibroblasts. Splenocytes from latently infected spleens were isolated, threefold serially diluted and plated on NIH3T3 monolayers in 96-well plates (24 wells/dilution). After 7 and 14 days, NIH3T3 cells in the plates were screened microscopically for a viral cytopathic effect.

To control for preexisting lytically infected cells in the spleen cell preparations, the reactivation assay was also performed on splenocytes that were previously mechanically destroyed by freezing and thawing. The frequency of reactivation was calculated by determining the number of spleen cells at which 63.2% of the wells scored positive for CPE. Paired student's t-test was performed over all dilutions to calculate the significance. As shown in Figure 41, control groups (PBS and MCMV Δm128) showed the highest frequency of reactivation (63.2% infection at 2889 and 5320 cells, respectively). In spleens of mice vaccinated with MCMV $_{\text{no MCK2}}$ ORF6 or MCMV $_{\text{no complex}}$ ORF6, the frequency was lower (63.2% infection at 29638 and 101600 cells, respectively. The differences were significant between mice vaccinated with MCMV Δm128 and those with MCMV $_{\text{no complex}}$ ORF6 or MCMV $_{\text{no MCK2}}$ ORF6 (P= 0.0078 and P= 0.0078, respectively). A significant difference was also detected between MCMV $_{\text{no chemokine}}$ ORF6 and MCMV $_{\text{no complex}}$ ORF6 (P= 0.03). No significant differences were detected between wt ORF6 and MCMV $_{\text{no chemokine}}$ ORF6, P value of 0.06 was detected between wt ORF6 and MCMV $_{\text{no MCK2}}$ ORF6 vectors. Vaccination of mice with wt ORF6 or MCMV $_{\text{no chemokine}}$ ORF6 showed the lowest reactivation and in this case, calculation of frequency of reactivated cells was not possible as it was lower than 63.2% for the range of cell numbers analyzed. In summary, MCMV vectors expressing the gH/gL/MCK2 complex suppress early latency better than vectors lacking the complex.

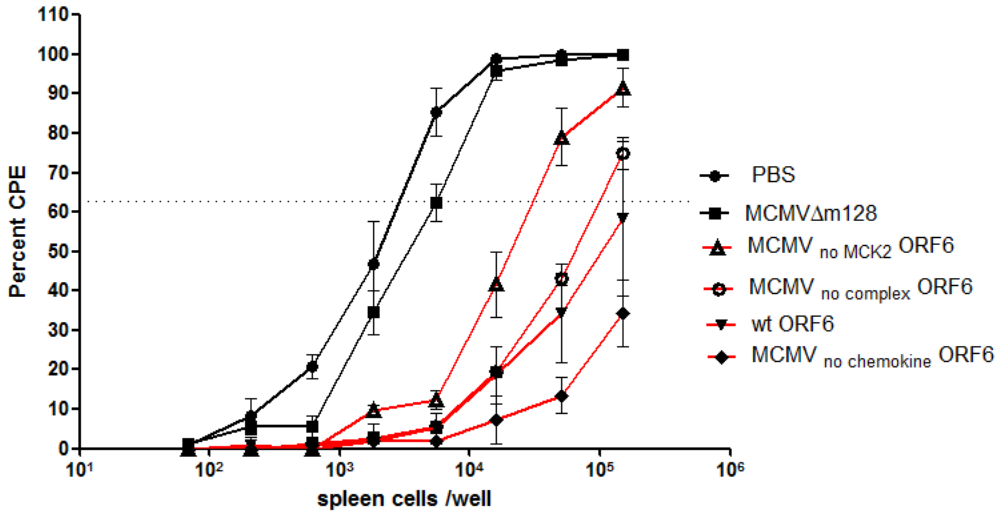

Figure 41: Reactivating splenocytes from mice vaccinated with MCMV vaccine vectors.
C57BL/6 mice were vaccinated i.p. with 5 × 10^5 PFU of MCMV vaccine vectors or injected with PBS. After 42 days, the mice were challenged i.n. with 5 × 10^4 PFU of MHV-68. The mice were sacrificed at day 17 post-challenge, the spleens were harvested, and the splenocytes were prepared. Three-fold dilutions of splenocytes were plated on monolayers of NIH3T3 cells in 96-well plates. Three independent experiments were performed, and frequency of reactivation of latent virus were calculated (n=5-7 mice /group) and shown as group means +/- SEM. The horizontal dotted line specifies the point of 63.2% Poisson distribution, set by the non-linear regression, and used for calculation of the frequency of reactivating cells. Paired t-test over all cell dilutions was performed to calculate significance.

4.3.5.3 Measurement of latent viral load by quantitative real-time PCR

An alternative to quantify latently infected splenocytes is to determine the viral load in spleens by real time PCR. For that, DNA was extracted from splenocytes using the DNeasy Blood & Tissue Kit. Viral DNA copy numbers were quantified by amplification of a 70-bp region of the MHV-68 glycoprotein B (gB) gene. Standard curves using known amounts of a plasmid containing the gB gene of MHV-68 were generated. In order to normalize input DNA between samples, the murine ribosomal protein L8 (rpl8) was also amplified in parallel. The data are presented as viral genome copy numbers relative to the copy number of rpl8. As shown in Figure 42, viral DNA loads in the spleens of all vaccinated mice were significantly reduced, when compared to mice infected with MCMV Δm128. Again, the loss of only the chemokine function of MCK2 resulted in a trend toward reduced numbers of latently infected cells. The MCMV vector lacking both the chemokine and the gH/gL/MCK2 complex of MCK2 showed higher viral load, compared to the MCMV vector lacking only the chemokine activity of MCK2. The data match exactly what was seen for the reactivation assay.

Collectively, the spleen weights, the frequency of reactivating cells, and viral loads were significantly reduced in all mice vaccinated with MCMV vaccine vectors, confirming that MCMV vaccine vectors could protect the immunized mice against MHV-68 latency. The differences between MCMV vaccine vectors in protection against MHV-68 latency, suggest a role of MCK2 in modulating the immune response after vaccination. Yet, there is no obvious correlation with $CD8^+$ T cell responses.

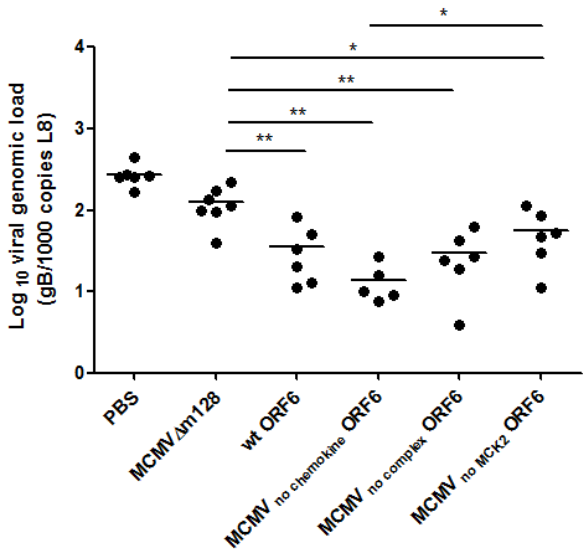

Figure 42: Latent viral DNA load after vaccination with MCMV vaccine vectors
C57BL/6 mice were vaccinated i.p. with 5×10^5 PFU of MCMV vaccine vectors or injected with PBS. After 42 days, the mice were anesthetized and challenged i.n. with 5×10^4 PFU of MHV-68. The mice were sacrificed at day 17 post-challenge, the spleens were harvested, and the splenocytes were prepared. DNA was extracted from the spleen cells and viral DNA copy numbers were quantified. The MHV-68 glycoprotein B (gB) gene was amplified. Amplification of rpl8 gene was also performed in parallel to normalize the input DNA between samples. The data are pooled from three independent experiments and the horizontal lines show means. Mann-Whitney test was performed for statistical analysis (* denotes $p<0.05$; ** denotes $p<0.01$).

5. Discussion

HCMV is the most common infectious cause of congenital disease following primary infection during pregnancy as well as many of life-threating diseases following infection or reactivation in immunocompromised individuals (Mocarski et al., 2013). Cytomegaloviruses encode for many immunomodulatory genes including viral chemokines, to evade from the host immune response (Miller-Kittrell & Sparer, 2009). Infection of mice with MCMV is a powerful model which helps to understand the interaction between the host's immune response and an HCMV infection (Reddehase &Lemmermann, 2018). The UL128 gene product of HCMV and its murine cytomegalovirus homolog MCK2 both have a dual function: They can act as chemokines and attract for example monocytes and additionally, as part of a gH/gL/chemokine entry complex, they can promote infection of host cells (Nguyen & Kamil, 2018). This study focused on analyzing the role of the viral MCK2 chemokine and/or the gH/gL/MCK2 complex in viral dissemination and antiviral immune responses. Secondly, the contribution of MCK2 to the vaccination success using MCMV as a vaccine vector was investigated.

5.1 A set of MCMV MCK2 mutants

5.1.1 Dual function of MCK2

MCK2 was first identified as a viral CC chemokine homolog with proinflammatory properties that enhances monocyte migration to the initial sites of infection, and thus may also enhance MCMV dissemination (MacDonald et al., 1999; Saederup et al., 1999; Noda et al., 2006). Studies using MCMV mutants lacking MCK2 revealed that MCK2 contributes to both, viral dissemination and immunomodulation of the host's antiviral immune response (Saederup et al., 2001; Stahl et al., 2015; Wikstrom et al., 2013; Daley-Bauer et al., 2014; Daley-Bauer et al., 2012; Farrell et al. 2019a; Jordan et al., 2011; Wagner et al., 2013; Farrell et al., 2016). Wagner et al., 2013, provided the first evidence that MCK2 is not only a viral chemokine but also has an entry function as a part of the virion gH/gL/MCK2 entry complex, promoting for example macrophage infection. It has been shown that the expression of MCK2 is associated with enhancement of viral titers in salivary glands (Fleming et al., 1999; Saederup et al., 2001; Jordan et al., 2011). It has also been shown that MCK2 increases the recruitment of inflammatory monocytes, which may act as vehicles to disseminate MCMV infection

to distal organs like salivary glands (Daley-Bauer et al., 2014). Furthermore, MCK2 promotes infection of macrophages *in vitro* and *in vivo* (Wagner et al., 2013; Stahl et al., 2015). MCMV lacking MCK2 showed higher infection in the lungs than wt MCMV at day 2 p.i. (Farrell et al., 2016).

Regarding immunomodulatory activities of MCK2, infection of mice with MCMV mutants lacking MCK2 promotes an early $CD8^+$ T cell response which accelerates viral clearance from organs (Daley-Bauer et al., 2012; Wikstrom et al., 2013). A key question was whether MCK2 exerts its roles through its chemokine activity or through gH/gL/MCK2-dependent infection of immunoregulatory cells like monocytes or macrophages. Dissemination could depend on attraction of cellular vehicles like patrolling monocytes, or on the gH/gL/MCK2-dependent infection of these cellular vehicles. Immunomodulation could depend on attraction of immunoregulatory cells like inflammatory monocytes (Daley-Bauer et al., 2012), or on inactivation of antigen presenting cells (APCs) like dendritic cells (Andrews et al., 2001). To address these questions, a set of MCK2 mutants was required, to discriminate between the chemokine function of MCK2 and its entry function as a part of the gH/gL/MCK2 complex.

5.1.2 MCMV MCK2 mutants

The MCK2 mutants used in this thesis are based on BAC-cloned MCMV strain Smith with intact MCK2 (Jordan et al., 2011). An MCK2-negative mutant was available, in which a stop mutation was introduced by inserting a stop cassette in the m131 domain of MCK2, thus preventing the expression of the MCK2 protein (MCMV $_{\text{no MCK2}}$) (Wagner et al. 2013). Additionally, a 129 stop mutant was available, which carries a stop cassette in the m129 domain of MCK2 (Wagner et al. 2013), resulting in a truncated MCK2 protein, which was shown to still have chemokine activity, but is no longer able to form a complex with gH/gL (MCMV $_{\text{no complex}}$). The only MCK2 mutant, which was missing at the start of the thesis, was a mutant, which lacks the chemokine function of MCK2 but maintains the entry function and forms a functional complex with gH/gL. This mutant was cloned by introducing a point mutation in the conserved CC motif of m131 domain of MCK2, exchanging a cysteine for glycine (AA 27), and was designated CC1 mutant, or (MCK2 $_{\text{no chemokine}}$). The CC1 mutant was cloned but not characterized at the start of the thesis. To test the entry function of the CC1 mutant, a double mutant (CC1 ΔgO) was generated using traceless mutagenesis, to remove gO which would make

the entry strictly dependent on the gH/gL/MCK2 complex. The growth of CC1 ΔgO on fibroblasts showed the same growth pattern as the Δ gO mutant, which confirmed that the entry function of gH/gL/MCK2 was still intact. Additionally, the CC1 mutant virus grew in fibroblast cultures with the same kinetic as wt MCMV and showed the same protein pattern in Western blot as wt MCMV, in both extracts of infected cells and in virions. These results indicated that an gH/gL/MCK2-CC1 complex was incorporated into virions and that gH/gL/MCK2-dependent entry was maintained. The chemokine activity of a recombinant CC1 MCK2 protein was analyzed using a migration assay. It could be shown that the MCK2 chemokine function was abolished in the CC1 mutant. In summary, the characterization of the CC1 MCK2 mutant confirmed that the chemokine function of MCK2 was eliminated, while the entry function was still intact. Most of MCK2 studies used MCK2 mutants with a complete deletion of MCK2 (Stahl et al., 2015; Wikstrom et al., 2013; Daley-Bauer et al., 2014; Daley-Bauer et al., 2012; Farrell et al., 2019a; Farrell et al., 2016). Only one study included experiments with an MCK2 mutation, in which two cysteines (AA 27, 28) were mutated by exchanging the cysteines for glycines to generate the CC/MCK2 mutant (Saederup et al. 2001). It could now be shown that this point mutation in the CC/MCK2 mutant lead to a less glycosylated MCK2, which resulted in the failure to integrate the gH/gL/MCK2 complex in virions. Consequently, this CC/MCK2 mutant showed the same growth curve in MEF-infected cells like a mutant lacking MCK2. Now, for the first time, a complete set of MCK2 mutants was available to elucidate the roles of the MCK2 chemokine and the gH/gL/MCK2 complex.

5.2. *In vitro* infection of macrophages and dendritic cells is mediated by the gH/gL/MCK2 entry complex

MCMV, like HCMV, shows a very broad cell tropism, including a tropism for hematopoietic cells like dendritic cells and macrophages (Krmpotic et al., 2003). It has been reported that MCK2 promotes infection of macrophages *in vitro* and *in vivo* (Wagner et al., 2013; Stahl et al., 2015). The capacity of the above described MCMV MCK2 mutants to infect dendritic cells (D2SC1) and macrophages (ANA-1) was studied *in vitro*, to understand whether MCK2-dependent infection of macrophages is driven by the chemokine activity of MCK2 or its entry function as a part of the gH/gL/MCK2 entry complex. D2SC1 and ANA-1 cells were infected with virus titrated

on MEF cells, and one day after infection, the percentage of infected cells was determined by intracellular staining for the MCMV IE1 protein. It could be reproduced that the infection of ANA-1 was impaired after infection with MCMV lacking MCK2 or unable to form the gH/gL/MCK2 complex (Wagner et al., 2013). In contrast, the MCMV $_{\text{no chemokine}}$ mutant showed the same infection capacity as wt MCMV. The same observation was made for D2SC1 infection. Accordingly, MCK2 promotes MCMV infection of macrophages and dendritic cells through its entry function as a part of the gH/gL/MCK2 entry complex, independent of the chemokine function of MCK2.

Spread of MCMV infection depends mainly on infected dendritic cells, which work as vehicles to disseminate infection (Farrell et al., 2017; Farrell et al., 2019a). Furthermore, MCMV infection of dendritic cells dampens functions of dendritic cells, and accordingly inhibits antigen presentation and activation of $CD8^+$ T cells (Andrews et al., 2001). Therefore, infection of dendritic cells with MCMV may have a profound impact not only on the viral dissemination, but also on the immune response. Here, *in vitro* infection of dendritic cells with MCMV-lacking MCK2 was impaired. More *in vivo* studies will be needed to study infection of dendritic cells with MCMV MCK2 mutants. Infection of primary cells like BMDM using MCK2 mutants would provide more information about MCK2-dependent infection of monocytes. BMDM infection was investigated in another study (Wagner et al., 2013) and also showed a reduced infection with MCMV lacking MCK2.

5.3 The gH/gL/MCK2 entry complex enhances viral dissemination to salivary glands

Salivary glands are considered to be the major site of MCMV shedding and the infection of salivary glands reflects successful dissemination of MCMV (Lagenaur et al., 1994; Manning et al., 1992; Daley-Bauer et al., 2012). BALB/c mice were infected with wildtype MCMV and the above described MCK2 mutants, salivary glands harvested at day 14 p.i., and viral titers determined. Significantly higher viral loads were detected in the salivary glands of mice infected with wt MCMV or the MCMV $_{\text{no chemokine}}$ mutant. On the contrary, mice infected with MCK2 mutants which are unable to form the gH/gL/MCK2 entry complex, showed 100-fold lower viral loads in salivary glands. Reduced titers in salivary glands are one of the hallmarks of infection of mice with MCMV lacking MCK2 (Fleming et al. 1999; Saederup et al. 2001; Jordan et al. 2011).

This unique phenotype was originally assumed to be attributed to the chemokine activity of MCK2, since MCK2 increases the recruitment of myelomonocytic leukocytes and was considered to enhance this way the number of infected cells, followed by dissemination of infected cells to salivary glands (Fleming et al., 1999; Noda et al., 2006; Saederup et al., 1999). Here, the data indicate that rather the gH/gL/MCK2 entry complex promotes viral dissemination to salivary glands. Infected dendritic cells have been proposed to be the main vehicles, which transfer MCMV infection to the salivary glands (Farrell et al., 2017; Farrell et al. 2019b; Farrell et al., 2019a), confirming the crucial role of infected dendritic cells in MCMV dissemination to salivary glands.

It has been reported that no difference was detected between viral titers in salivary glands infected with wt MCMV and those infected with MCMV lacking MCK2 at day 5 p.i., whereas a clear difference in salivary gland titers was observed at day 10 p.i., indicating that both wt MCMV and MCMV lacking MCK2 could equally infect salivary glands during early phase of infection (Farrell et al., 2019a). Furthermore, the equal viral titers in salivary glands at day 5 p.i. coincided with equal infection of leukocytes. Here, infection of leukocytes in the peripheral blood was studied after i.p. infection of BALB/c mice with wildtype MCMV and the above described MCK2 mutants, and blood samples were collected at day 4 p.i. The numbers of viral genomes were quantified in infected leukocytes by real time PCR. The numbers of viral genomes in peripheral blood leukocytes were comparable in all groups of mice. This data are in accordance with recent studies (Farrell et al., 2016; Farrell et al., 2019a), confirming that there is no difference between number of infected leukocytes in blood infected with wildtype MCMV and those infected with MCK2-negative MCMV at day 4 and 5 p.i. On the other hand, the data are in contradiction to previous studies (Saederup et al. 2001,1999), suggesting that the number of infected peripheral blood leukocytes decreases after infection of BALB/c mice with MCK2-negative MCMV at day 5 p.i., when compared to wt MCMV infection. To make sure that this contradiction is not due to the applied assay, another assay was also used, and the blood samples were subjected to an infectious center assay as in (Saederup et al., 1999, 2001) studies. The numbers of infected peripheral blood leukocytes were again comparable for all MCK2 mutants, confirming the results of quantification of viral genomes by real time PCR. Consequently, the data suggest that MCK2 is not relevant for leukocyte infection in the blood, during early acute MCMV infection.

MCK2 recruits both, patrolling monocytes and inflammatory monocytes, but only patrolling monocytes get infected and enhance viral dissemination, whereas inflammatory monocytes are not infected by MCMV and rather modulate the antiviral immune response (Daley-Bauer et al., 2012; Daley-Bauer et al., 2014). Thus, MCK2 mediates its effect on viral dissemination via recruitment and infection of particular lineages of monocytes. Here, it was concluded that for infection of leukocytes during acute MCMV infection, MCK2 is not relevant. Yet, the effect of MCK2 on infection of leukocytes might be more pronounced at later timepoints or in a specific population of myeloid cells, like resident dendritic cells, which play the major role in spread of MCMV infection (Farrell et al., 2017; Farrell et al., 2019a). Infection of macrophages may contribute to viral clearance (Farrell et al., 2016). It has been reported that the majority of viral genomes in blood infected with wildtype MCMV were $CD11c^{+}$-associated at day 4 p.i., confirming the contribution of infected dendritic cells to viral spread during acute MCMV infection (Farrell et al., 2017). Collectively, the gH/gL/MCK2 entry complex might enhance viral dissemination to salivary glands through promoting dendritic cell infection. Infection of mice with MCMV MCK2 mutants and investigating dendritc cells infection in blood or organs at different time points would help to confirm this approach.

5.4. The antiviral response is shaped by the chemokine activity of MCK2

5.4.1. The clearance of MCMV infection from lungs is mediated by the chemokine activity of MCK2

Besides viral titers in salivary glands and numbers of infected leukocytes in the blood, the clearance of infection from spleen, liver, and lungs was also studied. BALB/c mice were infected with wildtype MCMV and the above described MCK2 mutants.

At days 4 and 6 p.i, lungs, spleens, and livers were harvested, and viral titers determined in organ homogenates. Comparable viral titers were detected in spleens and livers of all groups at day 4 p.i., followed by a comparable control of infection and a reduction in viral titers at day 6 p.i., suggesting that clearance of MCMV infection from spleens and livers is MCK2-independent. In contrast, clearance of infection from lungs at day 6 p.i. was more pronounced in mice infected with MCMV MCK2 mutants lacking the chemokine activity (MCMV $_{\text{no chemokine}}$ or MCMV $_{\text{no MCK2}}$ mutants), whereas

the infection with wildtype MCMV or the MCMV $_{\text{no complex}}$ mutant did not start to become cleared at day 6 p.i. Furthermore, for the infection with the MCMV $_{\text{no complex}}$ mutant, even an increase in viral titers was observed at that timepoint.

(Saederup et al., 2001) showed that infection of organs was equally cleared after infection of BALB/c with wt MCMV or MCMV lacking MCK2, and no differences were detected between wt MCMV and MCK2-negative MCMV, with the exception of inconsistent differences in lung titers. It has also been described that infection of BALB/c mice with MCK2-negative MCMV, was cleared more rapidly from liver and spleen at day 5 p.i. (Fleming et al., 1999) or spleen at day 6 p.i. (Wikstrom et al. 2013), or lung and spleen at day 5 p.i. (Daley-Bauer et al., 2012), when compared to clearance after infection with wt MCMV. Notably, the differences between wt MCMV and MCMV lacking mutant in these studies were not consistent and only detected at specific timepoints.

Here, another pattern was observed. Infections with wt MCMV and MCK2 mutants were equally cleared from spleen and liver, independent of MCK2, but the clearance of infection from lungs was dependent on the chemokine activity of MCK2. These differences in different studies could for example be explained by different MCMV strains. In all previous studies, MCMV K181 strain was used for infection of mice. (Daley-Bauer et al., 2012) used MCMV K181 strain, propagated in NIH3T3 murine fibroblasts, and (Fleming et al., 1999; Wikstrom et al. 2013) studies used MCMV K181 that was purified from the salivary glands of infected mice. The K181 strain MCMV (Fleming et al., 1999; Wikstrom et al. 2013; Daley-Bauer et al., 2012) is known to be more virulent (Misra & Hudson, 1980) and exhibits a different kinetics of clearance from organs than the Smith strain-derived BACs used in this study. Viral titers in mice infected with wt MCMV in spleen and lungs at day 4 and 6 p.i. match with a recent study (Oduro et al., 2016). The differences observed for lung clearance suggest that infection of mice with MCMV mutants lacking the chemokine function of MCK2 was more rapidly cleared from lungs, indicating that the clearance of wt MCMV infection from lungs is inhibited by the chemokine activity of MCK2.

In addition to early control of infection in lungs, mice infected with MCMV lacking MCK2 also did not show a weight loss, suggesting that MCK2 might be involved in pathogenesis of MCMV. In line with this, infection of mice with wt MCMV induces a larger inflammatory infiltrate in the livers than MCMV lacking MCK2 at day 2 p.i. (Fleming et al., 1999). Furthermore, the histological examination of spleens infected

with MCMV lacking MCK2 at day 4 p.i. revealed that, the spleens were preserved with less disruption of lymphoid follicles, compared to spleens infected with wt MCMV (Wikstrom et al. 2013). This confirms the role of MCK2 in induction of an early inflammatory response.

5.4.2 The early antiviral CD8$^+$ T cell response is shaped by the chemokine activity of MCK2

It has been shown that early antiviral CD8$^+$ T cell responses were elevated in BALB/c mice infected with MCMV lacking MCK2, compared to wt MCMV starting from day 4 p.i. (Wikstrom et al., 2013; Daley-Bauer et al., 2012). (Wikstrom et al., 2013; Daley-Bauer et al., 2012) studies evaluated early CD8$^+$ T cell responses to the immediate early protein 1 and agreed that MCK2 seems to dampen the early antiviral immune response. Here, early anti-IE1 CD8$^+$ T cell responses were studied after infection of BALB/c mice with wildtype MCMV and the above described MCK2 mutants. At day 4 p.i., the spleens were harvested from infected mice, the splenocytes were *ex vivo* stimulated with IE1 peptide and the number of IFN γ-producing CD8$^+$ T cells was determined by intracellular cytokine staining.

The results of previous studies (Daley-Bauer et al., 2012; Wikstrom et al., 2013) could be reproduced, and a significantly higher IE1-specific CD8$^+$ T cell response was detected in mice infected with MCMV lacking MCK2, compared to wt MCMV. Interestingly, an enhanced CD8$^+$ T cell response was also observed in mice infected with the MCMV $_{\text{no chemokine}}$ mutant. On the contrary, IE1-specific CD8$^+$ T cell response was even below the level observed for wt MCMV in mice infected with the MCMV $_{\text{no complex}}$ mutant, which maintains only the chemokine function of MCK2. This suggests that the chemokine function of MCK2 may be more active when MCK2 is not bound to the gH/gL complex. Consequently, the inhibitory effect of the chemokine function of MCK2 on CD8$^+$ T cell response was more pronounced in the MCMV $_{\text{no complex}}$ mutant.

Taken together, the improved early CD8$^+$ T cell responses in mice infected with MCMV MCK2 mutants lacking the chemokine function directly correlated with the early clearance of infection from lungs infected with these mutants. Therefore, the data in this study reinforce a crucial role of the chemokine activity of MCK2 in inhibiting the early antiviral CD8$^+$ T cell response, which consequently may allow a better establishment of a lytic and subsequently also a latent infection. Remarkably, the MCMV MCK2 mutant lacking the complete MCK2 could elicit higher early CD8$^+$ T cell

response than those elicited by the MCK2 chemokine-negative mutant, indicating that the absence of MCK2-dependent attraction and additionally of gH/gL/MCK2-dependent infection of immune regulatory cells might have an additive effect.

5.4.3 How could MCK2 affect the early CD8$^+$ T cell response?

Different scenarios try to explain how MCK2 inhibits the early antiviral CD8$^+$ T cell response. (Daley-Bauer et al., 2012) reported that MCK2 works as an agonist and cooperates with host CCR2 in mediating signaling to increase recruitment of inflammatory monocytes, which in turn inhibit the CD8$^+$ T cell response via an iNOS-mediated pathway. Another scenario discusses an enhanced antigen presentation by conventional dendritic (cDC), namely CD8α$^+$ cDC cell in the spleen, and accordingly an enhanced early CD8$^+$ T cell response when MCK2 is lacking (Wikstrom et al., 2013). Improved CD8$^+$ T cell responses in MCK2 chemokine-negative mutants argue for inhibiting MCK2-dependent recruitment of inflammatory monocytes and their diminishing effect on early CD8$^+$ T cell response. The higher CD8$^+$ T cell response in the MCMV MCK2 mutant lacking both of chemokine and complex function, argues that a lack of an MCK2-dependent infection of dendritic cells may additionally affect antigen presentation by dendritic cells, and thus activation of CD8$^+$ T cell response. Further studies will be needed to understand the exact mechanism by which the chemokine function of MCK2 interferes with CD8$^+$ T cell response, and the MCMV $_{\text{no chemokine}}$ mutant should be involved in these studies.

5.4.4 Expression of intact MCK2 is essential for production of early cytokines

The cooperation between cytokines is necessary for early control of MCMV infection. After MCMV infection, type I interferons (IFN-α /β) are produced from plasmacytoid dendritic cells (pDC) and mediate the localized production of CCR2-binding chemokines as CCL2, CCL7 and CCL12 in the bone marrow, which are required for mobilization of monocytes from bone marrow into inflamed tissues (Crane et al., 2009; Wikstrom et al., 2013). The enhanced antiviral CD8$^+$ T cell response in mice infected with MCMV lacking MCK2 coincided with lower production of IFN-α by plasmacytoid dendritic cells, indicating a role of MCK2 in the activation status of dendritic cells (Wikstrom et al., 2013). Furthermore, CCL2 is also released from spleens in response to inflammation (Wikstrom et al., 2013). It has been reported that IFN-γ play a crucial role in inhibiting lytic MCMV replication and controlling of MCMV infection (Gribaudo

et al., 1993; Lucin et al.,1994; Krmpotic et al., 2003). Therefore, the production of IFN-α, CCL2 and IFN-γ cytokines in spleen was investigated, to test whether their production is influenced by MCK2 or not. After harvesting of spleens of mice infected with wt MCMV and the above described MCK2 mutants, the concentration of IFN-α, CCL2 and IFN-γ were measured in spleen homogenates using ELISA. For IFN-α production, direct correlations were detected between viral titers and IFN-α levels in spleens for wt MCMV and all MCK2 mutants. Infection of mice with (wt MCMV or MCMV $_{\text{no chemokine}}$) induced high levels of IFN-α in response to high titers in spleens, whereas lower ranges of IFN-α were produced in mice infected with (MCMV $_{\text{no MCK2}}$ or MCMV $_{\text{no complex}}$) mutants, in response to the same titers. This opens the question of the role of the gH/gL/MCK2 entry complex in IFN-α production. Additionally, infection of mice with wt MCMV induced the higher levels of IFN-α, CCL2 and IFN-γ production than all MCK2 mutants. Therefore, the results of (Wikstrom et al., 2013) study could be reproduced. These data imply that may be both of chemokine and gH/gL binding domains of MCK2 work in a concert in the early stage of infection to regulate the immune response and IFN-α, IFN-γ and CCL2 productions.

5.5 Role of MCK2 as part of MCMV vaccine vectors

5.5.1 CMV as a vaccine vector

Not all pathogens are amenable to conventional vaccines, which predominantly induce a humoral response. This raises the need for a new platform of vaccine vectors. Many viruses like adenoviruses, adeno-associated viruses, vesicular stomatitis virus, lentivirus, and vaccinia virus have been proposed as vaccine vectors which are able to deliver vaccine antigens of different pathogens (Rollier et al., 2011; Méndez et al., 2019). CMV can induce a potent and long-lasting $CD8^+$ T lymphocyte response (Sylwester et al., 2005). In addition, the large genome of CMV allows insertion of multiple foreign genes, which is of course desirable (Méndez et al., 2019). Therefore, CMV have been investigated as vaccine vectors to deliver different vaccine antigens and combat pathogens, like *Clostridium tetani* (Tierney et al., 2012), *Mycobacterium tuberculosis* (Beverley et al. 2014; Hansen et al. 2018), Zaire ebolavirus (Tsuda et al., 2011), influenza A virus (Zheng et al., 2019), respiratory syncytial virus (Morabito et al., 2018), and human papillomavirus 16 (Nejad et al., 2019). Furthermore, CMV-vaccine vectors have been investigated for immunotherapy to protect from cancers like

prostate cancer (Klyushnenkova et al., 2012) and aggressive B16 lung metastatic melanoma (Qiu et al., 2015). For safety concerns, CMV must be used in an attenuated form to avoid serious diseases in immunocompromised people. Live-attenuated RhCMV vaccine vector has also shown to be effective and could protect 59% of vaccinated rhesus macaques (Hansen et al. 2019). Furthermore, a live-attenuated HCMV vector could elicit robust effector memory T cell responses in rhesus macaques, confirming that also a single-round CMV can be immunogenic and safe (Caposio et al., 2019).

5.5.2 Vaccination with a RhCMV vector elicited unconventional CD8$^+$ T cell responses

After vaccination of rhesus macaques with RhCMV strain 68-1 vaccine vector, which lacks the pentameric complex and immunoregulatory genes including the homolog of HCMV UL128, 50% of the vaccinated animals were protected from SIV infection (Hansen et al., 2009; Hansen et al., 2013). Importantly, the protection of rhesus macaques against SIV challenge was associated with the presence of MHC-E–restricted CD8$^+$ T cell responses elicited by this RhCMV68-1 vector (Malouli et al., 2020). In addition to MHC-E–restricted CD8$^+$ T cells, vaccination with RhCMV68-1 vector elicited also unconventional MHC-II–restricted CD8$^+$ T cell responses in vaccinated rhesus macaques (Hansen et al., 2013). Repairing the pentameric complex and HCMV UL128 homolog genes in the RhCMV68-1.2 vector, resulting in elimination of the priming of MHC-E–restricted CD8$^+$ T cells and non-protection of the immunized rhesus macaques against SIV infection (Malouli et al., 2020). This confirms the role of the pentameric complex and viral chemokines in directing immune response elicited by RhCMV vectors (Hansen et al. 2016; Früh & Picker, 2017).

5.5.3 Do CMV chemokines affect the vaccination success?

The protection of macaques against SIV infection and the unconventional CD8$^+$ T cell responses elicited after vaccination with RhCMV vectors lacking the pentameric complex or HCMV UL128 homologs, raises the question of the contribution of immunoregulatory genes to vaccination outcomes, and to what extent would the viral chemokine UL128 and pentameric complex affect the vaccination success.

To understand the potential role of UL128 and the pentameric complex of HCMV in shaping immune responses elicited by CMV vectors, the role of the viral chemokine

MCK2 of MCMV in the vaccination of mice with MCMV vaccine vector was studied. Does for example the chemokine function of MCK2, for which we could show that it dampens the early antiviral $CD8^+$ T cell response, also affect the vaccination outcome of an MCMV vaccine vector? Vaccination experiments were designed to test the efficiency of MCMV vaccine vectors carrying different MCK2 mutations and expressing the ORF6 of MHV-68 as a vaccine antigen. MHV-68 has been used before as a target for vaccination (El-Gogo et al., 2007; El-Gogo et al., 2008; Boilesen et al., 2019; Samreen et al., 2019). MHV-68 ORF6 codes for a single-stranded DNA binding protein and is known for its ability to induce $CD8^+$ T cell responses in C57BL/6 mice (Gredmark-Russ et al., 2008). Furthermore, the $CD8^+$ T cell response to epitopes derived from ORF6 is well characterized and known to control early MHV-68 infection (Liu et al. 1999; Stevenson et al. 1999; Obar et al. 2006).

5.5.4 Control of lytic infection in lungs is MCK2-independent

Here, after one round of immunization of mice with MCMV vaccine vectors (wt ORF6, MCMV $_{\text{no chemokine}}$ ORF6, MCMV $_{\text{no complex}}$ ORF6, and MCMV $_{\text{no MCK2}}$ ORF6), 5-10% of the $CD8^+$ T cells were IFN-γ-positive after stimulation with ORF6 peptide at day 8 p.i. Notably, MCMV vectors lacking the chemokine, but still able to form the gH/gL complex induced the highest ORF6-specific $CD8^+$ T cell response. Yet, these early differences between MCMV vaccine vectors did not translate into different protection from MHV-68 lytic infection, and all vaccinated mice could equally control lytic infection in lungs after MHV-68 challenge. Furthermore, the comparable control of virus replication in lungs of immunized mice was correlated with comparable ORF6-specific $CD8^+$ T cell responses at day 6 after MHV-68 challenge. Consequently, MCK2 does not play a role in the protective effect of MCMV vaccine vectors against MHV-68 lytic infection in lungs.

Interestingly, MCMV vaccine vectors used here were more efficient than MVA vectors in controlling MHV-68 lytic infection in lungs. After prime-boost immunization of mice with MVA-OVA vectors and challenge with MHV-68 virus expressing foreign antigen (OVA) (El-Gogo et al., 2007), MVA vectors could reduce the viral titers in lungs of immunized mice by about 1 log (Figure 43a). Here, MCMV vaccine vectors showed a reduction of about 2 logs after only one round of immunization (Figure 43b).

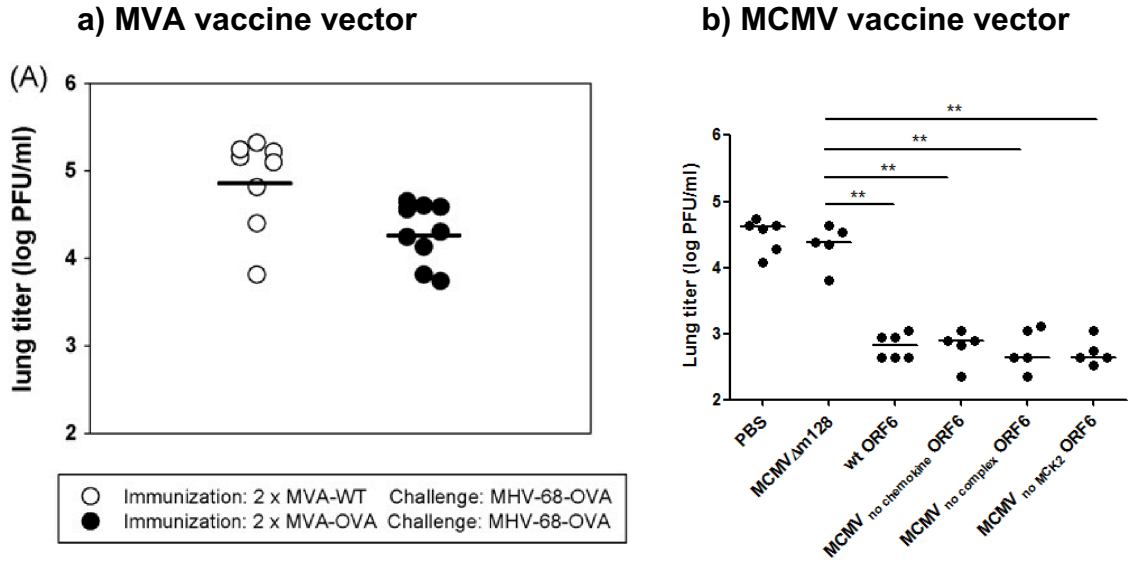

Figure 43: Comparison between MVA-vaccine vectors and MCMV vaccine vectors for reduction of viral titers in lungs of immunized mice after MHV-68 challenge.
a) C57BL/6 mice were immunized twice with MVA-OVA, at day 56 after the second immunization, the mice were challenged i.n. with MHV-68-OVA. At day 6 post-challenge, mice were sacrificed, lungs harvested, and viral titers determined (El-Gogo et al., 2007); b) C57BL/6 mice were immunized with MCMV vaccine vectors. After 42 days, the mice were challenged i.n. with MHV-68. The mice were sacrificed at day 6 post-challenge, lungs harvested, and viral titers determined.

5.5.5 Protection of vaccinated mice against MHV-68 latency is MCK2-dependent

Another important aspect of vaccination against herpesviruses is protection from latent infection. After immunization of mice with MCMV vaccine vectors, mice were challenged with MHV-68 at day 42 p.i. The mice were sacrificed at day 17 post-challenge, the timepoint of establishment of early MHV-68 latency. Spleens were harvested to determine the degree of splenomegaly and the frequency of reactivating splenocytes, which reflect the latent viral load in spleen. In all of the immunized mice, spleen weights, the frequency of reactivating splenocytes and the copies of viral genome in spleen cells were significantly reduced at day 17 post-challenge, confirming a protection from latency by MCMV vaccine vectors. Interestingly, the MCMV vector lacking both the chemokine and the complex-binding functions of MCK2, was the least effective vector, whereas the MCMV vector lacking only the chemokine function could provide the best protection against MHV-68 latency after calculating latency. This indicates that the chemokine and the complex-binding functions of MCK2 play separate roles in modulating the immune response. Consequently, the vaccination efficiencies of MCMV vectors carrying MCK2 mutations suggest a role of MCK2 in protection from MHV-68 latency.

Furthermore, MCMV vaccine vectors could provide higher protection for immunized mice against MHV-68 latency, than MVA vectors. After prime-boost protocol of immunization with MVA-ORF6, the frequency of splenocytes reactivated from latency was reduced in the immunized mice (Samreen et al., 2019) (Figure 44a), but after single dose of immunization of mice with MCMV vaccine vectors (wt ORF6 or MCMV $_{\text{no chemokine}}$ ORF6), the frequency of reactivated splenocytes was drastically reduced to a degree that its calculation was not possible, as shown in Figure 44b. Whereas the protective efficiency of MCMV vector lacking MCK2 is rather like MVA vectors, confirming the importance of an immunomodulatory protein like MCK2.

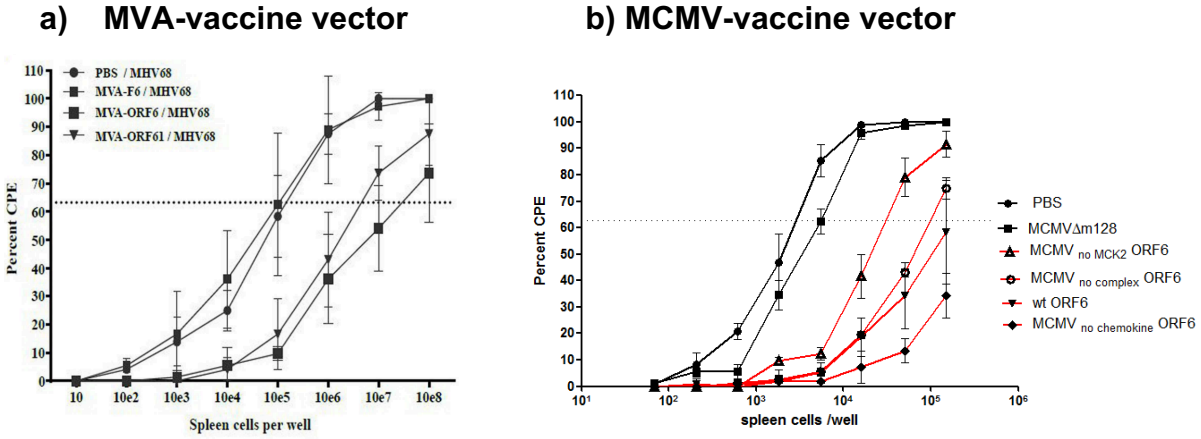

Figure 44: Comparison between MVA-vaccine vectors and MCMV-vaccine vectors for their protection against MHV-68 latency.
a) C57BL/6 mice were prime-boost vaccinated with MVA-ORF6. After 4 weeks, the mice were challenged with MHV-68. Spleens were harvested at day 17 post-challenge to determine latent viral load by *ex vivo* reactivation of splenocytes (Samreen et al., 2019); b) C57BL/6 mice were vaccinated with MCMV vaccine vectors, After 6 weeks, the mice were challenged with MHV-68. Spleens were harvested at day 17 post-challenge to determine latent viral load by *ex vivo* reactivation of splenocytes.

The differences between MCMV vaccine vectors in protection against MHV-68 latency are unexplained so far and were not correlated with $CD8^+$ T cell responses. All the MCMV vectors elicited a comparable ORF6-specific $CD8^+$ T cell response at day 17 post-challenge. The empty MCMV vector suppressed anti-MHV-68 $CD8^+$ T cells, indicating that MCMV vectors may shape the antiviral response in general.

The differences between MCMV vaccine vectors may also be attributed to their capacity to prime protective $CD4^+$ T cells, which may control establishment of MHV-68 latency. The ORF6-specific $CD4^+$ T cell response was reduced in mice immunized with MVA-ORF6 vaccine vectors at day 17 after MHV-68 challenge. Recently, the decline in ORF6-specific $CD4^+$ T cell responses was associated with protection

against MHV-68 latency (Samreen et al., 2019). Therefore, evaluation of ORF6-specific $CD4^+$ T cell response and neutralizing activities in serum of mice vaccinated with MCMV vaccine vector may be helpful to interpret the differences between the protective efficiency of MCMV vaccine vectors against MHV-68 latency.

Notably, MCMV vaccine vectors elicited stronger $CD8^+$ T cell responses than MVA vector expressing the same vaccine antigen (ORF6 of MHV-68), and at the same timepoints. After immunization of mice with MVA-ORF6, only 2% of ORF6-specific $CD8^+$ T cells were elicited at day 8 p.i., whereas MCMV vaccine vectors elicited higher ORF6-specific $CD8^+$ T cell responses (5-10%). Furthermore, only 0.2% of ORF6-specific $CD8^+$ T cells were induced by MVA-ORF6 vector at day 35 p.i., indicating that they showed contraction at the memory phase of infection. In contrast, ORF6-specific $CD8^+$ T cell responses elicited by MCMV vaccine vectors maintained at high frequencies until day 59 p.i. and did not contract, underlining the capacity of MCMV vectors in eliciting strong $CD8^+$ T cell responses

5.5.6 MCMV vaccine vectors compared to RhCMV vaccine vectors

The finding that MCMV lacking MCK2 equally protects from lytic infection of MHV-68, contradict the observations made with RhCMV, where a RhCMV vector lacking the MCK2 functional homolog provided the best protection for immunized animals against SIV infection (Hansen et al., 2009; Hansen et al., 2013). Yet, it should be taken into consideration that in the RhCMV-SIV model, patterns of many $CD8^+$ T cell epitopes were analyzed, while here only one epitope was investigated.

Infection of mice with MCMV has been proven to be a good model to study and predict the vaccination outcomes of RhCMV vaccine vectors. CMV-based vaccines against *Mycobacterium tuberculosis* have been investigated using MCMV and RhCMV vaccine vectors in mice and rhesus macaques. Both MCMV and RhCMV vaccine vectors could modulate the early innate immune response of their respective hosts, which was associated with their protection efficiency against *Mycobacterium tuberculosis* (Beverley et al. 2014; Hansen et al. 2018; Méndez et al., 2019). Moreover, the influence of previous CMV infection on the efficiency of CMV vaccine vectors was investigated using MCMV vaccine vectors. Like RhCMV, MCMV vaccine vectors has been shown to be immunogenic and could provide protection for mice with prior exposure to MCMV infection (Hansen et al., 2018; Beyranvand Nejad et al., 2019). This indicates that MCMV vaccine vectors could be a good starting point to predict the

vaccination outcomes of RhCMV vaccine vectors. However, infection of mice with MCMV may be not the suitable model to study all aspects of immune regulation and especially the MHC-E-restricted $CD8^+$ T cell response cannot be covered, since eliciting of MHC-E $CD8^+$ T cell restriction may be associated with recognition of specific epitopes, which are not recognized or processed in mice.

5.6 Outlook

In this thesis, it could be demonstrated that the chemokine activity and the gH/gL/MCK2 complex are distinct functions of MCK2. This is important for future studies to investigate in depth the contribution of the chemokine and complex-binding functions of MCK2 to MCMV infection, and may provide new therapeutic targets for the development of vaccines against CMV infection. Currently, the pentameric complex of HCMV draw much attention as a potential target for vaccination against HCMV, as a major target of neutralizing antibodies. Considering the findings in this thesis, it has to be taken into account that antibodies neutralizing MCK2 may also affect the antiviral immune response, and thus neutralizing antibodies target pentameric complex of HCMV may become counterproductive treatment strategies.

The contribution of viral chemokine and gH/gL/chemokine complex to vaccination success using CMV-based vectors, may be dependent on the pathogen under investigation. For example, the pentameric complex component and viral chemokines of RhCMV play a vital role in protection of rhesus macaques from SIV infection, but they have no role in protection from tuberculosis (Hansen et al. 2018). Consequently, investigating MCMV vaccine vectors against another pathogen or a vaccine antigen, which elicits predominantly a humoral response will be also interesting to get a more complete picture of CMV as vaccine vectors. Still, understanding the mechanism through which viral chemokine or entry complex promote the establishment of CMV infection is expected to reveal new targets for preventing CMV infection.

6. References

Adler, B., Scrivano, L., Ruzcics, Z., Rupp, B., Sinzger, C., & Koszinowski, U. (2006). Role of human cytomegalovirus UL131A in cell type-specific virus entry and release. *Journal of General Virology*, *87*(9), 2451–2460.

Adler, B., & Sinzger, C. (2009). Endothelial cells in human cytomegalovirus infection: one host cell out of many or a crucial target for virus spread? *Thrombosis and Haemostasis*, *102*(12), 1057–1063.

Adler, H., Messerle, M., Wagner, M., & Koszinowski, U. H. (2000). Cloning and mutagenesis of the murine gammaherpesvirus 68 genome as an infectious bacterial artificial chromosome. *Journal of Virology*, *74*(15), 6964–6974.

Akter, P., Cunningham, C., Mcsharry, B. P., Dolan, A., Addison, C., Dargan, D. J., Hassan-walker, A. F., Emery, V. C., Griffiths, P. D., Wilkinson, G. W. G., Davison, A. J., & Davison, A. (2003). *Communication Two novel spliced genes in human cytomegalovirus*. 1117–1122.

Akulian, J. A., Pipeling, M. R., John, E. R., Orens, J. B., Lechtzin, N., & McDyer, J. F. (2013). High-quality CMV-specific CD4+ memory is enriched in the lung allograft and is associated with mucosal viral control. *American Journal of Transplantation*, *13*(1), 146–156.

Alcami, A. (2003). Viral mimicry of cytokines, chemokines and their receptors. *Nature Reviews Immunology*, *3*(1), 36–50.

Alcami, A., & Lira, S. A. (2010). Modulation of chemokine activity by viruses. *Current Opinion in Immunology*, *22*(4), 482–487.

Anderholm, K. M., Bierle, C. J., & Schleiss, M. R. (2016). Cytomegalovirus vaccines: current status and future prospects. *Drugs*, *76*(17), 1625–1645.

Andrews, D. M., Andoniou, C. E., Fleming, P., Smyth, M. J., & Degli-Esposti, M. A. (2008). The early kinetics of cytomegalovirus-specific CD8+ T-Cell responses are not affected by antigen load or the absence of perforin or gamma Interferon. *Journal of Virology*, *82*(10), 4931–4937.

Andrews, Daniel M., Andoniou, C. E., Granucci, F., Ricciardi-Castagnoli, P., & Degli-Esposti, M. A. (2001). Infection of dendritic cells by murine cytomegalovirus induces functional paralysis. *Nature Immunology*, *2*(11), 1077–1084.

Appay, V., Dunbar, P. R., Callan, M., Klenerman, P., Gillespie, G. M. A., Papagno, L., Ogg, G. S., King, A., Lechner, F., & Spina, C. A. (2002). Memory CD8+ T cells vary in differentiation phenotype in different persistent virus infections. *Nature Medicine*, *8*(4), 379–385.

Bantug, G. R. B., Cekinovic, D., Bradford, R., Koontz, T., Jonjic, S., & Britt, W. J. (2008). CD8+ T lymphocytes control murine cytomegalovirus replication in the central nervous system of newborn animals. *The Journal of Immunology*, *181*(3), 2111–2123.

Beverley, P. C. L., Ruzsics, Z., Hey, A., Hutchings, C., Boos, S., Bolinger, B., Marchi, E., O'Hara, G., Klenerman, P., Koszinowski, U. H., & Tchilian, E. Z. (2014). A Novel Murine Cytomegalovirus Vaccine Vector Protects against Mycobacterium tuberculosis . *The Journal of Immunology*, *193*(5), 2306–2316.

Beyranvand Nejad, E., Ratts, R. B., Panagioti, E., Meyer, C., Oduro, J. D., Cicin-Sain, L., Früh, K., Van Der Burg, S. H., & Arens, R. (2019). Demarcated thresholds of tumor-specific CD8 T cells elicited by MCMV-based vaccine vectors provide robust correlates of protection. *Journal for ImmunoTherapy of Cancer*, *7*(1), 1–17.

Bissinger, A. L., Sinzger, C., Kaiserling, E., & Jahn, G. (2002). Human cytomegalovirus as a direct pathogen: correlation of multiorgan involvement and cell distribution with clinical and pathological findings in a case of congenital inclusion disease. *Journal of Medical Virology*, *67*(2), 200–206.

Boehme, K. W., Guerrero, M., & Compton, T. (2006). Human Cytomegalovirus Envelope Glycoproteins B and H Are Necessary for TLR2 Activation in Permissive Cells. *The Journal of Immunology*, *177*(10), 7094 LP – 7102.

Boilesen, D. R., Ragonnaud, E., Laursen, H., Andersson, A. M. C., Tolver, A., Spiess, K., & Holst, P. J. (2019). CD8+ T cells induced by adenovirus-vectored vaccine are capable of preventing establishment of latent murine γ-herpesvirus 68 infection. *Vaccine*, *37*(22), 2952–2959.

Boppana, S. B., Rivera, L. B., Fowler, K. B., Mach, M., & Britt, W. J. (2001). Intrauterine transmission of cytomegalovirus to infants of women with preconceptional immunity. *New England Journal of Medicine*, *344*(18), 1366–1371.

Britt, W. J., Vugler, L., Butfiloski, E. J., & Stephens, E. B. (1990). Cell surface expression of human cytomegalovirus (HCMV) gp55-116 (gB): use of HCMV-recombinant vaccinia virus-infected cells in analysis of the human neutralizing antibody response. *Journal of Virology*, *64*(3), 1079–1085.

Browne, E. P., & Shenk, T. (2003). Human cytomegalovirus UL83-coded pp65 virion protein inhibits antiviral gene expression in infected cells. *Proceedings of the National Academy of Sciences*, *100*(20), 11439–11444.

Bubić, I., Wagner, M., Krmpotić, A., Saulig, T., Kim, S., Yokoyama, W. M., Jonjić, S., & Koszinowski, U. H. (2004). Gain of virulence caused by loss of a gene in murine cytomegalovirus. *Journal of Virology*, *78*(14), 7536–7544.

Caposio, P., van den Worm, S., Crawford, L., Perez, W., Kreklywich, C., Gilbride, R. M., Hughes, C. M., Ventura, A. B., Ratts, R., & Marshall, E. E. (2019). Characterization of a live-attenuated HCMV-based vaccine platform. *Scientific Reports*, *9*(1), 1–19.

Cardin, R. D., Abenes, G. B., Stoddart, C. A., & Mocarski, E. S. (1995). Murine cytomegalovirus IE2, an activator of gene expression, is dispensable for growth and latency in mice. *Virology*, *209*(1), 236–241.

Centers, for D. C. and P. (1997). Update: trends in AIDS incidence, deaths and prevalence-United States, 1996. *MMWR Morb Mortal Wkly Rep*, *46*.

Chandler, S. H., Holmes, K. K., Wentworth, B. B., Gutman, L. T., Wiesner, P. J., Alexander, E. R., & Handsfield, H. H. (1985). The epidemiology of cytomegaloviral infection in women attending a sexually transmitted disease clinic. *Journal of Infectious Diseases*, *152*(3), 597–605.

Chandramouli, S., Malito, E., Nguyen, T. V., Luisi, K., Donnarumma, D., Xing, Y., Norais, N., Yu, D., & Carfi, A. (2017). Structural basis for potent antibody-mediated neutralization of human cytomegalovirus. *Science Immunology*, *2*(12), 1–11.

Cheeran, M. C.-J., Hu, S., Gekker, G., & Lokensgard, J. R. (2000). Decreased cytomegalovirus expression following proinflammatory cytokine treatment of primary human astrocytes. *The Journal of Immunology*, *164*(2), 926–933.

Ciferri, C., Chandramouli, S., Donnarumma, D., Nikitin, P. A., Cianfrocco, M. A., Gerrein, R., Feire, A. L., Barnett, S. W., Lilja, A. E., Rappuoli, R., Norais, N., Settembre, E. C., & Carfi, A. (2015). Structural and biochemical studies of HCMV gH/gL/gO and pentamer reveal mutually exclusive cell entry complexes. *Proceedings of the National Academy of Sciences of the United States of America*, *112*(6), 1767–1772.

Clark-Lewis, I., Kim, K., Rajarathnam, K., Gong, J., Dewald, B., Moser, B., Baggiolini, M., & Sykes, B. D. (1995). Structure-activity relationships of chemokines. *Journal of Leukocyte Biology*, *57*(5), 703–711.

Collins, T. M., Quirk, M. R., & Jordan, M. C. (1994). Biphasic viremia and viral gene expression in leukocytes during acute cytomegalovirus infection of mice. *Journal of Virology*, *68*(10), 6305–6311.

Compton, T., Kurt-Jones, E. A., Boehme, K. W., Belko, J., Latz, E., Golenbock, D. T., & Finberg, R. W. (2003). Human Cytomegalovirus Activates Inflammatory Cytokine Responses via CD14 and Toll-Like Receptor 2. *Journal of Virology*, *77*(8), 4588 LP – 4596.

Compton, T., Nepomuceno, R. R., & Nowlin, D. M. (1992). Human cytomegalovirus penetrates host cells by pH-independent fusion at the cell surface. *Virology*, *191*(1), 387–395.

Cox, G. W., Mathieson, B. J., Gandino, L., Blasi, E., Radzioch, D., & Varesio, L. (1989). Heterogeneity of hematopoietic cells immortalized by v-myc/v-raf recombinant retrovirus infection of bone marrow or fetal liver. *JNCI: Journal of the National Cancer Institute*, *81*(19), 1492–1496.

Crane, M. J., Hokeness-Antonelli, K. L., & Salazar-Mather, T. P. (2009). Regulation of Inflammatory Monocyte/Macrophage Recruitment from the Bone Marrow during Murine Cytomegalovirus Infection: Role for Type I Interferons in Localized Induction of CCR2 Ligands. *The Journal of Immunology*, *183*(4), 2810–2817.

Crough, T., & Khanna, R. (2009). Immunobiology of human cytomegalovirus: from bench to bedside. *Clinical Microbiology Reviews*, *22*(1), 76–98.

Daley-Bauer, L. P., Roback, L. J., Wynn, G. M., & Mocarski, E. S. (2014). Cytomegalovirus hijacks CX3CR1hi patrolling monocytes as immune-privileged vehicles for dissemination in mice. *Cell Host and Microbe*, *15*(3), 351–362.

Daley-Bauer, L. P., Wynn, G. M., & Mocarski, E. S. (2012). Cytomegalovirus impairs antiviral CD8+ T cell immunity by recruiting inflammatory monocytes. *Immunity*, *37*(1), 122–133.

Dalod, M., Hamilton, T., Salomon, R., Salazar-Mather, T. P., Henry, S. C., Hamilton, J. D., & Biron, C. A. (2003). Dendritic cell responses to early murine cytomegalovirus infection: subset functional specialization and differential regulation by interferon α/β. *The Journal of Experimental Medicine*, *197*(7), 885–898.

Davison, A. J., Dolan, A., Akter, P., Addison, C., Dargan, D. J., Alcendor, D. J., McGeoch, D. J., & Hayward, G. S. (2003). The human cytomegalovirus genome revisited: Comparison with the chimpanzee cytomegalovirus genome. *Journal of General Virology*, *84*(1),17–28.

de Munnik, S. M., Smit, M. J., Leurs, R., & Vischer, H. F. (2015). Modulation of cellular signaling by herpesvirus-encoded G protein-coupled receptors. *Frontiers in Pharmacology*, *6*, 40.

Dekhtiarenko, I., Jarvis, M. A., Ruzsics, Z., & Čičin-Šain, L. (2013). The context of gene expression defines the immunodominance hierarchy of cytomegalovirus antigens. *The Journal of Immunology*, *190*(7), 3399–3409.

Delannoy, A., Hober, D., Bouzidi, A., & Wattre, P. (1999). Role of Interferon Alpha (IFN-α) and Interferon Gamma (IFN-γ) in the Control of the Infection of Monocyte-Like Cells with Human Cytomegalovirus (HCMV). *Microbiology and Immunology*, *43*(12), 1087–1096.

Drago, F., Aragone, M. G., Lugani, C., & Rebora, A. (2000). Cytomegalovirus infection in normal and immunocompromised humans. *Dermatology*, *200*(3), 189–195.

Dulbecco, R., & Vogt, M. (1954). Plaque formation and isolation of pure lines with poliomyelitis viruses. *Journal of Experimental Medicine*, *99*(2), 167–182.

Dutia, B. M., Clarke, C. J., Allen, D. J., & Nash, A. A. (1997). Pathological changes in the spleens of gamma interferon receptor-deficient mice infected with murine gammaherpesvirus: a role for CD8 T cells. *Journal of Virology*, *71*(6), 4278–4283.

El-Gogo, S., Staib, C., Meyr, M., Erfle, V., Sutter, G., & Adler, H. (2007). Recombinant murine gammaherpesvirus 68 (MHV-68) as challenge virus to test efficacy of vaccination against chronic virus infections in the mouse model. *Vaccine*, *25*(20), 3934–3945.

El-Gogo, S., Staib, C., Lasarte, J. J., Sutter, G., & Adler, H. (2008). Protective vaccination with hepatitis C virus NS3 but not core antigen in a novel mouse challenge model. *The Journal of Gene Medicine: A Cross-disciplinary Journal for Research on the Science of Gene Transfer and Its Clinical Applications*, *10*(2), 177–186.

Farrell, H. E., Bruce, K., Lawler, C., Oliveira, M., Cardin, R., Davis-Poynter, N., & Stevenson, P. G. (2017). Murine cytomegalovirus spreads by dendritic cell recirculation. *MBio*, *8*(5), e01264-17.

Farrell, H. E., Bruce, K., Redwood, A. J., & Stevenson, P. G. (2019a). Murine cytomegalovirus disseminates independently of CX3CR1, CCL2 or its m131/m129 chemokine homologue. *The Journal of General Virology*, *100*(12), 1695–1700.

Farrell, H. E., Bruce, K., Lawler, C., & Stevenson, P. G. (2019b). Murine Cytomegalovirus Spread Depends on the Infected Myeloid Cell Type. *Journal of Virology*, *93*(15).

Farrell, H. E., Lawler, C., Oliveira, M. T., Davis-Poynter, N., & Stevenson, P. G. (2016). Alveolar Macrophages Are a Prominent but Nonessential Target for Murine Cytomegalovirus Infecting the Lungs. *Journal of Virology*, *90*(6), 2756–2766.

Fauriat, C., Long, E. O., Ljunggren, H.-G., & Bryceson, Y. T. (2010). Regulation of human NK-cell cytokine and chemokine production by target cell recognition. *Blood*, *115*(11), 2167–2176.

Flaño, E., Husain, S. M., Sample, J. T., Woodland, D. L., & Blackman, M. A. (2000). Latent murine γ-herpesvirus infection is established in activated B cells, dendritic cells, and macrophages. *The Journal of Immunology*, *165*(2), 1074–1081.

Flaño, E., Jia, Q., Moore, J., Woodland, D. L., Sun, R., & Blackman, M. A. (2005). Early establishment of γ-herpesvirus latency: implications for immune control. *The Journal of Immunology*, *174*(8), 4972–4978.

Fleming, P., Davis-Poynter, N., Degli-Esposti, M., Densley, E., Papadimitriou, J., Shellam, G., & Farrell, H. (1999). The Murine Cytomegalovirus Chemokine Homolog, m131/129, Is a Determinant of Viral Pathogenicity. *Journal of Virology*, *73*(8), 6800–6809.

Fodil-Cornu, N., Lee, S.-H., Belanger, S., Makrigiannis, A. P., Biron, C. A., Buller, R. M., & Vidal, S. M. (2008). Ly49h -Deficient C57BL/6 Mice: A New Mouse Cytomegalovirus-Susceptible Model Remains Resistant to Unrelated Pathogens Controlled by the NK Gene Complex . *The Journal of Immunology*, *181*(9), 6394–6405.

Foolad, F., Aitken, S. L., & Chemaly, R. F. (2018). Letermovir for the prevention of cytomegalovirus infection in adult cytomegalovirus-seropositive hematopoietic stem cell transplant recipients. *Expert Review of Clinical Pharmacology*, *11*(10), 931–941.

Forbes, B. A. (1989). Acquisition of cytomegalovirus infection: an update. *Clinical Microbiology Reviews*, *2*(2), 204–216.

Fouts, A. E., Chan, P., Stephan, J.-P., Vandlen, R., & Feierbach, B. (2012). Antibodies against the gH/gL/UL128/UL130/UL131 complex comprise the majority of the anti-cytomegalovirus (anti-CMV) neutralizing antibody response in CMV hyperimmune globulin. *Journal of Virology*, *86*(13), 7444–7447.

Fowler, K. B., Stagno, S., Pass, R. F., Britt, W. J., Boll, T. J., & Alford, C. A. (1992). The outcome of congenital cytomegalovirus infection in relation to maternal antibody status. *New England Journal of Medicine*, *326*(10), 663–667.

Frascaroli, G., Varani, S., Moepps, B., Sinzger, C., Landini, M. P., & Mertens, T. (2006). Human Cytomegalovirus Subverts the Functions of Monocytes, Impairing Chemokine-Mediated Migration and Leukocyte Recruitment. *Journal of Virology*, *80*(15), 7578 LP – 7589.

Friel, T. J., Hirsch, M. S., & Thorner, A. R. (2010). Epidemiology, clinical manifestations, and treatment of cytomegalovirus infection in immunocompetent hosts. *UpToDate February*.

Früh, K., & Picker, L. (2017). CD8+ T cell programming by cytomegalovirus vectors: applications in prophylactic and therapeutic vaccination. *Current Opinion in Immunology*, *47*, 52–56.

Gao, J.-L., & Murphy, P. M. (1994). Human cytomegalovirus open reading frame US28 encodes a functional beta chemokine receptor. *Journal of Biological Chemistry*, *269*(46), 28539–28542.

Geissmann, F., Jung, S., & Littman, D. R. (2003). Blood monocytes consist of two principal subsets with distinct migratory properties. *Immunity*, *19*(1), 71–82.

Gerna, G., Percivalle, E., Lilleri, D., Lozza, L., Fornara, C., Hahn, G., Baldanti, F., & Revello, M. G. (2005). Dendritic-cell infection by human cytomegalovirus is restricted to strains carrying functional UL131–128 genes and mediates efficient viral antigen presentation to CD8+ T cells. *Journal of General Virology*, *86*(2), 275–284.

Gibson, W. (1996). Structure and assembly of the virion. *Intervirology*, *39*(5–6), 389–400.

Gil, M. P., Bohn, E., O'Guin, A. K., Ramana, C. V, Levine, B., Stark, G. R., Virgin, H. W., & Schreiber, R. D. (2001). Biologic consequences of Stat1-independent IFN signaling. *Proceedings of the National Academy of Sciences*, *98*(12), 6680–6685.

Goldberg, M. D., Honigman, A., Weinstein, J., Chou, S., Taraboulos, A., Rouvinski, A., Shinder, V., & Wolf, D. G. (2011). Human cytomegalovirus UL97 kinase and nonkinase functions mediate viral cytoplasmic secondary envelopment. *Journal of Virology*, *85*(7), 3375–3384.

Goodier, M. R., Jonjić, S., Riley, E. M., & Juranić Lisnić, V. (2018). CMV and natural killer cells: shaping the response to vaccination. *European Journal of Immunology*, *48*(1), 50–65.

Gredmark-Russ, S., Cheung, E. J., Isaacson, M. K., Ploegh, H. L., & Grotenbreg, G. M. (2008). The CD8 T-cell response against murine gammaherpesvirus 68 is directed toward a broad repertoire of epitopes from both early and late antigens. *Journal of Virology*, *82*(24), 12205–12212.

Green, M. R., & Sambrook, J. (2018). Touchdown polymerase chain reaction (PCR). *Cold Spring Harbor Protocols*, *2018*(5), pdb-prot095133.

Gribaudo, G., Ravaglia, S., Caliendo, A., Cavallo, R., Gariglio, M., Martinotti, M. G., & Landolfo, S. (1993). Interferons inhibit onset of murine cytomegalovirus immediate-early gene transcription. *Virology*, *197*(1), 303–311.

Hahn, G., Revello, M. G., Patrone, M., Percivalle, E., Campanini, G., Sarasini, A., Wagner, M., Gallina, A., Milanesi, G., Koszinowski, U., Baldanti, F., & Gerna, G. (2004). Human Cytomegalovirus UL131-128 Genes Are Indispensable for Virus Growth in Endothelial Cells and Virus Transfer to Leukocytes. *Journal of Virology*, *78*(18), 10023–10033.

Hansen, S. G., Marshall, E. E., Malouli, D., Ventura, A. B., Hughes, C. M., Ainslie, E., Ford, J. C., Morrow, D., Gilbride, R. M., Bae, J. Y., Legasse, A. W., Oswald, K., Shoemaker, R., Berkemeier, B., Bosche, W. J., Hull, M., Womack, J., Shao, J., Edlefsen, P. T., … Picker, L. J. (2019). A live-attenuated RhCMV/SIV vaccine shows long-term efficacy against heterologous SIV challenge. *Science Translational Medicine*, *11*(501).

Hansen, S. G., Powers, C. J., Richards, R., Ventura, A. B., Ford, J. C., Siess, D., Axthelm, M. K., Nelson, J. A., Jarvis, M. A., Picker, L. J., & Früh, K. (2010). Evasion of CD8⁺ T Cells Is Critical for Superinfection by Cytomegalovirus. *Science*, *328*(5974), 102 LP – 106.

Hansen, S. G., Sacha, J. B., Hughes, C. M., Ford, J. C., Burwitz, B. J., Scholz, I., Gilbride, R. M., Lewis, M. S., Gilliam, A. N., Ventura, A. B., Malouli, D., Xu, G., Richards, R., Whizin, N., Reed, J. S., Hammond, K. B., Fischer, M., Turner, J. M., Legasse, A. W., … Picker, L. J. (2013). Cytomegalovirus vectors violate CD8+ T cell epitope recognition paradigms. *Science*, *340*(6135).

Hansen, S. G., Vieville, C., Whizin, N., Coyne-Johnson, L., Siess, D. C., Drummond, D. D., Legasse, A. W., Axthelm, M. K., Oswald, K., Trubey, C. M., Piatak, M., Lifson, J. D., Nelson, J. A., Jarvis, M. A., & Picker, L. J. (2009). Effector memory T cell responses are associated with protection of rhesus monkeys from mucosal simian immunodeficiency virus challenge. *Nature Medicine*, *15*(3), 293–299.

Hansen, S. G., Zak, D. E., Xu, G., Ford, J. C., Marshall, E. E., Malouli, D., Gilbride, R. M., Hughes, C. M., Ventura, A. B., Ainslie, E., Randall, K. T., Selseth, A. N., Rundstrom, P., Herlache, L., Lewis, M. S., Park, H., Planer, S. L., Turner, J. M., Fischer, M., … Picker, L. J. (2018). Prevention of tuberculosis in rhesus macaques by a cytomegalovirus-based vaccine. *Nature Medicine*, *24*(2), 130–143.

Härter, G., & Michel, D. (2012). *Antiviral treatment of cytomegalovirus infection: an update*. Taylor & Francis.

Heise, M. T., & Virgin, H. W. T. (1995). The T-cell-independent role of gamma interferon and tumor necrosis factor alpha in macrophage activation during murine cytomegalovirus and herpes simplex virus infections. *Journal of Virology*, *69*(2), 904–909.

Heldwein, E. E., & Krummenacher, C. (2008). Entry of herpesviruses into mammalian cells. *Cellular and Molecular Life Sciences*, *65*(11), 1653–1668.

Hughes, C. E., & Nibbs, R. J. B. (2018). A guide to chemokines and their receptors. *The FEBS Journal*, *285*(16), 2944–2971.

Hui-hui, G., Ran, T., Qi, Z., Jun, X., & Shi-qiang, S. (2013). Recombinant HCMV UL128 expression and functional identification of PBMC-attracting activity in vitro. *Archives of Virology*, *158*(1), 173–177.

Jarvis, M. A., Hansen, S. G., Nelson, J. A., Picker, L. J., Früh, K., & Reddehase, M. J. (2013). *Cytomegaloviruses: From Molecular Pathogenesis to Intervention*.

Jordan, S., Krause, J., Prager, A., Mitrovic, M., Jonjic, S., Koszinowski, U. H., & Adler, B. (2011). Virus progeny of murine cytomegalovirus bacterial artificial chromosome pSM3fr show reduced growth in salivary Glands due to a fixed mutation of MCK-2. *Journal of Virology*, *85*(19), 10346–10353.

Jordan, S., Ruzsics, Z., Mitrović, M., Baranek, T., Arapović, J., Krmpotić, A., Vivier, E., Dalod, M., Jonjić, S., Dölken, L., & Koszinowski, U. H. (2013). Natural killer cells are required for extramedullary hematopoiesis following murine cytomegalovirus infection. *Cell Host and Microbe*, *13*(5), 535–545.

Kabanova, A., Marcandalli, J., Zhou, T., Bianchi, S., Baxa, U., Tsybovsky, Y., Lilleri, D., Silacci-Fregni, C., Foglierini, M., & Fernandez-Rodriguez, B. M. (2016). Platelet-derived growth factor-α receptor is the cellular receptor for human cytomegalovirus gHgLgO trimer. *Nature Microbiology*, *1*(8), 1–8.

Kaech, S. M., Tan, J. T., Wherry, E. J., Konieczny, B. T., Surh, C. D., & Ahmed, R. (2003). Selective expression of the interleukin 7 receptor identifies effector CD8 T cells that give rise to long-lived memory cells. *Nature Immunology*, *4*(12), 1191–1198.

Kari, B., & Gehrz, R. (1992). A human cytomegalovirus glycoprotein complex designated gC-II is a major heparin-binding component of the envelope. *Journal of Virology*, *66*(3), 1761–1764.

Karrer, U., Sierro, S., Wagner, M., Oxenius, A., Hengel, H., Koszinowski, U. H., Phillips, R. E., & Klenerman, P. (2003). Memory inflation: continuous accumulation of antiviral CD8+ T cells over

time. *The Journal of Immunology*, *170*(4), 2022–2029.

Karstentischer, B., von Einem, J., Kaufer, B., & Osterrieder, N. (2006). Two-step red-mediated recombination for versatile high-efficiency markerless DNA manipulation in Escherichia coli. *Biotechniques*, *40*(2), 191–197.

Keyvani, H., Saroukalaei, S. T., & Mohseni, A. H. (2016). Assessment of the human cytomegalovirus UL97 gene for identification of resistance to ganciclovir in iranian immunosuppressed patients. *Jundishapur Journal of Microbiology*, *9*(5).

Kledal, T. N., Rosenkilde, M. M., & Schwartz, T. W. (1998). Selective recognition of the membrane-bound CX3C chemokine, fractalkine, by the human cytomegalovirus-encoded broad-spectrum receptor US28. *FEBS Letters*, *441*(2), 209–214.

Klenerman, P., & Oxenius, A. (2016). T cell responses to cytomegalovirus. *Nature Reviews Immunology*, *16*(6), 367–377.

Klyushnenkova, E. N., Kouiavskaia, D. V, Parkins, C. J., Caposio, P., Botto, S., Alexander, R. B., & Jarvis, M. A. (2012). A cytomegalovirus-based vaccine expressing a single tumor-specific CD8+ T cell epitope delays tumor growth in a murine model of prostate cancer. *Journal of Immunotherapy (Hagerstown, Md.: 1997)*, *35*(5), 390.

Krmpotic, A., Bubic, I., Polic, B., Lucin, P., & Jonjic, S. (2003). Pathogenesis of murine cytomegalovirus infection. *Microbes and Infection*, *5*(13), 1263–1277.

Kschonsak, M., Rougé, L., Arthur, C. P., Hoangdung, H., Patel, N., Kim, I., Johnson, M. C., Kraft, E., Rohou, A. L., & Gill, A. (2021). Structures of HCMV Trimer reveal the basis for receptor recognition and cell entry. *Cell*, *184*(5), 1232–1244.

Kuhn, D. E., Beall, C. J., & Kolattukudy, P. E. (1995). The cytomegalovirus US28 protein binds multiple CC chemokines with high affinity. *Biochemical and Biophysical Research Communications*, *211*(1), 325–330.

Kurz, S., Steffens, H.-P., Mayer, A., Harris, J. R., & Reddehase, M. J. (1997). Latency versus persistence or intermittent recurrences: evidence for a latent state of murine cytomegalovirus in the lungs. *Journal of Virology*, *71*(4), 2980–2987.

Lachmann, R., Loenenbach, A., Waterboer, T., Brenner, N., Pawlita, M., Michel, A., Thamm, M., Poethko-Müller, C., Wichmann, O., & Wiese-Posselt, M. (2018). Cytomegalovirus (CMV) seroprevalence in the adult population of Germany. *PLoS One*, *13*(7), e0200267.

Lagenaur, L. A., Manning, W. C., Vieira, J., Martens, C. L., & Mocarski, E. S. (1994). Structure and function of the murine cytomegalovirus sgg1 gene: a determinant of viral growth in salivary gland acinar cells. *Journal of Virology*, *68*(12), 7717–7727.

Lee, E.-C., Yu, D., De Velasco, J. M., Tessarollo, L., Swing, D. A., Court, D. L., Jenkins, N. A., & Copeland, N. G. (2001). A highly efficient Escherichia coli-based chromosome engineering system adapted for recombinogenic targeting and subcloning of BAC DNA. *Genomics*, *73*(1), 56–65.

Lemmermann, N. A. W., Krmpotic, A., Podlech, J., Brizic, I., Prager, A., Adler, H., Karbach, A., Wu, Y., Jonjic, S., & Reddehase, M. J. (2015). Non-redundant and redundant roles of cytomegalovirus gH/gL complexes in host organ entry and intra-tissue spread. *PLoS Pathog*, *11*(2), e1004640.

Leung, W. C., Hashimoto, K., Umehara, K., & Hata, J. (1991). Murine cytomegalovirus infection model in Balb/c mice. 3. Immunoglobulin production during infection. *The Tokai Journal of Experimental and Clinical Medicine*, *16*(1), 11–20.

Li, G., & Kamil, J. P. (2016). Viral regulation of cell tropism in human cytomegalovirus. *Journal of Virology*, *90*(2), 626–629.

Lilja, A. E., & Shenk, T. (2008). Efficient replication of rhesus cytomegalovirus variants in multiple rhesus and human cell types. *Proceedings of the National Academy of Sciences*, *105*(50), 19950–19955.

Lilleri, D., Kabanova, A., Revello, M. G., Percivalle, E., Sarasini, A., Genini, E., Sallusto, F., Lanzavecchia, A., Corti, D., & Gerna, G. (2013). Fetal human cytomegalovirus transmission correlates with delayed maternal antibodies to gH/gL/pUL128-130-131 complex during primary infection. *PloS One*, *8*(3), e59863.

Lilley, B. N., Ploegh, H. L., & Tirabassi, R. S. (2001). Human cytomegalovirus open reading frame TRL11/IRL11 encodes an immunoglobulin G Fc-binding protein. *Journal of Virology*, *75*(22), 11218–11221.

Lischka, P., & Zimmermann, H. (2008). Antiviral strategies to combat cytomegalovirus infections in transplant recipients. *Current Opinion in Pharmacology*, *8*(5), 541–548.

Liu, J., Jaijyan, D. K., Tang, Q., & Zhu, H. (2019). Promising cytomegalovirus-based vaccine vector induces robust CD8+ T-cell response. *International Journal of Molecular Sciences*, *20*(18).

Liu, L., Flaño, E., Usherwood, E. J., Surman, S., Blackman, M. A., & Woodland, D. L. (1999). Lytic cycle T cell epitopes are expressed in two distinct phases during MHV-68 infection. *The Journal of Immunology*, *163*(2), 868–874.

Longo, P. A., Kavran, J. M., Kim, M.-S., & Leahy, D. J. (2013). Transient mammalian cell transfection with polyethylenimine (PEI). In *Methods in enzymology* (Vol. 529, pp. 227–240). Elsevier.

Loomis, R. J., Lilja, A. E., Monroe, J., Balabanis, K. A., Brito, L. A., Palladino, G., Franti, M., Mandl, C. W., Barnett, S. W., & Mason, P. W. (2013). Vectored co-delivery of human cytomegalovirus gH and gL proteins elicits potent complement-independent neutralizing antibodies. *Vaccine*, *31*(6), 919–926.

Lucia, H. L., & Booss, J. (1981). Immune stimulation, inflammation, and changes in hematopoiesis. Host responses of the murine spleen to infection with cytomegalovirus. *The American Journal of Pathology*, *104*(1), 90.

Lucin, P., Jonjic, S., Messerle, M., Polic, B., Hengel, H., & Koszinowski, U. H. (1994). Late phase inhibition of murine cytomegalovirus replication by synergistic action of interferon-gamma and tumour necrosis factor. *Journal of General Virology*, 101–110.

Lüttichau, H. R. (2010). The cytomegalovirus UL146 gene product vCXCL1 targets both CXCR1 and CXCR2 as an agonist. *Journal of Biological Chemistry*, *285*(12), 9137–9146.

Macagno, A., Bernasconi, N. L., Vanzetta, F., Dander, E., Sarasini, A., Revello, M. G., Gerna, G., Sallusto, F., & Lanzavecchia, A. (2010). Isolation of human monoclonal antibodies that potently neutralize human cytomegalovirus infection by targeting different epitopes on the gH/gL/UL128-131A complex. *Journal of Virology*, *84*(2), 1005–1013.

MacDonald, M. R., Burney, M. W., Resnick, S. B., & Virgin, H. W. (1999). Spliced mRNA encoding the murine cytomegalovirus chemokine homolog predicts a β chemokine of novel structure. *Journal of Virology*, *73*(5), 3682–3691.

MacDonald, M. R., Li, X.-Y., & Virgin, Hw. (1997). Late expression of a beta chemokine homolog by murine cytomegalovirus. *Journal of Virology*, *71*(2), 1671–1678.

Magri, G., Muntasell, A., Romo, N., Sáez-Borderías, A., Pende, D., Geraghty, D. E., Hengel, H., Angulo, A., Moretta, A., & López-Botet, M. (2011). NKp46 and DNAM-1 NK-cell receptors drive the response to human cytomegalovirus-infected myeloid dendritic cells overcoming viral immune evasion strategies. *Blood, The Journal of the American Society of Hematology*, *117*(3), 848–856.

Malm, G., & Engman, M.-L. (2007). Congenital cytomegalovirus infections. *Seminars in Fetal and Neonatal Medicine*, *12*(3), 154–159.

Malouli, D., Hansen, S. G., Hancock, M. H., Hughes, C. M., Ford, J. C., Gilbride, R. M., Ventura, A. B., Morrow, D., Randall, K. T., Taher, H., Uebelhoer, L. S., McArdle, M. R., Papen, C. R., Espinosa Trethewy, R., Oswald, K., Shoemaker, R., Berkemeier, B., Bosche, W. J., Hull, M., … Picker, L. J. (2020). Cytomegaloviral determinants of CD8 + T cell programming and RhCMV/SIV vaccine efficacy. *BioRxiv*, *5413*(March).

Malouli, D., Nakayasu, E. S., Viswanathan, K., Camp, D. G., Chang, W. L. W., Barry, P. A., Smith, R. D., & Früh, K. (2012). Reevaluation of the coding potential and proteomic analysis of the BAC-derived rhesus cytomegalovirus strain 68-1. *Journal of Virology*, *86*(17), 8959–8973.

Manning, W. C., Stoddart, C. A., Lagenaur, L. A., Abenes, G. B., & Mocarski, E. S. (1992). Cytomegalovirus determinant of replication in salivary glands. *Journal of Virology*, *66*(6), 3794–3802.

Marshall, G. S., Rabalais, G. P., Stout, G. G., & Waldeyer, S. L. (1992). Antibodies to recombinant-derived glycoprotein B after natural human cytomegalovirus infection correlate with neutralizing activity. *Journal of Infectious Diseases*, *165*(2), 381–384.

Martinez-Martin, N., Marcandalli, J., Huang, C. S., Arthur, C. P., Perotti, M., Foglierini, M., Ho, H., Dosey, A. M., Shriver, S., & Payandeh, J. (2018). An unbiased screen for human cytomegalovirus identifies neuropilin-2 as a central viral receptor. *Cell*, *174*(5), 1158–1171.

McGeoch, D. J., & Gatherer, D. (2005). Integrating reptilian herpesviruses into the family herpesviridae. *Journal of Virology*, *79*(2), 725–731.

Méndez, A. C., Rodríguez-Rojas, C., & Del Val, M. (2019). Vaccine vectors: the bright side of cytomegalovirus. *Medical Microbiology and Immunology*, *208*(3–4), 349–363.

Messerle, M., Crnkovic, I., Hammerschmidt, W., Ziegler, H., & Koszinowski, U. H. (1997). Cloning and mutagenesis of a herpesvirus genome as an infectious bacterial artificial chromosome. *Proceedings of the National Academy of Sciences*, *94*(26), 14759–14763.

Miller-Kittrell, M., & Sparer, T. E. (2009). Feeling manipulated: Cytomegalovirus immune manipulation. *Virology Journal*, *6*, 1–20.

Misra, V., & Hudson, J. B. (1980). Minor base sequence differences between the genomes of two strains of murine cytomegalovirus differing in virulence. *Archives of Virology*, *64*(1), 1–8.

Mocarski, E. S. (n.d.). J., Shenk, T., Griffiths, PD, and Pass, RF (2013) Cytomegaloviruses. *Fields Virology, 6th Ed., Lippincott Williams & Wilkins, Philadelphia*.

Morabito, K. M., Ruckwardt, T. J., Bar-Haim, E., Nair, D., Moin, S. M., Redwood, A. J., Price, D. A., & Graham, B. S. (2018). Memory inflation drives tissue-resident memory CD8+ T cell maintenance in the lung after intranasal vaccination with murine cytomegalovirus. *Frontiers in Immunology*, *9*(AUG), 1–13.

Munks, M. W., Cho, K. S., Pinto, A. K., Sierro, S., Klenerman, P., & Hill, A. B. (2006). Four distinct patterns of memory CD8 T cell responses to chronic murine cytomegalovirus infection. *The Journal of Immunology*, *177*(1), 450–458.

Murray, S. E., Nesterenko, P. A., Vanarsdall, A. L., Munks, M. W., Smart, S. M., Veziroglu, E. M., Sagario, L. C., Lee, R., Claas, F. H. J., & Doxiadis, I. I. N. (2017). Fibroblast-adapted human CMV vaccines elicit predominantly conventional CD8 T cell responses in humans. *Journal of Experimental Medicine*, *214*(7), 1889–1899.

Ndjamen, B., Joshi, D. S., Fraser, S. E., & Bjorkman, P. J. (2016). Characterization of antibody bipolar bridging mediated by the human cytomegalovirus Fc Receptor gp68. *Journal of Virology*, *90*(6), 3262–3267.

Nguyen, C. C.,& Kamil, J. P. (2018). *Pathogen at the Gates : Human Cytomegalovirus Entry and Cell Tropism*. Viruses, 10(12), 704.

Nielsen, S. L., Sørensen, I., & Andersen, H. K. (1988). Kinetics of specific immunoglobulins M, E, A, and G in congenital, primary, and secondary cytomegalovirus infection studied by antibody-capture enzyme-linked immunosorbent assay. *Journal of Clinical Microbiology*, *26*(4), 654–661.

Nigro, G., & Adler, S. P. (2013). Hyperimmunoglobulin for prevention of congenital cytomegalovirus disease. *Clinical Infectious Diseases*, *57*(suppl_4), S193–S195.

Noda, S., Aguirre, S. A., Bitmansour, A., Brown, J. M., Sparer, T. E., Huang, J., & Mocarski, E. S. (2006). Cytomegalovirus MCK-2 controls mobilization and recruitment of myeloid progenitor cells to facilitate dissemination. *Blood*, *107*(1), 30–38.

Noriega, V. M., & Tortorella, D. (2009). Human cytomegalovirus-encoded immune modulators partner to downregulate major histocompatibility complex class I molecules. *Journal of Virology*, *83*(3), 1359–1367.

O'Hara, G. A., Welten, S. P. M., Klenerman, P., & Arens, R. (2012). Memory T cell inflation: understanding cause and effect. *Trends in Immunology*, *33*(2), 84–90.

Obar, J. J., Fuse, S., Leung, E. K., Bellfy, S. C., & Usherwood, E. J. (2006). Gammaherpesvirus persistence alters key CD8 T-cell memory characteristics and enhances antiviral protection. *Journal of Virology*, *80*(17), 8303–8315.

Oduro, J. D., Redeker, A., Lemmermann, N. A. W., Ebermann, L., Marandu, T. F., Dekhtiarenko, I., Holzki, J. K., Busch, D. H., Arens, R., & Čičin-Šain, L. (2016). Murine cytomegalovirus (CMV) infection via the intranasal route offers a robust model of immunity upon mucosal CMV infection. *Journal of General Virology*, *97*(1), 185–195.

Paglia, P., Girolomoni, G., Robbiati, F., Granucci, F., & Ricciardi-Castagnoli, P. (1993). Immortalized dendritic cell line fully competent in antigen presentation initiates primary T cell responses in vivo. *The Journal of Experimental Medicine*, *178*(6), 1893–1901.

Palella Jr, F. J., Delaney, K. M., Moorman, A. C., Loveless, M. O., Fuhrer, J., Satten, G. A., Aschman, D. J., Holmberg, S. D., & Investigators, H. I. V. O. S. (1998). Declining morbidity and mortality among patients with advanced human immunodeficiency virus infection. *New England Journal of Medicine*, *338*(13), 853–860.

Pass, R. F. (2001). Cytomegalovirus. *Fields Virology*, 2675–2705.

Pass, R. F., & Anderson, B. (2014). Mother-to-child transmission of cytomegalovirus and prevention of congenital infection. *Journal of the Pediatric Infectious Diseases Society*, *3*(suppl_1), S2–S6.

Patro, A. (2019). Subversion of immune response by human cytomegalovirus. *Frontiers in Immunology*, *10*, 1155.

Penfold, M. E. T., Dairaghi, D. J., Duke, G. M., Saederup, N., Mocarski, E. S., Kemble, G. W., & Schall, T. J. (1999). Cytomegalovirus encodes a potent α chemokine. *Proceedings of the National Academy of Sciences*, *96*(17), 9839–9844.

Pereira, L. H., Empii, J. A., Haase, D. A., & Manley, K. M. (1990). Cytomegalovirus infection among women attending a sexually transmitted disease clinic: association with clinical symptoms and other sexually transmitted diseases. *American Journal of Epidemiology*, *131*(4), 683–692.

Pollock, J. L., & Virgin, H. W. 4th. (1995). Latency, without persistence, of murine cytomegalovirus in the spleen and kidney. *Journal of Virology*, *69*(3), 1762–1768.

Pontejo, S. M., & Murphy, P. M. (2017a). Chemokines encoded by herpesviruses. *Journal of Leukocyte Biology*, *102*(5), 1199–1217.

Pontejo, S. M., & Murphy, P. M. (2017b). Two glycosaminoglycan-binding domains of the mouse cytomegalovirus-encoded chemokine MCK-2 are critical for oligomerization of the full-length protein. *Journal of Biological Chemistry*, *292*(23), 9613–9626.

Pontejo, S. M., Murphy, P. M., & Pease, J. E. (2018). Chemokine Subversion by Human Herpesviruses. *Journal of Innate Immunity*, *10*(5–6), 465–478.

Prod'homme, V., Tomasec, P., Cunningham, C., Lemberg, M. K., Stanton, R. J., McSharry, B. P., Wang, E. C. Y., Cuff, S., Martoglio, B., & Davison, A. J. (2012). Human cytomegalovirus UL40 signal peptide regulates cell surface expression of the NK cell ligands HLA-E and gpUL18. *The Journal of Immunology*, *188*(6), 2794–2804.

Qiu, Z., Huang, H., Grenier, J. M., Perez, O. A., Smilowitz, H. M., Adler, B., & Khanna, K. M. (2015). Cytomegalovirus-based vaccine expressing a modified tumor antigen induces potent tumor-specific CD8+ T-cell response and protects mice from melanoma. *Cancer Immunology Research*, *3*(5), 536–546.

Rajarathnam, K., Sykes, B. D., Dewald, B., Baggiolini, M., & Clark-Lewis, I. (1999). Disulfide bridges in interleukin-8 probed using non-natural disulfide analogues: dissociation of roles in structure from function. *Biochemistry*, *38*(24), 7653–7658.

Razonable, R. R. (2011). Antiviral drugs for viruses other than human immunodeficiency virus. *Mayo Clinic Proceedings*, *86*(10), 1009–1026.

Reddehase, M. J. (2002). Antigens and immunoevasins: Opponents in cytomegalovirus immune surveillance. *Nature Reviews Immunology*, *2*(11), 831–844.

Reddehase, M. J., & Lemmermann, N. A. W. (2018). Mouse model of cytomegalovirus disease and immunotherapy in the immunocompromised host: Predictions for medical translation that survived the "test of time." *Viruses*, *10*(12).

Reddehase, M. J., Podlech, J., & Grzimek, N. K. A. (2002). Mouse models of cytomegalovirus latency: overview. *Journal of Clinical Virology*, *25*, 23–36.

Redpath, S., Angulo, A., Gascoigne, N. R. J., & Ghazal, P. (2001). Immune checkpoints in viral latency. *Annual Reviews in Microbiology*, *55*(1), 531–560.

Reed, L. J., & Muench, H. (1938). A simple method of estimating fifty per cent endpoints. *American Journal of Epidemiology*, *27*(3), 493–497.

Reschke, M. (1994). Detailed 2d model of HCMV. *Institute of Virology, University of Marburg, Germany*.

Revello, M. G., Lazzarotto, T., Guerra, B., Spinillo, A., Ferrazzi, E., Kustermann, A., Guaschino, S., Vergani, P., Todros, T., & Frusca, T. (2014). A randomized trial of hyperimmune globulin to prevent congenital cytomegalovirus. *New England Journal of Medicine*, *370*(14), 1316–1326.

Robbins, S. H., Bessou, G., Cornillon, A., Zucchini, N., Rupp, B., Ruzsics, Z., Sacher, T., Tomasello, E., Vivier, E., & Koszinowski, U. H. (2007). Natural killer cells promote early CD8 T cell responses against cytomegalovirus. *PLoS Pathog*, *3*(8), e123.

Roizman, B., Whitley, R. J., & Lopez, C. (1993). *The human herpesviruses: biology, pathogenesis, and treatment*. Raven Pr.

Rollier, C. S., Reyes-Sandoval, A., Cottingham, M. G., Ewer, K., & Hill, A. V. S. (2011). Viral vectors as vaccine platforms: deployment in sight. *Current Opinion in Immunology*, *23*(3), 377–382.

Ruiss, R., Ohno, S., Steer, B., Zeidler, R., & Adler, H. (2012). Murine gammaherpesvirus 68 glycoprotein 150 does not contribute to latency amplification in vivo. *Virology Journal*, *9*(1), 107.

Ryckman, B. J., Jarvis, M. A., Drummond, D. D., Nelson, J. A., & Johnson, D. C. (2006). Human cytomegalovirus entry into epithelial and endothelial cells depends on genes UL128 to UL150 and occurs by endocytosis and low-pH fusion. *Journal of Virology*, *80*(2), 710–722.

Ryckman, B. J., Rainish, B. L., Chase, M. C., Borton, J. A., Nelson, J. A., Jarvis, M. A., & Johnson, D. C. (2008). Characterization of the human cytomegalovirus gH/gL/UL128-131 complex that mediates entry into epithelial and endothelial cells. *Journal of Virology*, *82*(1), 60–70.

Saederup, N., Aguirre, S. A., Sparer, T. E., Bouley, D. M., & Mocarski, E. S. (2001). Murine Cytomegalovirus CC Chemokine Homolog MCK-2 (m131-129) Is a Determinant of Dissemination That Increases Inflammation at Initial Sites of Infection. *Journal of Virology*, *75*(20), 9966–9976.

Saederup, N., Lin, Y. C., Dairaghi, D. J., Schall, T. J., & Mocarski, E. S. (1999). Cytomegalovirus-encoded β chemokine promotes monocyte-associated viremia in the host. *Proceedings of the National Academy of Sciences of the United States of America*, *96*(19), 10881–10886.

Sainz, B., LaMarca, H. L., Garry, R. F., & Morris, C. A. (2005). Synergistic inhibition of human cytomegalovirus replication by interferon-alpha/beta and interferon-gamma. *Virology Journal*, *2*(1), 14.

Samreen, B., Tao, S., Tischer, K., Adler, H., & Drexler, I. (2019). ORF6 and ORF61 expressing MVA vaccines impair early but not late latency in murine gammaherpesvirus MHV-68 infection. *Frontiers in Immunology*, *10*, 2984.

Sandonís, V., García-Ríos, E., McConnell, M. J., & Pérez-Romero, P. (2020). Role of Neutralizing Antibodies in CMV Infection: Implications for New Therapeutic Approaches. *Trends in Microbiology*, *28*(11), 900–912.

Sarkar, S., Kalia, V., Haining, W. N., Konieczny, B. T., Subramaniam, S., & Ahmed, R. (2008). Functional and genomic profiling of effector CD8 T cell subsets with distinct memory fates. *The Journal of Experimental Medicine*, *205*(3), 625–640.

Schleiss, M. R. (2002). Animal models of congenital cytomegalovirus infection: an overview of progress in the characterization of guinea pig cytomegalovirus (GPCMV). *Journal of Clinical Virology : The Official Publication of the Pan American Society for Clinical Virology*, *25 Suppl 2*, S37-49.

Schleiss, M. R. (2013). Developing a vaccine against congenital CMV infection: what have we learned from animal models? Where should we go next? *Future Virology*, *8*(12), 1161–1182.

Schreiber, A., Härter, G., Schubert, A., Bunjes, D., Mertens, T., & Michel, D. (2009). Antiviral treatment of cytomegalovirus infection and resistant strains. *Expert Opinion on Pharmacotherapy*, *10*(2), 191–209.

Scrivano, L., Esterlechner, J., Muhlbach, H., Ettischer, N., Hagen, C., Grunewald, K., Mohr, C. A., Ruzsics, Z., Koszinowski, U., & Adler, B. (2010). The m74 Gene Product of Murine Cytomegalovirus (MCMV) Is a Functional Homolog of Human CMV gO and Determines the Entry Pathway of MCMV. *Journal of Virology*, *84*(9), 4469–4480.

Shizuya, H., Birren, B., Kim, U.-J., Mancino, V., Slepak, T., Tachiiri, Y., & Simon, M. (1992). Cloning and stable maintenance of 300-kilobase-pair fragments of human DNA in Escherichia coli using an F-factor-based vector. *Proceedings of the National Academy of Sciences*, *89*(18), 8794–8797.

Simas, J. P., & Efstathiou, S. (1998). Murine gammaherpesvirus 68: a model for the study of gammaherpesvirus pathogenesis. *Trends in Microbiology*, *6*(7), 276–282.

Simon, C. O., Seckert, C. K., Dreis, D., Reddehase, M. J., & Grzimek, N. K. A. (2005). Role for tumor necrosis factor alpha in murine cytomegalovirus transcriptional reactivation in latently infected lungs. *Journal of Virology*, *79*(1), 326–340.

Simon, C. O., Seckert, C. K., Grzimek, N. K. A., & Reddehase, M. J. (2006). Murine model of cytomegalovirus latency and reactivation: the silencing/desilencing and immune sensing hypothesis. *Cytomegaloviruses: Molecular Biology and Immunology. Caister Academic Press, Wymondham, Norfolk, United Kingdom*, 483–500.

Smith, H. R. C., Heusel, J. W., Mehta, I. K., Kim, S., Dorner, B. G., Naidenko, O. V, Iizuka, K., Furukawa, H., Beckman, D. L., & Pingel, J. T. (2002). Recognition of a virus-encoded ligand by a natural killer cell activation receptor. *Proceedings of the National Academy of Sciences*, *99*(13), 8826–8831.

Smith, L. R., Wloch, M. K., Chaplin, J. A., Gerber, M., & Rolland, A. P. (2013). Clinical development of a cytomegalovirus DNA vaccine: from product concept to pivotal phase 3 trial. *Vaccines*, *1*(4), 398–414.

Smith, M. G. (1954). Propagation of salivary gland virus of the mouse in tissue cultures. *Proceedings of the Society for Experimental Biology and Medicine*, *86*(3), 435–440.

Snyder, C. M., Cho, K. S., Bonnett, E. L., Allan, J. E., & Hill, A. B. (2011). Sustained CD8+ T cell memory inflation after infection with a single-cycle cytomegalovirus. *PLoS Pathogens*, *7*(10), e1002295.

Sprague, E. R., Reinhard, H., Cheung, E. J., Farley, A. H., Trujillo, R. D., Hengel, H., & Bjorkman, P. J. (2008). The human cytomegalovirus Fc receptor gp68 binds the Fc CH2-CH3 interface of immunoglobulin G. *Journal of Virology*, *82*(7), 3490–3499.

Stahl, F. R., Keyser, K. A., Heller, K., Bischoff, Y., Halle, S., Wagner, K., Messerle, M., & Förster, R. (2015). Mck2-dependent infection of alveolar macrophages promotes replication of MCMV in nodular inflammatory foci of the neonatal lung. *Mucosal Immunology*, *8*(1), 57–67.

Staras, S. A. S., Dollard, S. C., Radford, K. W., Flanders, W. D., Pass, R. F., & Cannon, M. J. (2006). Seroprevalence of cytomegalovirus infection in the United States, 1988–1994. *Clinical Infectious Diseases*, *43*(9), 1143–1151.

Stegmann, C., Hochdorfer, D., Lieber, D., Subramanian, N., Stöhr, D., Laib Sampaio, K., & Sinzger, C. (2017). A derivative of platelet-derived growth factor receptor alpha binds to the trimer of human cytomegalovirus and inhibits entry into fibroblasts and endothelial cells. *PLoS Pathogens*, *13*(4), e1006273.

Steinberg, C., Eisenächer, K., Gross, O., Reindl, W., Schmitz, F., Ruland, J., & Krug, A. (2009). The IFN regulatory factor 7-dependent type I IFN response is not essential for early resistance against murine cytomegalovirus infection. *European Journal of Immunology*, *39*(4), 1007–1018.

Stevenson, P. G., Belz, G. T., Altman, J. D., & Doherty, P. C. (1999). Changing patterns of dominance in the CD8+ T cell response during acute and persistent murine γ-herpesvirus infection. *European Journal of Immunology*, *29*(4), 1059–1067.

Stoddart, C. A., Cardin, R. D., Boname, J. M., Manning, W. C., Abenes, G. B., & Mocarski, E. S. (1994). Peripheral blood mononuclear phagocytes mediate dissemination of murine cytomegalovirus. *Journal of Virology*, *68*(10), 6243–6253.

Straschewski, Sarah, Patrone, M., Walther, P., Gallina, A., Mertens, T., & Frascaroli, G. (2011). Protein pUL128 of human cytomegalovirus is necessary for monocyte infection and blocking of migration. *Journal of Virology*, *85*(10), 5150–5158.

Sunil-Chandra, N. P., Efstathiou, S., Arno, J., & Nash, A. A. (1992). Virological and pathological features of mice infected with murine gammaherpesvirus 68. *Journal of General Virology*, *73*(9), 2347–2356.

Sylwester, A. W., Mitchell, B. L., Edgar, J. B., Taormina, C., Pelte, C., Ruchti, F., Sleath, P. R., Grabstein, K. H., Hosken, N. A., Kern, F., Nelson, J. A., & Picker, L. J. (2005). Broadly targeted human cytomegalovirus-specific CD4+ and CD8+ T cells dominate the memory compartments of exposed subjects. *Journal of Experimental Medicine*, *202*(5), 673–685.

Tabata, T., Petitt, M., Fang-Hoover, J., Freed, D. C., Li, F., An, Z., Wang, D., Fu, T.-M., & Pereira, L. (2019). Neutralizing monoclonal antibodies reduce human cytomegalovirus infection and spread in developing placentas. *Vaccines*, *7*(4), 135.

Tarantal, A. F., Salamat, M. S., Britt, W. J., Luciw, P. A., Hendrickx, A. G., & Barry, P. A. (1998). Neuropathogenesis Induced by Rhesus Cytomegalovirus in Fetal Rhesus Monkeys (Macaca mulatta). *The Journal of Infectious Diseases*, *177*(2), 446–450.

Tierney, R., Nakai, T., Parkins, C. J., Caposio, P., Fairweather, N. F., Sesardic, D., & Jarvis, M. A. (2012). A single-dose cytomegalovirus-based vaccine encoding tetanus toxin fragment C induces sustained levels of protective tetanus toxin antibodies in mice. *Vaccine*, *30*(20), 3047–3052.

Tsuda, Y., Caposio, P., Parkins, C. J., Botto, S., Messaoudi, I., Cicin-Sain, L., Feldmann, H., & Jarvis, M. A. (2011). A replicating cytomegalovirus-based vaccine encoding a single Ebola virus nucleoprotein CTL epitope confers protection against Ebola virus. *PLoS Neglected Tropical Diseases*, *5*(8), 1–10.

Upadhyayula, S., & Michaels, M. G. (2013). Ganciclovir, foscarnet, and cidofovir: antiviral drugs not just for cytomegalovirus. *Journal of the Pediatric Infectious Diseases Society*, *2*(3), 286–290.

van Stijn, A., Rowshani, A. T., Yong, S. L., Baas, F., Roosnek, E., ten Berge, I. J. M., & van Lier, R. A. W. (2008). Human cytomegalovirus infection induces a rapid and sustained change in the expression of NK cell receptors on CD8+ T cells. *The Journal of Immunology*, *180*(7), 4550–4560.

Vanarsdall, A. L., Chin, A. L., Liu, J., Jardetzky, T. S., Mudd, J. O., Orloff, S. L., Streblow, D., Mussi-Pinhata, M. M., Yamamoto, A. Y., Duarte, G., Britt, W. J., & Johnson, D. C. (2019). HCMV trimer- and pentamer-specific antibodies synergize for virus neutralization but do not correlate with congenital transmission. *Proceedings of the National Academy of Sciences of the United States of America*, *116*(9), 3728–3733.

Verweij, M., Hansen, S. G., Iyer, R., John, N., Malouli, D., Morrow, D., Scholz, I., Womack, J., Abdulhaqq, S., & Gilbride, R. M. (2021). Modulation of MHC-E transport by viral decoy ligands is required for RhCMV/SIV vaccine efficacy. *Science*.

Vieira, J., Farrell, H. E., Rawlinson, W. D., & Mocarski, E. S. (1994). Genes in the HindIII J fragment of the murine cytomegalovirus genome are dispensable for growth in cultured cells: insertion mutagenesis with a lacZ/gpt cassette. *Journal of Virology*, *68*(8), 4837–4846.

Virgin IV, H. W., & Speckt, S. H. (1999). Unraveling immunity to γ-herpesviruses: a new model for understanding the role of immunity in chronic virus infection. *Current Opinion in Immunology*, *11*(4), 371–379.

Volkmer, H., Bertholet, C., Jonjić, S., Wittek, R., & Koszinowski, U. H. (1987). Cytolytic T lymphocyte recognition of the murine cytomegalovirus nonstructural immediate-early protein pp89 expressed by recombinant vaccinia virus. *The Journal of Experimental Medicine*, *166*(3), 668–677.

Wagner, F. M., Brizic, I., Prager, A., Trsan, T., Arapovic, M., Lemmermann, N. A. W., Podlech, J., Reddehase, M. J., Lemnitzer, F., Bosse, J. B., Gimpfl, M., Marcinowski, L., MacDonald, M., Adler, H., Koszinowski, U. H., & Adler, B. (2013). The Viral Chemokine MCK-2 of Murine Cytomegalovirus Promotes Infection as Part of a gH/gL/MCK-2 Complex. *PLoS Pathogens*, *9*(7).

Wagner, M., Jonjić, S., Koszinowski, U. H., & Messerle, M. (1999). Systematic excision of vector sequences from the BAC-cloned herpesvirus genome during virus reconstitution. *Journal of Virology*, *73*(8), 7056–7060.

Wang, D., & Shenk, T. (2005). Human cytomegalovirus UL131 open reading frame is required for epithelial cell tropism. *Journal of Virology*, *79*(16), 10330–10338.

Ward, S. M., Jonsson, J. R., Sierro, S., Clouston, A. D., Lucas, M., Vargas, A. L., Powell, E. E., & Klenerman, P. (2004). Virus-specific CD8+ T lymphocytes within the normal human liver. *European Journal of Immunology*, *34*(6), 1526–1531.

Warming, S., Costantino, N., Court, D. L., Jenkins, N. A., & Copeland, N. G. (2005). Simple and highly efficient BAC recombineering using galK selection. *Nucleic Acids Research*, *33*(4), e36–e36.

Watanabe, K. S., Goodrich, J. M., Li, C. R., Agha, M. E., & Greenberg, P. D. (1992). Restoration of viral immunity in immunodeficient humans by the adoptive transfer of T cell clones. *Science*, *257*(5067), 238–241.

Weck, K. E., Dal Canto, A. J., Gould, J. D., O'Guin, A. K., Roth, K. A., Saffitz, J. E., Speck, S. H., & Virgin, H. W. (1997). Murine γ-herpesvirus 68 causes severe large-vessel arteritis in mice lacking interferon-γ responsiveness: a new model for virus-induced vascular disease. *Nature Medicine*, *3*(12), 1346–1353.

Weinberg, J. B., Lutzke, M. L., Alfinito, R., & Rochford, R. (2004). Mouse strain differences in the chemokine response to acute lung infection with a murine gammaherpesvirus. *Viral Immunology*, *17*(1), 69–77.

Weller, T. H., Macauley, J. C., Craig, J. M., & Wirth, P. (1957). Isolation of intranuclear inclusion producing agents from infants with illnesses resembling cytomegalic inclusion disease. *Proceedings of the Society for Experimental Biology and Medicine*, *94*(1), 4–12.

Wen, Y., Monroe, J., Linton, C., Archer, J., Beard, C. W., Barnett, S. W., Palladino, G., Mason, P. W., Carfi, A., & Lilja, A. E. (2014). Human cytomegalovirus gH/gL/UL128/UL130/UL131A complex elicits potently neutralizing antibodies in mice. *Vaccine*, *32*(30), 3796–3804.

Wikstrom, M. E., Fleming, P., Comerford, I., McColl, S. R., Andoniou, C. E., & Degli-Esposti, M. A. (2013). A Chemokine-Like Viral Protein Enhances Alpha Interferon Production by Plasmacytoid Dendritic Cells but Delays CD8+ T Cell Activation and Impairs Viral Clearance. *Journal of Virology*, *87*(14), 7911–7920.

Wille, P. T., Knoche, A. J., Nelson, J. A., Jarvis, M. A., & Johnson, D. C. (2010). A human cytomegalovirus gO-null mutant fails to incorporate gH/gL into the virion envelope and is unable to enter fibroblasts and epithelial and endothelial cells. *Journal of Virology*, *84*(5), 2585–2596.

Wille, P. T., Wisner, T. W., Ryckman, B., & Johnson, D. C. (2013). Human cytomegalovirus (HCMV) glycoprotein gB promotes virus entry in trans acting as the viral fusion protein rather than as a receptor-binding protein. *MBio*, *4*(3).

Wloch, M. K., Smith, L. R., Boutsaboualoy, S., Reyes, L., Han, C., Kehler, J., Smith, H. D., Selk, L., Nakamura, R., & Brown, J. M. (2008). Safety and immunogenicity of a bivalent cytomegalovirus DNA vaccine in healthy adult subjects. *Journal of Infectious Diseases*, *197*(12), 1634–1642.

Wu, C. A., Paveglio, S. A., Lingenheld, E. G., Zhu, L., Lefrançois, L., & Puddington, L. (2011). Transmission of murine cytomegalovirus in breast milk: a model of natural infection in neonates. *Journal of Virology*, *85*(10), 5115–5124.

Wu, Y., Prager, A., Boos, S., Resch, M., Brizic, I., Mach, M., Wildner, S., Scrivano, L., & Adler, B. (2017). *Human cytomegalovirus glycoprotein complex gH / gL / gO uses PDGFR- α as a key for entry*. 1–24.

Wu, Z., Sinzger, C., Frascaroli, G., Reichel, J., Bayer, C., Wang, L., Schirmbeck, R., & Mertens, T. (2013). Human cytomegalovirus-induced NKG2Chi CD57hi natural killer cells are effectors dependent on humoral antiviral immunity. *Journal of Virology*, *87*(13), 7717–7725.

Wussow, F., Chiuppesi, F., Contreras, H., & Diamond, D. J. (2017). Neutralization of human cytomegalovirus entry into fibroblasts and epithelial cells. *Vaccines*, *5*(4), 39.

Xiaofei, E., Meraner, P., Lu, P., Perreira, J. M., Aker, A. M., McDougall, W. M., Zhuge, R., Chan, G. C., Gerstein, R. M., Caposio, P., Yurochko, A. D., Brass, A. L., & Kowalik, T. F. (2019). OR14I1 is a receptor for the human cytomegalovirus pentameric complex and defines viral epithelial cell tropism. *Proceedings of the National Academy of Sciences of the United States of America*, *116*(14), 7043–7052.

Ye, L., Qian, Y., Yu, W., Guo, G., Wang, H., & Xue, X. (2020). Functional Profile of Human Cytomegalovirus Genes and Their Associated Diseases: A Review. *Frontiers in Microbiology*, *11*(September), 1–13.

Young, N. T., & Uhrberg, M. (2002). KIR expression shapes cytotoxic repertoires: a developmental program of survival. *Trends in Immunology*, *23*(2), 71–75.

Yu, D., Ellis, H. M., Lee, E.-C., Jenkins, N. A., & Copeland, N. G. (2000). An efficient recombination system for chromosome engineering in Escherichia coli. *Proceedings of the National Academy of Sciences*, *97*(11), 5978–5983.

Zheng, X., Oduro, J. D., Boehme, J. D., Borkner, L., Ebensen, T., Heise, U., Gereke, M., Pils, M. C., Krmpotic, A., & Guzmán, C. A. (2019). Mucosal CD8+ T cell responses induced by an MCMV based vaccine vector confer protection against influenza challenge. *PLoS Pathogens*, *15*(9), e1008036.

Zhou, M., Lanchy, J.-M., & Ryckman, B. J. (2015). Human cytomegalovirus gH/gL/gO promotes the fusion step of entry into all cell types, whereas gH/gL/UL128-131 broadens virus tropism through a distinct mechanism. *Journal of Virology*, *89*(17), 8999–9009.

7. Appendix

7.1 List of abbreviations

aa	amino acid
ADCC	antibody-dependent cellular cytotoxicity
APCs	antigen presenting cells
APS	ammonium persulfate
BAC	bacterial artificial chromosome
BSA	bovine serum albumin
CAM	chloramphenicol
CCMV	chimpanzee cytomegalovirus
cDC	conventional dendritic cell
CMV	cytomegalovirus
CPE	cytopathogenic effect
DMEM	Dulbecco's Modified Eagle Medium
DMSO	dimethyl sulfoxide
DNA	desoxyribonucleic acid
dNTP	desoxynucleotide triphosphate
E.coli	Escherichia coli
EDTA	ethylene diamine tetraacetic acid
ELISA	enzyme-linked immunosorbent assay
FACS	fluorescence activated cell staining
FCS	fetal calf serum
FITC	fluorescein isothiocyanate
gB (H, L, M, N, O)	glycoprotein (H, L, M, N, O)
h	hour(s)
HA	hemagglutinin
HCMV	human cytomegalovirus
HIV	human immunodeficiency virus
HPV	human papillomavirus
HSCT	hematopoietic stem cell transplants
IAV	influenza A virus

ICS	intracellular cytokine staining
IE	immediate early
IFN	interferon
I.p	intraperitoneal
I.n	intranasal
iNOS	Inducible nitric oxide synthase
KAN	kanamycin
KLRG1	killer cell lectin-like receptor subfamily G member 1
MCMV	murine cytomegalovirus
MEF	mouse embryonic fibroblasts
MHC	major histocompatibility complex
MHV-68	murine gammaherpesvirus 68
μg	microgram
μl	microliter
mM	micromolar
M	molar
min	minute(s)
MOI	multiplicity of infection
MVA	Modified vaccinia ankara
MΦ	macrophage(s)
pDC	plasmacytoid dendritic cells
nm	nanometer
OD	optical density
ORF	open reading frame
OVA	ovalbumin
PAGE	polyacrylamide gel electrophoresis
PBMC	peripheral blood mononuclear cells
PBL	peripheral blood leukocytes
PBS	phosphate buffered saline
PC	pentameric complex
PCR	polymerase chain reaction
PDGF-α	platelet-derived growth factor-α

Pen/Strep	penicillin/streptomycin
PEI	Polyethyleneimine
PFA	paraformaldehyde
PFU	plaque forming unit
PTHrP	parathyroid hormone-related protein
PRRs	pattern recognition receptors
RCMV	rat cytomegalovirus
RhCMV	rhesus cytomegalovirus
RT	room temperature
RNA	ribonucleic acid
RPL8	murine ribosomal protein L8
SCMV	simian cytomegalovirus
SDS	sodium dodecyl sulfate
SDS-PAGE	SDS polyacrylamide gel electrophoresis
SIV	simian immunodeficiency
TAE	Tris-Acetate-EDTA
TC	Trimeric complex
TCID	tissure cuture infective dose
TEMED	N,N,N',N' – Tetramethylethylendiamin
TLR	toll-like receptors
TNF	tumor necrosis factor
WB	Western Blot
Wt	wildtype
ZEBOV	Zaire ebolavirus

7.2 Publications and posters

This thesis describes work performed at the Max von Pettenkofer-Institute, in Munich between April 2017 and September 2020. Parts of the thesis were presented at conferences or will be published.

Publications to come

1. The MCK2 protein of murine cytomegalovirus: chemokine activity and gH/gL/MCK2-dependent entry are independent functions. **Marwa Eletreby**, Thomas Deiler, Lucie Kubic, Katharina Jäger, Josipa Jerak, Laura Jochem, Krizan Jurinovic, Max Holzwarth, Barbara Adler

(in preparation).

2. The MCMV gH/gL/MCK2 complex as a target of neutralizing antibodies. Ilija Brizic, Katharina Jäger, Lucie Kubic, **Marwa Eletreby**, Stipan Jonjic, Barbara Adler

(in preparation).

Poster presentations

1. **Marwa Eletreby**, Katharina Jäger, Ursula Rambold, Thomas Deiler, Lena Thiessen, Lucie Kubic, Barbara Adler (2021). The importance of the viral chemokine MCK2 for MCMV vaccine vectors. 30th Annual Meeting of the Society for Virology, 2021.

2. **Marwa Eletreby**, Josipa Jerak, Laura Jochem, Thomas Deiler, Ilia Brizic, Stipan Jonjic and Barbara Adler (2018). MCK2-viral chemokine and key to entry. Gene center retreat (2018)